

Electronic Thesis and Dissertation Repository

10-26-2020 1:00 PM

Inducing DNA-Mismatch Repair Deficiency In Tumours: A Strategy To Enhance Anti-Tumour Immunity

Mikal El-Hajjar, *The University of Western Ontario*

Supervisor: Maleki, Saman, *The University of Western Ontario*

Joint Supervisor: Koropatnick, James, *The University of Western Ontario*

A thesis submitted in partial fulfillment of the requirements for the Master of Science degree in Microbiology and Immunology

© Mikal El-Hajjar 2020

Follow this and additional works at: <https://ir.lib.uwo.ca/etd>



Part of the [Immunity Commons](#)

Recommended Citation

El-Hajjar, Mikal, "Inducing DNA-Mismatch Repair Deficiency In Tumours: A Strategy To Enhance Anti-Tumour Immunity" (2020). *Electronic Thesis and Dissertation Repository*. 7432.
<https://ir.lib.uwo.ca/etd/7432>

This Dissertation/Thesis is brought to you for free and open access by Scholarship@Western. It has been accepted for inclusion in Electronic Thesis and Dissertation Repository by an authorized administrator of Scholarship@Western. For more information, please contact wlsadmin@uwo.ca.

Abstract

Immunotherapy has improved patient outcomes in advanced or metastatic settings across a number of cancers. Patients with tumours deficient in the DNA mismatch repair (DNA-MMR) pathway often show high response rates to immune checkpoint inhibitors (ICIs) with a rise in immune surveillance. However, little is known about the immune sensitization effects of inducing DNA-MMR-deficiency in low tumour mutational burden (TMB) cancers, such as ICI refractory neuroblastoma. In addition, the dynamic T-cell profile that results from such a DNA-MMR inactivation, and whether this may confer a therapeutic benefit, is poorly understood. Here, I used CRISPR/CAS9 genome editing technology to knock out (KO) *MLH1*, a crucial molecule in the DNA-MMR pathway, in mouse neuroblastoma (neuro-2a) cells – a low TMB pediatric cancer refractory to ICIs – to induce MMR deficiency. To analyze tumour growth inhibition in response to ICIs and immunophenotype the tumour-infiltrating lymphocytes (TILs), tumours with intact or induced MMR deficiency were injected subcutaneously into immunocompetent mice. Tumour growth were measured after treatment with anti-PD1 antibodies and TILs were analyzed for activation, exhaustion, and effector markers, allowing for an in-depth flow cytometric analysis of T-cell subsets in these tumours. This study shows that inducing MMR-deficiency induces a robust anti-tumour response in a low TMB cancer. Moreover, this sensitization was accompanied by specific phenotypic changes of T-cells in response to anti-PD1 therapy in the tumour.

Keywords

Cancer, DNA-MMR Repair, Immunotherapy, Immune checkpoint inhibitors, MLH1, T-cells

Summary for Lay Audience

Immunotherapy is a new form of cancer treatment that utilizes the immune system to recognize and kill cancer cells. In this thesis, I focus on immune checkpoint inhibitors (ICIs), which is a form of cancer immunotherapy that binds to “immune checkpoints” found on immune cells. These immune checkpoints typically serve to tamper down the immune response in order to prevent a harmful overactivation of the immune system. ICIs therefore bind to immune checkpoint molecules, blocking them from exerting their function, which then allows for immune cells to become re-invigorated and target cancer cells. Over the past few years, clinical trials have shown that a number of patients that are treated with immunotherapy have a long-term response to treatment. Moreover, responders to ICIs often have a very high number of mutations in their tumours. A subset of cancer patients that show a favorable response to ICIs are cancer patients that have a deficiency in their ability to repair DNA mistakes, which results in a large number of mutations in their tumour. Unfortunately, many cancer patients with a low number of tumour mutations do not respond to ICIs. In this thesis, I studied the effect of inducing a deficiency of DNA repair in a tumour with a low number of mutations and hypothesized that this would result in an increase in mutations in the tumour and a better response to ICIs.

Co-Authorship Statement

Experiments in this thesis were performed by Mikal El-Hajjar with the help of members of the Koropatnick/Maleki laboratory as follows:

Rene Figueredo generated the neuroblastoma knockout cell lines used in these studies and helped with tumour injections.

Ronak Zareardalan aided in expanding the neuroblastoma cell lines and taught me how to perform western blot analysis.

Acknowledgments

I would first like to thank all the members of the Koropatnick/Maleki lab for their support and friendship throughout my 2 years at the lab.

I want to also thank my family for supporting me throughout my master's, through all the good and bad days. Their support meant everything to me, and I could not have done this without them.

Thank you to Dr. Koropatnick for his wisdom and help. His advice and mentorship allowed me to better develop my skills and overall knowledge as a scientist in training. I also want to thank my advisory committee, Dr. Mymryk and Dr. Gunaratnam, for their invaluable guidance. I learned so much thanks to your advice and help.

Finally, I want to thank Dr. Maleki for your constant guidance and support throughout my 2 years. You gave me invaluable advice on what it means to be a scientist. I am truly lucky to have been your student and appreciate everything that you have done for me. The lessons you have taught me will be ones that I take with me throughout the rest of my career.

Table of Contents

Abstract.....	i
Summary for Lay Audience.....	ii
Co-Authorship Statement.....	iii
Acknowledgments.....	iv
Table of Contents.....	v
List of Tables.....	viii
List of Abbreviations.....	xi
Chapter 1.....	1
<i>Introduction</i>	<i>1</i>
1.1 – Cancer and the immune system.....	1
1.1.1 Cancer and the immune system.....	1
1.1.2 Role of the adaptive immune system in anti-tumour immunity.....	1
1.2.1 Immune checkpoint inhibitors.....	5
1.2.2 Predictors of response to anti-PD1 therapy.....	7
1.3.1 Immunogenic tumour microenvironment.....	8
1.3.2 Tumour mutational burden and TME.....	8
1.4 – Hot tumours and microsatellite instability.....	11
1.4.1 DNA mismatch repair pathway and microsatellite instability.....	11
1.4.2 DNA mismatch repair pathway and tumour immunogenicity.....	13
1.4.3 Inducing MMR-deficiency in poorly immunogenic tumours: turning “cold” tumours “hot”.....	13
1.5 – Neuroblastoma: “cold tumours” and immunotherapy.....	15
1.6 Rationale, hypothesis and aims.....	16
Rationale.....	16
Hypothesis.....	16
Aims.....	16
Chapter 2.....	17

<i>Methods</i>	17
2.1 – Cell culture.....	17
2.2 – CRISPR Cas9 MLH1 KO Plasmid	18
2.3 - CRISPR Cas9 transfection.....	19
2.4 – Western blot.....	19
2.5 – Proliferation assay.....	20
2.6 – Mice	21
2.7 – Tumour implantation, immune checkpoint inhibitor treatment, tumour measurement and blood collection.....	21
2.7.1 – Immune checkpoint inhibitor experiments	21
2.7.2 – Tumour growth in immunodeficient mice experiments.....	21
2.7.3 – Blood collection	22
2.8 – Isolation of splenocytes, lymph nodes and TILs from mice	22
2.8.1 – Isolation of splenocytes and lymph nodes from mice.....	22
2.8.2 – Isolation of tumour infiltrating lymphocytes (TILs) from mice	23
2.9 – Flow cytometry	24
2.10 – TCGA data mining.....	25
2.11 – Statistical analysis	26
Chapter 3.....	27
<i>Results</i>	27
3.1 Colorectal cancer patients with microsatellite instability ^{HIGH} tumours express lower levels of the DNA-MMR repair gene <i>MLH1</i>	27
3.2 MSI-h tumours are associated with higher numbers of T-cells and levels of pro- inflammatory molecules.....	30
3.3 Generating an <i>MLH1</i> knock-out mouse neuroblastoma cell line.....	34
3.4 Baseline tumour growth of pMMR and dMMR neuro-2a cells was similar in immunodeficient mice	37
3.5 Inducing DNA-MMR deficiency results in an increased anti-tumour response in immunocompetent mice.....	39
3.6 Combination of inducing MMR-deficiency and treating with anti-PD1 prolongs survival of immune competent mice.....	45

3.7 DNA-mismatch repair deficient tumours express higher levels of MHC-I <i>in vitro</i>	48
3.8 Colorectal cancer patients with highly microsatellite instable tumours express higher levels of MHC-I related genes	51
3.9 Effect of inducing DNA-MMR repair in neuro-2a cells on PD-L1 expression.....	54
3.10 Effect of inducing MMR-deficiency and treating with anti-PD1 on T-cell infiltration of the tumour-draining lymph nodes	58
3.11 T-cell infiltration into tumours in response to dMMR induction and anti-PD1 treatment	60
3.12 CD8 ⁺ T-cell infiltration into tumours in response to dMMR induction and anti-PD1 treatment	63
3.13 The effect of inducing MMR deficiency and treating with anti-PD1 on T-cell activation and exhaustion	66
3.14 The effect of inducing MMR-deficiency and treating with anti-PD1 blockade on T-cell cytotoxic activity.....	71
3.15 Effect of inducing MMR-deficiency and treating with anti-PD1 on CD39 ⁺ PD1 ⁺ CD8 ⁺ T-cells infiltrated into tumours	74
3.16 Effect of inducing MMR-deficiency and treating with anti-PD1 on stimulating immunosuppressive T-regulatory cells in tumours.....	77
3.17 Effect of inducing MMR deficiency and treating with anti-PD1 on CD4 ⁺ T-cell activation and exhaustion.....	80
3.18 A combination of inducing MMR-deficiency and anti-PD1 treatment results in a significant decrease in dysfunctional T-cells	83
.....	84
3.19 Immune markers associated with improved overall survival in high-risk neuroblastoma patients	85
Chapter 4.....	88
<i>Discussion</i>	88
References.....	93

List of Tables

Table 1. Antibodies and reagents table	24
--	----

List of Figures

Figure 1.1. DNA MMR-deficiency in tumours results in heightened tumour immunogenicity...	10
Figure 1.2. DNA mismatch repair pathway	12
Figure 2.1 CRISPR Cas9 MLH1 KO Plasmid.....	18
Figure 3.1. MLH1 is downregulated in microsatellite instable human COAD READ tumours. .	29
Figure 3.2. MSI-h tumours express higher levels of T-cells marker and proinflammatory genes.	33
Figure 3.3. Inducing MMR deficiency in neuroblastoma mouse cancer cells and the impact on growth in vitro.....	36
Figure 3.4. Growth of pMMR and dMMR neuro-2a cells in immunodeficient mice was not significantly different.....	38
.....	42
.....	42
Figure 3.5.1. Inducing tumour MMR deficiency results in increased anti-tumour response.	42
Figure 3.5.2. A combination of inducing MMR-deficiency and treating with anti-PD1 immune checkpoint blockade starting at day 7 can cure a subset of mice.....	44
Figure 3.6. Inducing tumour MMR deficiency and treating with anit-PD1 increases survival of mice.....	47
Figure 3.7. Inducing MMR-deficiency enhances MHC-I expression in neuro-2a cells.	50
Figure 3.8. MSI-h tumours express higher levels of MHC-I genes.....	53
Figure 3.9.1 MSI-h colorectal tumours express higher levels of PD-L1 mRNA.	55
Figure 3.9.2 Effect of inducing MMR-deficiency on PD-L1 expression.	57
Figure 3.10. Inducing MMR-deficiency enhances T-cell recruitment to tumour draining lymph nodes in response to anti-PD1 treatment.	59

Figure 3.11. Effect of inducing MMR-deficiency on T-cell infiltration of mouse neuroblastoma tumours.	62
Figure 3.12. Effect of inducing MMR-deficiency on CD8 ⁺ T-cell infiltration into mouse neuroblastoma tumours.	65
Figure 3.13. Tumour infiltrating lymphocyte activation and exhaustion in mice bearing induced DNA mismatch repair deficient tumours.	70
Figure 3.14. CD8 ⁺ T-cell degranulation activity from tumours following MMR-induction and anti-PD1 treatment.	73
Figure 3.15. Tumour infiltrating lymphocyte exhaustion in mice bearing induced DNA mismatch repair deficient tumours.	76
Figure 3.16. T-regulatory cell infiltration into pMMR and dMMR tumours.	79
Figure 3.17. CD4 ⁺ T-cell exhaustion in pMMR and dMMR tumours.	82
Figure 3.18. A combination of MMR-induction and anti-PD1 treatment results in a decrease in dysfunctional T-cells.	84
Figure 3.19. CD8a expression is associated with improved overall survival in high-risk neuroblastoma patients.	87

List of Abbreviations

ATCC	American Type Culture Collection
BCR	B-cell receptor
C12	Clone 12
C4	Clone 4
COAD READ	Colorectal adenocarcinoma
CRC	Colorectal cancer
CTLA-4	Cytotoxic T-lymphocyte-associated protein
DC	Dendritic cell
DNA-MMR	DNA mismatch repair
FACS	Fluorescence activated cell sorting
FBS	Fetal bovine serum
GZMb	Granzyme B
HLA	Human leukocyte antigen
ICI	Immune checkpoint inhibitor
IFN γ	Interferon gamma
IP	Intraperitoneal
KO	Knock-out
MDSC	Myeloid derived suppressor cell
MHC	Major histocompatibility complex
MLH1	MutL homologue 1
MMR	Mismatch repair
MMR-d	Mismatch repair deficient
MSI	Microsatellite stable instable
MSI-h	Microsatellite stable instable high
MSH2	MutS homologue 2
MSH6	MutS homologue 6MSS
MSS	Microsatellite stable
NK	Natural killer
PBS	Phosphate buffered saline
PD-1	Programmed cell death 1
PD-L1	Programmed cell death ligand 1
PMS2	Postmeiotic segregation increase 2
PRF1	Perforin 1
RBC	Red blood cell
RSEM	RNA-seq by expectation maximization
RT	Room temperature
SC	Subcutaneously
SD	Standard deviation
SEM	Standard error mean
TCR	T-cell receptor
TMB	Tumour mutational burden
TIL	Tumour infiltrating lymphocyte
TME	Tumour microenvironment
Treg	T-regulatory

UV

Ultra-violet

Chapter 1

Introduction

1.1 – Cancer and the immune system

1.1.1 Cancer and the immune system

Cancer is a disease in which cells divide uncontrollably and no longer abide by typical growth-control mechanisms¹. Cancer cells are transformed “normal cells” that progressively mutate and evolve to continuously proliferate and can ultimately spread to other organs and kill the host². More recently, it has become apparent that the immune system plays a critical role in the development and control of tumours. The term “cancer immunoediting” has been coined to describe the role that the immune system plays in both limiting and promoting tumour growth³. Immunoediting involves three stages: elimination, equilibrium and escape³. In the first phase, *elimination*, both the innate and adaptive components of the immune system work together to eliminate tumour cells before they are clinically detectable⁴. This is likely a reasonably effective process, as many individuals do not develop clinically detectable cancer in their lifetimes. In the equilibrium phase, the tumour and the immune system reach an equilibrium where the immune system is able to control tumour growth, but not completely eliminate all tumour cells. The immune system is therefore able to keep the net number of cancer cells constant or at a number below that necessary to generate detectable tumours during equilibrium⁵. While this prevents the tumour from forming clinically detectable disease, certain cancer cells that escape the elimination phase remain alive, as immune selection and pressure favours cells with lower immunogenicity⁶. In the escape phase, the immune system is no longer able to suppress tumour growth as some tumour cells generate mutations that mediate resistance to immune control. This results in the clinical presentation of the disease⁴. As all tumours go through the process of immunoediting, clinically detectable tumours are commonly resistant to immune control and either evade or actively suppress anti-tumour immunity.

1.1.2 Role of the adaptive immune system in anti-tumour immunity

Innate immunity is the first barrier of defense in the fight against foreign pathogens. The innate immune system is activated rapidly after detection of a pathogen; however, it does not develop a pathogen-specific response or immunological memory against the foreign entity. Adaptive immunity, on the other hand, is capable of mounting a specific response tailored to the invading pathogen or neoplastic cells. Adaptive immunity is also responsible for immunological memory against pathogens and tumours⁷. This highlights the significance of adaptive immunity in targeting cancer in a sustainable manner.

Adaptive immunity consists of T-cells and B-cells and, unlike innate immunity, is *antigen-specific*. Antigens (*antibody generators*) are molecules that can stimulate an immune response in the body³. This type of immunity is quite powerful because it targets cancer cells on the basis of recognition of tumour-specific and/or tumour-associated antigens and stimulates immunological memory to continuously recognize and eradicate tumour cells expressing those antigens⁸. Antigen-specific recognition is due to the generation of a vast number of possible receptors found on T-cells (TCRs) and B-cells (BCRs)⁸. Collectively, these cells are able to recognize a large number of unique antigen-specific peptides due to their VD(J) recombination⁹. This genetic recombination takes place between variable, diversity, and joining segments of TCRs or BCRs, which allows for the generation of millions of different unique and specific receptors⁹. B-cells and T-cells recognize foreign antigens and in the context of pro-inflammatory cytokines are able to mount a proper antigen-specific clonal response to neutralize the threat⁸. Importantly, T-cells recognize only foreign antigens that are presented on MHC molecules while B-cell responses are MHC-independent⁸. Conventional T-cells are divided into two different types: CD4⁺ T-cells and CD8⁺ T-cells. CD4⁺ T-cells recognize peptides bound to MHC-II molecules, which are present only on antigen-presenting cells. Such peptides or neopeptides (“new peptides”) can arise from mutated proteins that go on to be detected as a “non-self” protein¹⁰. Once the CD4⁺ T-cell is bound to MHC-II, it can differentiate into either a T-helper cell or a T-regulatory cell (Treg), depending on the cytokine context. T-helper cells, as their name suggest, aid in the activation of NK cells, B-cells and CD8⁺ T-cells. However, Tregs are generated when CD4⁺ T-cells recognize an MHC-II bound antigen in the context

of immunosuppressive cytokine⁸. Unlike T-helper cells, Tregs dampen the immune response and play an important role in immune homeostasis and tumour immune evasion¹¹.

Conversely, CD8⁺ T-cells have the potential to differentiate into cells with cytotoxic capacity to eliminate virally infected and tumour cells: these T-cells have been termed “the foot soldiers of the immune system”¹². CD8⁺ T-cells differ from CD4⁺ T-cells in that they recognize foreign peptides presented onto MHC-I molecules, which are found on all nucleated cells¹². Peptides presented onto MHC-I molecules allow CD8⁺ T-cells to recognize these cells as *non-self*¹⁰. CD8⁺ T-cells have an anti-tumour function and exert cell-mediated cytotoxicity to kill cancer cells¹². T-cells, in general, play an essential role in anti-tumour immunity, as increased T-cell infiltration (both CD4⁺ and CD8⁺ T-cells) is often associated with improved prognosis of cancer patients⁷. The focus of this thesis will be on stimulating a T-cell response, mainly CD8⁺ T-cells, in tumours that are typically devoid of T-cells.

In order to understand the manner in which T-cells are primed and trafficked into tumours, an overall understanding of the “Cancer-Immunity Cycle” is essential. This cycle begins with the release of tumour antigens, which are engulfed and processed by antigen-presenting cells, more specifically dendritic cells (DCs)¹³. DCs make their way through the lymphatic system and traffic to lymphoid organs. In the lymphoid organs, DCs, with their respective antigens loaded onto surface MHC-I or MHC-II molecules, will present peptides to CD8⁺ or CD4⁺ T-cells, respectively¹⁴. Importantly, the process in which DCs internalize and present endogenous antigens from tumours cells that do not directly infect DCs is called cross presentation¹⁵. Cross presentation is critical in generating an immune response against tumour cells¹⁵. Following the presentation of tumour antigens onto MHCI molecules, T-cells with a TCR that recognizes their respective antigen results in the priming of naïve T-cells¹⁵. Fully activated CD8⁺ T-cells then traffic to the tumour where they recognize MHC-I bound tumour antigens on the surface of tumour cells and target them for destruction¹⁴. This tumour cell killing results in the release of other tumour antigens including neoantigens (true foreign antigens) and the cancer immunity cycle continues¹⁴. Cancer cells are often able to disrupt this cycle through different mechanisms and overcome anti-tumour

immunity. An important example of such a disruption is the expression by tumour cells of ligands for immune checkpoint molecules present on T-cells, which dampen the anti-tumour functions of T-cells⁷. Thus, immune checkpoint inhibitors (ICIs) are important as they allow for the reinvigoration of T-cells and, consequently, restoration of the cancer immunity cycle⁷. Despite the promise of ICIs, many cancers do not respond to these drugs. Thus, studying ICI-refractory tumour cells and discovering a novel mechanism to sensitize these tumours to ICIs can serve as an important way to trigger anti-tumour immunity.

1.2 – Immunotherapy with immune checkpoint inhibitors

1.2.1 Immune checkpoint inhibitors

Immune checkpoints are molecules expressed on T-cells that negatively regulate activation or effector functions of these cells¹⁶. The evolutionary purpose of immune checkpoints is to prevent a harmful overactivation of the immune system and to maintain immune homeostasis¹⁶. However, cancer cells exploit immune checkpoints to dampen anti-tumour immune responses¹⁷. Immune checkpoint inhibitors (ICIs) are monoclonal antibodies that bind to these regulatory proteins and hinder the immune dampening effects of immune checkpoints¹⁷. Two major immune checkpoints studied in the context of cancer are “cytotoxic T-lymphocyte-associated protein 4” (CTLA-4) and “programmed cell death protein 1” (PD-1) and its ligand PD-L1. PD-1 will be the main focus of this thesis; however, it is important to understand the differences between these two immune checkpoints and their distinct role in dampening the immune response.

CTLA-4 is an immune checkpoint that plays a role in early T-cell activation stage¹⁸. CTLA-4 is expressed on T-cells upon binding of T-cell receptor (TCR) to an antigen MHC complex on antigen-presenting cells. CTLA-4 competes with CD28 (a costimulatory molecule expressed on T-cells) in binding to CD80 (B7-1) and CD86 (B7-2) ligands expressed on antigen-presenting cells¹⁸. CD28 binding to CD80 and CD86 is required for proper T-cell activation as it provides a co-stimulatory signal for effective T-cell activation¹⁸. CTLA-4 binds to CD80 and CD86 with a higher affinity and often outcompetes CD28, which prevents T-cell activation and instead induces T-cell anergy¹⁸. Moreover, as T-cells become activated, CTLA-4 is trafficked from intracellular vesicles, where it is stored in T-cells, to the cell surface to prevent overactivation of T-cells¹⁷. Anti-CTLA-4 antibodies were first tested, in preclinical models, as a treatment against tumours by James Allison and his group¹⁹. Their study remarkably showed that CTLA-4 blockade *in vivo* enhanced immune-related anti-tumour responses with durable efficacy¹⁹. Since then, anti-CTLA-4 has been used to treat melanoma patients. These patients have a very high TMB due to the ultraviolet (UV) DNA damage induced nature of the cancer²⁰. In randomized controlled trials, 22% of melanoma patients showed sustained long-term (>3

years) benefits in response to ipilimumab, an anti-CTLA-4 ICI¹⁸. CTLA-4 is mainly expressed on CD4⁺ T-cells, therefore ipilimumab primarily activates CD4⁺ T-cells²¹. It is important to note that this drug can also have some serious side effects related to the activation of the immune system against self-antigens²². These can include skin rashes, colitis and endocrinopathies²².

PD-1, another immune checkpoint molecule, inhibits T-cell effector functions including cytokine secretion and cytotoxicity¹⁸. PD-1-mediated immune regulation most often involves T-cells that have been activated before and occurs in peripheral tissues rather than lymph nodes¹⁸. T-cells express PD-1 after activation, as a mechanism to prevent overactivation of the immune system¹⁸. PD-1 binds to its ligands, PD-L1 and PD-L2, which are often found on antigen-presenting cells, myeloid cells, and tumour cells²³. The PD-1/PD-L1 interaction hinders T-cell activation and proliferation¹⁸. Tumour cells take advantage of this axis of inhibition in order to downregulate the T-cell's cytotoxic capacity and induce a state of T-cell exhaustion¹⁸. Monoclonal antibodies that target either PD-1, or PD-L1, in order to block this ligand receptor interaction, can re-invigorate T-cells²⁴. More specifically, these monoclonal antibodies reinvigorate cytotoxic CD8⁺ T-cells and they can then go on to target and kill cancer cells²⁴.

T-cells express a number of other co-inhibitory receptors that play an important role in regulating the T-cell immune response²⁵. These immune checkpoints include lymphocyte-activation gene 3 (LAG-3), T-cell immunoglobulin mucin domain-3 (TIM-3) and T-cell immunoreceptor with Ig and ITIM domains (TIGIT)²⁶. LAG-3 is expressed on activated CD8⁺ and CD4⁺ T-cells and binds to a number of molecules including MHCII, (with higher affinity than CD4), LSECtin and galectin3 (found on tumour cells)²⁵. When LAG-3 binds to these molecules, it negatively regulates T-cell signalling and results in reduced T-cell proliferation and cytokine production²⁵. TIM-3, another immune checkpoint, binds to galectin9 found on various tumour cells²⁵. Binding of TIM-3 and galectin9 results in the phosphorylation of tyrosine residues on the TIM-3 tail and stimulates downstream inhibitory signals that negatively regulate the T-cell response²⁵. Interestingly, the co-inhibitory receptor TIGIT was discovered through bioinformatic analysis²⁵. TIGIT binds

CD155 and through its immunoreceptor tyrosine inhibitory domains, TIGIT inhibits T-cell proliferation and dampens the overall T-cell effector capacity²⁵.

1.2.2 Predictors of response to anti-PD1 therapy

Clinical success of anti-PD1 therapy depends on a number of factors, including PD-L1 expression on tumour cells. For example, patients with tumours expressing higher levels of PD-L1 respond better to ICI therapy¹⁸. Higher somatic mutation frequency in tumours is also associated with better overall response rates to anti-PD1 treatment²⁰. The heightened response in patients with high TMB tumours is thought to occur due to the increase in neoantigens resulting from somatic mutations. Neoantigens are “new antigens” that have not been otherwise recognized as “self” by T-cells during thymic development, therefore, they are considered true foreign antigens by the immune system¹⁰. Neoantigens render tumours more immunogenic, allowing cytotoxic T-cells to recognize them as non-self and target them for destruction²⁰. Microsatellite instable (MSI) tumours have some of the highest somatic mutation frequencies and also display heightened overall responses to ICIs²⁰. Interestingly, pembrolizumab, which targets PD-1, was the first ICI that was FDA approved on a molecular biomarker basis and is used for all microsatellite instability-high (MSI-h) and mismatch repair-deficient (MMR-d) cancers. This underscores the importance of microsatellite instability for favorable ICI response²⁰. A growing shift in ICI research has moved towards studying factors, such as the ones listed above, that influence T-cell infiltration into tumours and promote ICI response²⁷.

1.3 - Tumour microenvironment and immune checkpoint inhibitors

1.3.1 Immunogenic tumour microenvironment

The immunogenicity of tumours can have a substantial impact on prognosis of cancer patients and success of their response to immunotherapies such as ICIs²⁸. Highly immunogenic tumours, termed “hot tumours”, refer to a T-cell-inflamed tumour microenvironment (TME)²⁸. Hot tumours are highly infiltrated with T-cells and show signs of immune activation²⁸. However, cold tumours are characterized as having a TME where T-cells are excluded²⁸. The presence of cytotoxic T-lymphocytes in the TME demonstrates that the adaptive immune system recognizes the cancer as foreign and is able to infiltrate the tumour. However, in order for a tumour to be considered as highly immunogenic or “hot”, it not only has to be infiltrated with T-cells, but it also has to be *inflamed*. Within *infiltrated-inflamed* tumours, cytotoxic lymphocytes express high levels of effector molecules such as interferon gamma (IFN γ) and granzyme B²⁷. The presence of these activation markers indicates that cytotoxic T-lymphocytes in the tumour are not simply bystanders but are able to recognize cancer cells as foreign and elicit an immune response²⁷.

1.3.2 Tumour mutational burden and TME

High tumour mutational burden (TMB) of tumours correlates with tumour immunogenicity²⁷. A high TMB may seem paradoxical, as mutations acquired by cancer cells are what allow them to gain the ability to proliferate uncontrollably and escape cell death¹⁰. However, a higher number of mutations within the tumour can lead to more neoantigens that can be recognized by the immune system as foreign¹⁰. Moreover, a high TMB is associated with higher immune cell infiltration¹⁰. As these tumours acquire more mutations, they are able to present more foreign peptides on their MHC-I molecules that can then be recognized as foreign by the cytotoxic T-cells that infiltrate the tumour²⁹. Immune cell infiltration, along with high levels of foreign peptides in high TMB tumours, is likely responsible for their enhanced ICI response²⁹. ICIs often show efficacy in such patients, because as immune cells become exhausted in this highly immunogenic TME,

ICIs rescue them from their exhausted state, and they become re-invigorated to recognize and kill tumour cells in an antigen specific manner¹⁰.

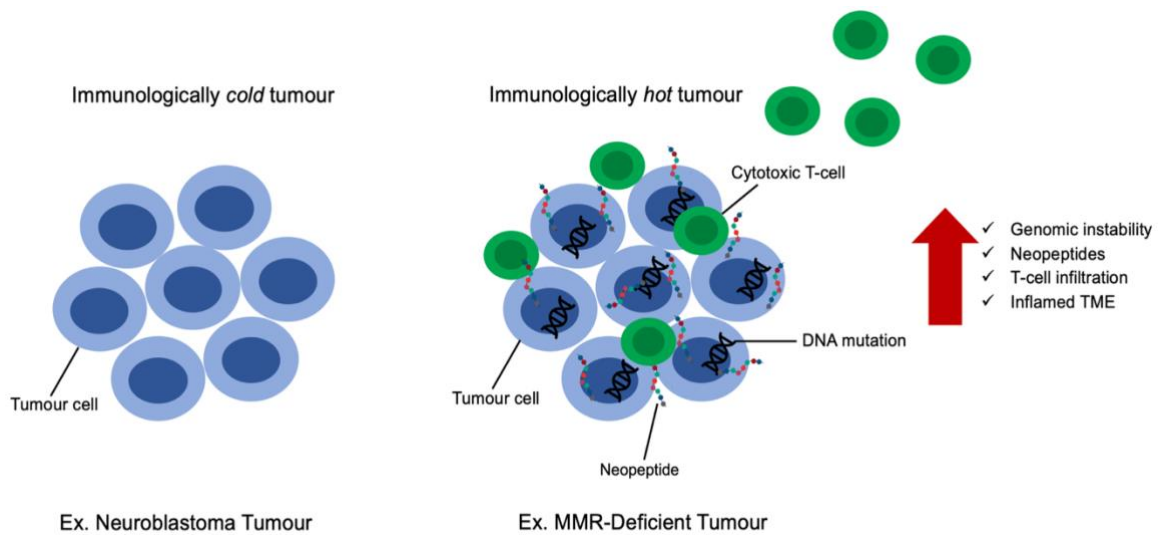


Figure 1.1. DNA MMR-deficiency in tumours results in heightened tumour immunogenicity.

Immunologically hot tumours are characterized by an increase in T-cell infiltration and immune recognition. Such tumours respond favorably to ICIs because of their pre-existing anti-tumour immunity. Recently, mismatch repair deficient patients have been shown to respond well to ICIs and have a TME that has been characterized as immunologically hot and conducive to ICI response. These immunologically hot tumours have genomic instability, which leads to many genomic mutations. When such mutations occur in coding regions of the genome, leading to new potentially antigenic peptides (neopeptides) being produced. These neopeptides can then be presented by MHC-I molecules and tumours are subsequently recognized as non-self by the immune system. This recognition of the tumour as *foreign* results in the infiltration of cytotoxic T-cells into the tumour and the release of pro-inflammatory cytokines and cytolytic enzymes to target and kill cancer cells. However, the immune system has evolved mechanisms to prevent the overactivation of the immune system and it therefore dampens the T-cell response. As such, these cytotoxic T-cells express activation and exhaustion immune checkpoint molecules such as PD-1, TIM-3, LAG-3 and TIGIT, which hinder the T-cell response against tumours. Notably, this pre-existing T-cell infiltration and immune checkpoint expression results in a favorable response of MMR-deficient patients when compared to patients with genomically stable cold tumours. Genomically stable tumours such as neuroblastoma tumours often lack a pre-existing anti-tumour response, and therefore show little benefit to ICIs.

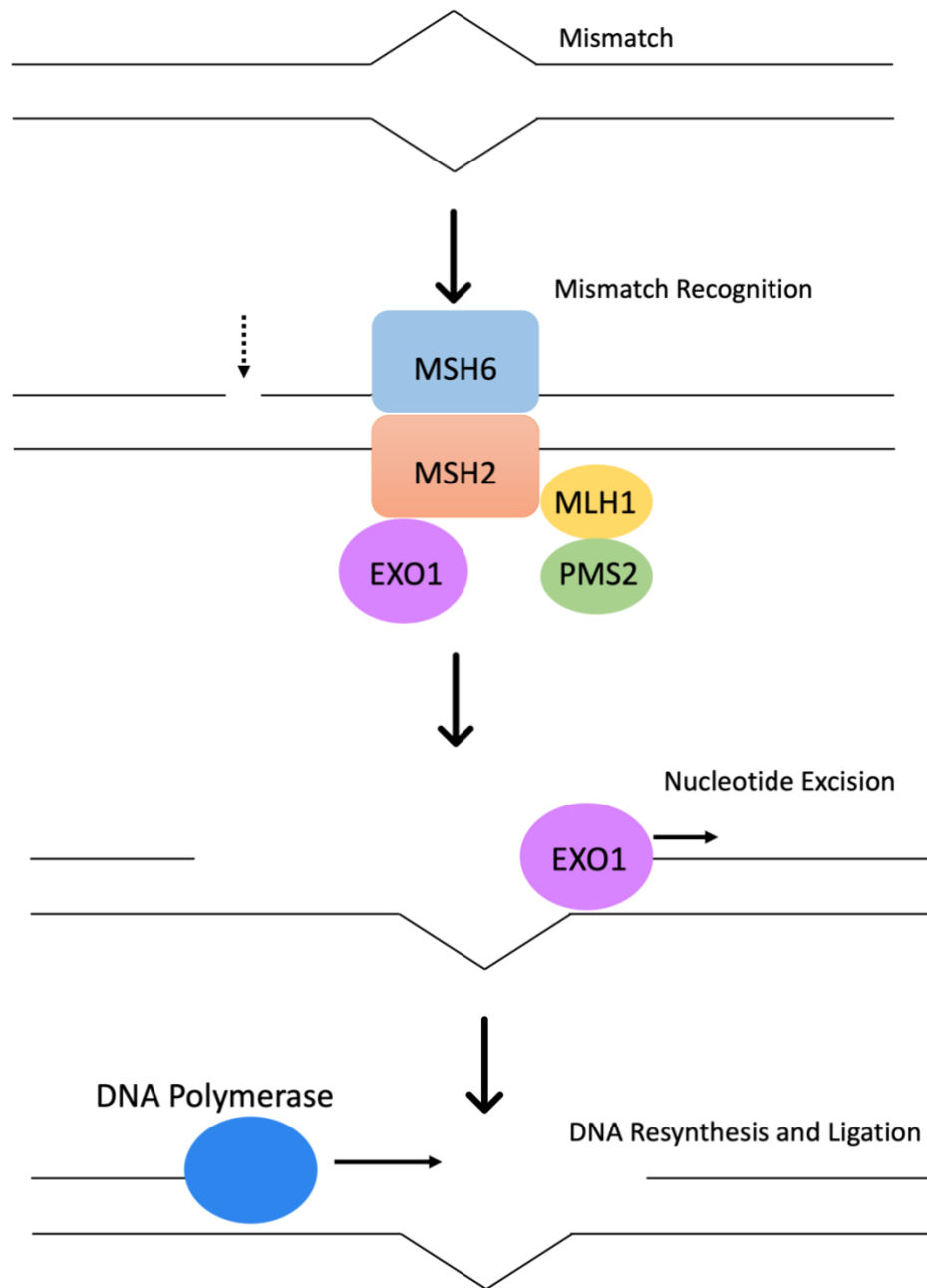
1.4 – Hot tumours and microsatellite instability

The tumour mutational burden (TMB) is a strong biomarker for immunogenicity as previously discussed. A major example of highly immunogenic cancers with a high TMB signature is a subset of colorectal adenocarcinoma (COAD READ) patients with highly microsatellite instable (MSI-h) or DNA mismatch repair-deficient tumours²⁷. As a result of this TMB signature, these patients respond favorably to immune checkpoint inhibitors (ICIs). It is important to note that deficiencies in other types of DNA repair mechanisms may also result in a high TMB and favorable response to ICIs. However, the focus of this thesis will be on the DNA-MMR pathway, as tumours with a DNA-MMR deficiency have been clinically shown to respond to ICIs across a number of cancers.

1.4.1 DNA mismatch repair pathway and microsatellite instability

Microsatellites are repetitive DNA sequences that range from 1 to 6 nucleotides in length³⁰. These repetitive sequences are error prone during DNA replication as slippage between the primer and template strand occurs. This slippage results in an insertion deletion loop that can then be recognized and repaired by the DNA-MMR machinery³¹. However, when DNA-MMR is impaired, these mutations are not corrected, and the result is microsatellite instability. Four important genes in the DNA mismatch repair complex are the mutL homologue (MLH1), mutS homologue (MSH2), mutS homologue 6 (MSH6) and post-meiotic segregation increase 2 (PMS2)³². When a mismatch occurs, MSH2 binds to MSH6 forming the mutS homologue and MLH1 associates with PMS2 forming the mutL homologue³². The mutS and mutL guide mismatch recognition and recruit exonuclease 1 to remove mismatching nucleotides³². Polymerase δ fills in the gap created by the exonuclease and DNA ligase repairs the phospho-diester backbone³². Importantly, mutation or silencing of any one of the four genes responsible for mismatch recognition can result in microsatellite instability (MSI or MSI-high)³². However, in MSI-h COAD READ patients, the most common cause of MMR deficiency is the hypermethylation of the MLH1 promoter, leading to loss of gene expression²⁹.

Figure 1.2. DNA mismatch repair pathway



*Adapted from: Alexinna MN et al. *Nature* 2015

1.4.2 DNA mismatch repair pathway and tumour immunogenicity

Tumours that are DNA-MMR-deficient (dMMR) acquire more mutations in comparison to DNA-MMR-proficient tumours (pMMR) (>12 mutations/10⁶ DNA bases vs <8.24 mutations/10⁶ DNA bases, respectively)²⁹. This high mutation load results in more new peptides generated by the tumours and presented onto their MHC I molecule²⁹. As such, MMR deficiency renders tumours more immunogenic as these tumours become highly infiltrated and inflamed²⁷. More specifically, these tumours have a large number of cytotoxic T-lymphocytes that express markers of activation, such as PD-1²⁷. These tumours also express higher levels of type I IFN genes, which aids in triggering anti-tumour immunity, when compared to their mismatch repair-proficient counterparts.²⁹ As such, MSI-h COAD READ tumours are considered “hot tumours” and these patients have a better prognosis when compared to microsatellite stable (MSS) COAD READ patients³². Additionally, due to their highly immune inflamed TME, dMMR MSI-h patients respond better to ICIs²⁹.

1.4.3 Inducing MMR-deficiency in poorly immunogenic tumours: turning “cold” tumours “hot”

MMR-deficient tumours have been characterized as immunologically hot, with higher immune cell infiltration and by definition, these tumours illicit a stronger immune response when compared to cold tumours²⁷. A number of scientists have therefore studied the effect of inducing MMR-deficiency on immunologically cold tumours in order to render these tumours more immunogenic. Germano *et al.* showed that inducing MMR-deficiency in the immunologically cold pancreatic tumour resulted in a heightened anti-tumour response against these tumours when compared to their MMR proficient counterparts³³. Mandal *et al.* similarly showed that inducing MMR-deficiency in a murine colorectal cell line resulted in an enhanced immune dependent anti-tumour response in mice³⁴. Interestingly, both groups also showed that inducing MMR-deficiency resulted in higher tumour immunogenicity, which sensitized these immunologically cold, ICI refractory tumours, to this treatment^{33,34}. Unfortunately, this concept of inducing MMR-deficiency in cold tumours has not been well studied in childhood cancers, which are an important subset of tumours that do not respond to ICI treatment. Cancers, such as

neuroblastoma, accounts for disproportionate mortality among childhood cancers³⁵. Neuroblastoma tumours are immunologically cold and do not illicit a strong anti-tumour response and consequently do not benefit from ICI treatment³⁵.

1.5 – Neuroblastoma: “cold tumours” and immunotherapy

In the previous section, hot tumours and their heightened response to immunotherapy were discussed. Conversely, “cold tumours” are characterized as non-immune-inflamed tumours largely devoid of immune cells²⁸. One example of such a tumour is neuroblastoma, which is the most common extra-cranial solid tumour diagnosed in children³⁵. Patients diagnosed after 18 months of age often display metastatic or unresectable disease and have a very poor prognosis (40-50%)³⁵. Neuroblastoma is largely non-immunogenic. These tumours have a low TMB, which prevents the body from mounting an effective immune response against the tumour.

Immunotherapy with ICIs largely relies on the re-invigoration of a pre-existing immune response to restore effective immune targeting of cancer cells. However, in the case of neuroblastoma, tumour antigen availability is very limited, preventing such an immune response against the tumour³⁶. Neuroblastoma cells are therefore largely invisible to cytotoxic T-cells limiting T-cell infiltration into tumours. Neuroblastoma cells also express negatively charged carbohydrate epitopes on their surface that are not only non-immunogenic, but also immunosuppressive³⁶. Additionally, these tumours release immunosuppressive molecules such as FAS ligand into the TME, further rendering the microenvironment tumour-suppressive³⁶. Pro-tumourigenic immune cells are also recruited to the TME, such as anti-inflammatory macrophages that promote tumour growth and inhibit anti-tumour natural killer (NK) cells³⁶. Some studies have also shown that the immune-suppressive populations, such as myeloid derived suppressor cells (MDSCs) and Treg cells, play a role in creating an immunosuppressive tumour microenvironment³⁶.

This highly immunosuppressive tumour microenvironment along with the limited epitope landscape renders these tumours immunologically cold³⁶. Immunologically cold tumours cannot induce a proper immune response and are devoid of cytotoxic T-lymphocytes needed for a successful response to ICIs.

1.6 Rationale, hypothesis and aims

Rationale

Patients with DNA-MMR repair deficiencies have highly immune infiltrated and inflamed tumours²⁷. This phenotype is thought to arise due to the increase in somatic mutations in these tumours, ultimately producing more neopeptides that can stimulate an immune response²⁷. Moreover, because of this highly infiltrated and immune-inflamed phenotype, patients with DNA-MMR deficiencies respond well to immune checkpoint inhibitors²⁰. Therefore, I hypothesize that impairing DNA-MMR machinery in an otherwise stable and non-immunogenic cancer, neuroblastoma, would stimulate an anti-tumour immune response. Furthermore, I propose that this activation of the immune system can, in turn, sensitize these tumours to immune checkpoint inhibitors.

Hypothesis

Induction of DNA-MMR deficiency in an immunologically cold tumour will result in increased tumour immunogenicity with a heightened anti-tumour response in immune-competent mice. This induction will also produce a robust anti-tumour response characterized by phenotypic changes in tumour infiltrating lymphocytes (TILs).

Aims

Aim 1: Induce MMR deficiency in the neuro-2a neuroblastoma cell line (representing a low TMB cancer).

Aim 2: Study the effect of inducing MMR-deficiency on neuro-2a cells.

Aim 3: Analyze anti-tumour response of mice bearing MMR-deficient (dMMR) and MMR-proficient (pMMR) tumours and treated with ICIs.

Aim 4: Compare the immune phenotype of TILs from dMMR and pMMR tumour-bearing-mice using multicolour flow cytometry.

Chapter 2

Methods

2.1 – Cell culture

The murine neuroblastoma cell line, neuro-2a, was obtained from the American Type Culture Collection (ATCC) and was used for the experiments described below. These cells were grown in culture at 37 degrees Celsius, 5% CO₂. Cells were cultured in RPMI140 media (Wisent Bio Products, Saint-Jean Baptise, QC) supplemented with 10% fetal bovine serum (ThermoFisher Scientific, Waltham, MA, USA). For the majority of the experiments, cells were expanded to a ~70-80% confluency. In order to detach cells from cell culture plates/flasks, media was removed, and plates/flasks were washed with PBS (Wisent Bio Products, Saint-Jean Baptise, QC, CA) to remove any residual FBS. Trypsin (Wisent Bio Products, Saint-Jean Baptise, QC, CA) was added (0.5-1.5ml) to detach cells from the surface of plates and these were placed in an incubator at 37 degrees Celsius, 5% CO₂ for ~3 minutes. Once cells were visibly detached, 10ml of RPMI media (Wisent Bio Products) supplemented with FBS (ThermoFisher Scientific) was added to the trypsin-cell mixture. Harvested cells were then processed following the methods described below.

2.2 – CRISPR Cas9 MLH1 KO Plasmid

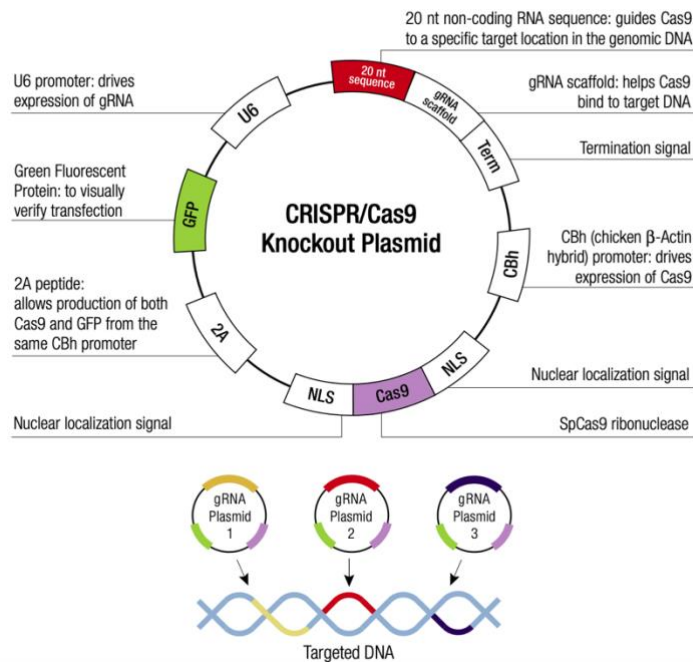


Figure 2.1 **CRISPR Cas9 MLH1 KO Plasmid**

Clustered Regularly Interspaced Short Palindromic Repeats (CRISPR) and the CRISPR-associated protein (Cas9) are used to degrade target genetic material in order to knock-out a gene of interest. I used the MLH1 CRISPR Cas9 KO Plasmid from Santa Cruz Biotechnology in order to knock-out the MLH1 gene in the murine neuroblastoma (neuro-2a) cell line. This CRISPR Cas9 plasmid consists of a pool of 3 different plasmids with distinct target-specific guide RNAs, a GFP encoding region and a Cas9 encoding region. A pool of 3 plasmids targeting different portions of the MLH1 gene, was used in order to maximize knock-out efficiency. Other important regions of the plasmids are indicated in the figure above obtained from the Santa Cruz Biotechnology website (<https://www.scbt.com/p/mlh1-crispr-knockout-and-activation-products-m>).

2.3 - CRISPR Cas9 transfection

MLH1 CRISPR CAS9 KO plasmid was purchased from Santa Cruz Biotechnology (Santa Cruz Biotechnology, Dallas, TX, USA). In a 6-well plate, 50 000 neuro-2a neuroblastoma cells were seeded in 3 ml of RPMI 140 (Wisent Bio Products, Saint-Jean Baptise, QC) supplemented with 10% FBS (ThermoFisher Scientific) and grown to 80% confluency. After 24 hours, 1ug of plasmid DNA (Santa Cruz Biotechnology) was mixed with 3ml of lipofectamine 3000 (ThermoFisher Scientific, Waltham, MA, USA) and 500ul of medium. Cells were incubated for 24 hours. Successful plasmid transfection was visualized using fluorescence activated cell sorting (FACS) for green fluorescence protein (GFP) fluorescence. GFP+ cells were sorted, 1 cell per well in a 96-well plate. Cells were grown until a colony was formed and were then trypsinized (Wisent Bio Products) and transferred onto a 24-well plate. They were further expanded and finally transferred onto a T25 plate.

2.4 – Western blot

Selection of successful *MLH1* KO clones was confirmed by western blot. Wild type neuro-2a cells and neuro-2a cells transfected with the *MLH1*CRISPR Cas9 KO plasmid, were grown *in vitro*. Protein was collected from neuro-2a cells using 100 µl of RIPA (name derived from its original intended application, radio-immunoprecipitation assay) lysis buffer with protease inhibitors (ThermoFisher Scientific, Waltham, MA, USA), which lyses and extracts protein from mammalian cells. A cell scraper was then used, and the lysate was transferred to a 15 ml tube and left on ice for ~15 minutes. Cells were sonicated twice, 2 seconds each time, and again left on ice for 15 minutes. Cells were centrifuged at 13000g for 5 minutes at 4 degrees Celsius. The concentration of protein from the sample was measured using the Bio-Rad Protein Assay (Bio-Rad, Hercules, CA, USA) and reading through the spectrophotometer. Samples were then reduced and denatured (105 degrees Celsius) and Sodium Dodecyl Sulfate (SDS) sample buffer with β-mercaptoethanol were added to the protein sample. SDS is a detergent that denature proteins and gives them all an overall negative charge in order for the proteins to separate based off of size. Cell lysates (30 µg) were loaded into every well of the 10% SDS-PAGE gel and run at 120V for ~1

hour in a Bio-Rad electrophoresis apparatus (Bio-Rad, Hercules, CA, USA) with running buffer (28.8g of glycine, 6.04g of Tris base, 2 ml of 10% SDS). Protein samples that had then separated were then transferred onto a membrane using transfer buffer (25mM Tris, 192 mM glycine at a pH of 8.3 with 20% methanol). Transfer to membrane was carried out within a cassette with filter paper and fiber pads and was run at 30V overnight. After proteins were transferred onto the membrane, the membrane was submerged in 2 ml of 5% skim milk (prepared from powder) for 1 hour on a shaker. Primary anti-*MLH1* antibodies at a 1:2000 (Abcam, Cambridge, UK) concentration were then added to the membrane for ~2 hours on a shaker at room temperature (RT). This was then washed with TBST for 5 minutes, 3 times. Finally, HRP-conjugated secondary anti-rabbit antibody at a 1:2000 (Millipore Sigma, Burlington, MA, USA) concentration was added to the membrane. HRP chemiluminescent substrate, luminata forte (Millipore Sigma, Burlington, MA, USA), was thinly layered onto the membrane and this was then imaged.

2.5 – Proliferation assay

Neuro-2a clones 12 (pMMR cell line) and clone 4 (dMMR cell line) were grown for 7 weeks *in vitro*, passaged ~3 times per week, to allow for mutations to accumulate. In order to ensure that neuro-2a cells with the *MLH1* KO (dMMR) and that neuro-2a cells still expressing *MLH1* (pMMR) were growing at similar rate *in vitro*, a proliferation assay was conducted. Neuro-2a cells were thawed and then given a day to adhere to the T75 flasks. The following day, cells were trypsinized (Wisent Bio Products) and spun down at 300g for 6 minutes at 4 degrees Celsius. Cells were then washed twice with PBS (Wisent Bio Products) and spun down at 300g for 6 minutes at 4 degrees Celsius. Cells were counted using the Beckman Coulter cell counter (Beckman Coulter, Brea, CA, USA) and they were then spun down at 300g for 6 minutes at 4 degrees Celsius. Neuro-2a cells were then diluted for a final concentration of 50,000 cells per 100 ul and 100 ul was added to a T25 flask with 10 ml of RPMI media (Wisent Bio Products) with 10% FBS (ThermoFisher Scientific). There was a total of 6 flasks with pMMR neuro-2a cells and 6 flasks with dMMR neuro-2a cells. Cells were placed in an incubator at 30 degrees Celsius, 5% CO₂ to grow. The next day, 3 flasks with pMMR neuro-2a cells and 3 flasks with dMMR neuro-2a cells were removed from the incubator to calculate the number of cells that adhered onto

the flasks and establish the baseline number of cells for each clone. Cells were left to grow for an additional 4 days. At day 4, the rest of the flasks with pMMR and dMMR neuro-2a cells were counted using the Beckman Coulter cell counter (Beckman Coulter). This cell count represents the total number of cells after a 4-day growth period. The proliferation rate was calculated by simply dividing the number of cells at day 4 by the initial number of cells that adhered onto the flasks to obtain the fold increase of cell growth.

2.6 – Mice

A/J mice were purchased from the Jackson Laboratory (Jackson Laboratory, Bar Harbor, ME, USA) and immunodeficient SHO mice were purchased from Charles river (Charles river, Wilmington, MA, USA). Mice were 6-8 weeks of age when acquired and were all female. These mice were housed at the Victoria Research Lab Vivarium. Protocols involving animals were approved by the Animal Care Committee (ACC) at Western University.

2.7 – Tumour implantation, immune checkpoint inhibitor treatment, tumour measurement and blood collection.

2.7.1 – Immune checkpoint inhibitor experiments

For the *in vivo* experiments, 5×10^5 pMMR and dMMR neuro-2a cells were injected subcutaneously into the right flank of mice (day 0). Tumours were palpable ~10 days post tumour injection. Therefore, at day 7 or 10 depending on the experiment, mice were given 250 ug of anti-PD1 antibody in 100 ul of PBS injected intraperitoneally (i.p.) every 3 days for a total of 3 injections on days 10, 13, and 16. Tumour volumes were measured using callipers, and calculated by measuring their length and width, and recorded in mm^3 . When the first tumour volumes reached $\sim 1400 \text{mm}^3$, all mice were euthanized.

2.7.2 – Tumour growth in immunodeficient mice experiments

When analyzing tumour growth *in vivo* in immunodeficient animals, 500 000 pMMR neuro-2a cells (C12) and dMMR neuro-2a cells (C4) were injected subcutaneously into the

right flank of mice (day 0). Tumour volumes were measured at days 7, 10, 13, 16, 20, 24. Mice were sacrificed individually when their tumour volumes reached ~1400 mm³.

2.7.3 – Blood collection

Blood was collected at 2 time points from A/J mice. The first time point was at day 7, the “before treatment time point”. The second time point was at day 14 and this was the “after treatment time point”. For blood collection, blood was collected from the saphenous vein on the right leg of mice. The blood was then left to settle at RT for 30 minutes. After 30 minutes, blood was centrifuged at 15000 RPM at room temperature and the supernatant was collected and frozen at -80 degrees Celsius.

2.8 – Isolation of splenocytes, lymph nodes and TILs from mice

2.8.1 – Isolation of splenocytes and lymph nodes from mice

Mice were euthanized by being placed in a chamber with carbon monoxide for 30 seconds. Spleens were removed and placed in ice-cold RPMI media (Wisent Bio Products) and kept on ice. The spleen was placed in a 70um strainer (ThermoFisher Scientific, Waltham, MA, USA) and the plunger end of a sterile syringe was used to homogenize the spleen into a well of a 6-well plate with RPMI media (Wisent Bio Products). Media was then transferred from the plate to a 15 ml tube and placed on ice. To acquire a single cell suspension, the cell suspension was then centrifuged at 300 g for 8 minutes at 4 degrees Celsius. The cell pellet was broken up with 1 ml of PBS (Wisent Bio Products) and then 13 ml of PBS were added to wash cells. Tube was transferred to the centrifuge for the wash at 300 g for 8 minutes at 4 degrees Celsius. This wash was repeated one more time. One ml of red blood cell (RBC) lysis (NH₄Cl (ammonium chloride) 8.02gm NaHCO₃ (sodium bicarbonate) 0.84gm EDTA (disodium) 0.37gm)) buffer was added to break up the pellet and 2 more ml of buffer were added and the tube was placed on ice for 3 minutes (mixing suspension every 30 seconds). Ten ml of RPMI media (Wisent Bio Products) was subsequently added and the tube was centrifuged at 300 g for 8 minutes at 4 degrees Celsius. Pellet was once again broken up with 1 ml of PBS (Wisent Bio Products) and 13 ml of PBS was added to wash

the cells. PBS (Wisent Bio Products) was added for a final wash, and 500 ul was removed prior to centrifugation to obtain a cell count using the Beckman Coulter (Beckman Coulter) cell counter. After the final wash, the pellet was broken up with 1 ml of PBS (Wisent Bio Products) and additional PBS was added as needed to have ~1 million cells/ml. 250 ul of this suspension (250,000 cells) was then transferred to a well on a 96-well plate for further antibody staining.

2.8.2 – Isolation of tumour infiltrating lymphocytes (TILs) from mice

Mice were sacrificed by being exposed to carbon monoxide in an enclosed chamber for 30 seconds. Dead animals were then removed, and the tumour was extracted and placed in RPMI (Wisent Bio Products) media on ice. Tumour was cut into small 2-4mm pieces and placed in a 50 ml tube with RPMI media (Wisent Bio Products) using the Miltenyi Biotec Tumour Dissociation Kit (Miltenyi Biotec, Bergisch, GL, DE). The tumour sample was homogenized using the GentleMacs Dissociator (Miltenyi Biotec, Bergisch, GL, DE), on the “tumour mouse sample 03” setting, for solid tumour homogenization. Tubes were then rested on a rotator, which was placed in an incubator (37 degrees Celsius) for 40 minutes. Samples were removed and run through a 70um strainer (ThermoFisher Scientific) and then centrifuged at 300 g for 8 minutes at 4 degrees Celsius. Cell pellet was broken up with 1 ml of PBS (Wisent Bio Products) and then 30 ml of PBS was added to wash the pellet. Suspension was centrifuged at 300 g for 8 minutes at 4 degrees Celsius. This washing step was repeated. One ml of RBC lysis buffer was added to break up the pellet and 4 more ml of the lysis buffer was added, and the tube was placed on ice for 5 minutes (mixing suspension every 30 seconds). Thirty ml of RPMI media (Wisent Bio Products) were then added and the tube was centrifuged at 300 g for 8 minutes at 4 degrees Celsius. Pellet was once again broken up with 1 ml of PBS and 30 ml of PBS (Wisent Bio Products) were added to wash the cells. PBS (Wisent Bio Products) was added for a final wash, and prior to centrifugation, 500 ul of the mixture was removed to count the number of cells using the Beckman Coulter Cell counter (Beckman Coulter). After the final wash, the pellet was broken up with 1 ml of PBS (Wisent Bio Products) and additional PBS was added as needed to have ~5 million cells/ml. 200 ul of this suspension (1 million cells) was then transferred to a well on a 96-well plate for further antibody staining.

2.9 – Flow cytometry

Flow cytometry was required for experiments involving neuro-2a cells (grown *in vitro*), splenocytes, lymph node cells, and tumour cells extracted from mice post-euthanasia. All cells were seeded in a 96-well plate with 200,000 – 1×10^6 cells per well suspended in 250 ul of PBS. Cells were spun down at 3000g for 6 minutes at 4 degrees Celsius. Supernatant was removed and cells were suspended in a live/dead zombie dye (Biolegend, San Diego, CA, USA) for 15 minutes at RT in the dark. Cells were washed with FACS buffer (1x PBS with 5% FBS) and spun down at 1800 g for 6 minutes at 4 degrees Celsius. Supernatant was then removed and 20 ul of Fc Block (Biolegend, San Diego, CA, USA) with a concentration of 10 ug/ml was added to each well and left for 15 minutes at RT in the dark. Mixes of antibodies were then added to the wells and left for 30 minutes on ice without removing the Fc block. Cells were washed with the FACS buffer (PBS with 5% FBS) and centrifuged at 3000g for 6 minutes at 4 degrees Celsius, twice. In order to fix cells, fixation buffer (Biolegend, San Diego, CA, USA) was diluted 1:2 with deionized water and 50 ul of the diluted fixation buffer was added to each well and left for 20 minutes at RT. Cells were washed twice with FACS buffer. Supernatant was removed and cells were transferred from each well in 100 ul of FACS buffer to a polystyrene tube with 300 ul of FACS buffer. Tubes were placed in the refrigerator (4 degrees Celsius) in the dark and run the next day on the BD LSRII Cytometer.

Table 1. **Antibodies and reagents table**

Antibody	Fluorophore	Clone	Source
CD3	Brilliant Violet 711	17A2	BioLegend
CD4	Alexa Fluor 700	GK1.5	BioLegend
CD8a	PerCP/Cyanine5.5	53-6.7	BioLegend
PD1	PE/Dazzle 594	29F.1A12	BioLegend
LAG3	PE/Cyanine 7	C9B7W	BioLegend
TIM3	PE	B8.2C12	BioLegend

TIGIT	APC	IG9	BioLegend
CD39	Alexa Fluor 647	Duha59	BioLegend
CD107a	Brilliant Violet 421	1D4B	BioLegend
CD38	Alexa Fluor 488	90	BioLegend
CD25	Brilliant Violet 605	PC61	BioLegend
CD152	Brilliant Violet 605	UC10-4B9	BioLegend

2.10 – TCGA data mining

The Cancer Genome Atlas database was bioinformatically mined to extract data from the colorectal adenocarcinoma (COAD READ) dataset. mRNA sequencing data was obtained from the Broad Genome Data Analysis Firehose database (<https://gdac.broadinstitute.org/>). This dataset was level 3 RSEM (RNA-Seq by Expectation Maximization) normalized illumina high throughput sequencing data. The normalized RNA seq data file name is “illuminahisec_rnaseqv2-RSEM_genes_normalized (MD5)” and was subsequently converted into a CSV file format. The COAD READ cohort has 631 total samples. Using Python libraries (csv, os and itertools), 3 excel files were created with patient ID information for each sample along with RNAseq values for a number of genes. Samples were divided into the 3 excel files according to whether they were classified as “normal”, “MSS” or “MSI-h” in the clinical file titled “Merge Clinical (MD5)” on the Firehose database website (<https://gdac.broadinstitute.org/>). COAD READ patient samples with both microsatellite status information along with gene expression data were therefore grouped into normal (n=51), MSS (n=257) and MSI-h (n=51) primary tumour tissue samples. Metastatic samples were not included in the analysis. Using the python library Seaborn, box plots were generated in order to compare gene expression between groups. The center line of boxplots represents the media and the upper and lower limits indicate the 75th and 25th percentiles respectively. Mann-Whitney U test was used to statistically compare the groups. In order to generate the overall survival graphs, I analyzed gene

expression as described above. Moreover, I stratified patients according to their gene expression into “high” and “low” groups and used the lifelines library to generate the overall survival plots. The 2-sided log-rank test was used to compare the overall survival in patients highly expressing a gene and patients expressing the gene to a lower extent.

2.11 – Statistical analysis

In vitro data are represented as mean \pm standard deviation (SD). Results were analyzed using Student’s t-two-tailed unpaired t test. Moreover, *in vivo* experiments requiring the comparison between more than 2 groups statistical analysis was performed using the one-way ANOVA test. These results are represented as mean \pm standard deviation (SD). Finally, for the survival experiments statistical analysis was performed using the two-sided log-rank (Mantel-Cox) test. For all tests, a p value < 0.05 (indicated by an asterisk [*] in graphed data) was chosen *a priori* as an indication that the null hypothesis could be rejected. However, data showing differences at more stringent bars of significance (** $p \leq 0.01$, *** $p \leq 0.001$, **** $p \leq 0.0001$) are also shown as matter of interest only: where significance is ascribed, only $p < 0.05$ was considered. Where p values were greater than 0.05, “ns” indicates “not significant”.

Chapter 3

Results

3.1 Colorectal cancer patients with microsatellite instability^{HIGH} tumours express lower levels of the DNA-MMR repair gene *MLH1*

DNA-MMR repair genes *MLH1*, *MSH2*, *MSH6* and *PMS2* are essential components of the DNA-MMR pathway and decreases in expression of these genes is characteristic of a large number of DNA-mismatch repair deficient (dMMR) tumours. Moreover, MMR-deficiency often results in microsatellite instability, an event correlated with favourable responses to ICIs. I therefore set out to determine the levels of 4 major DNA-MMR repair genes: *MLH1*, *MSH2*, *MSH6* and *PMS2* in the colorectal adenocarcinoma (COAD READ) cohort of The Cancer Genome Atlas (TCGA) database. I specifically aimed to determine whether these DNA-MMR genes were significantly downregulated in samples with high microsatellite instability. I included patients with both microsatellite status information along with RNA sequencing data. COAD READ primary samples were grouped into 3 major categories: microsatellite stable (MSS), high microsatellite instability^{high} (MSI-h) and normal (samples obtained from normal adjacent tissues from both MSI-h and MSS patients) samples. Importantly, *MLH1* transcript levels were significantly lower in the MSI-h group when compared to *both* the MSS and normal tissue groups, whereas MSS samples did not exhibit any significant differences in their *MLH1* transcript levels when compared to the normal group (Fig.3.1a). Notably, gene expression (mRNA) levels of *MSH2* and *MSH6* were not significantly different between MSS and MSI-h subsets (Fig.3.1b, c). Finally, *PMS2* levels were slightly lower in the MSI-h group when compared to the MSS subset: they were, however, higher than the normal sample group (Fig.3.1d). Together, these results demonstrate that downregulation of expression of *MLH1* DNA-MMR repair genes is a highly conserved characteristic of highly microsatellite instable primary human colorectal tumours.

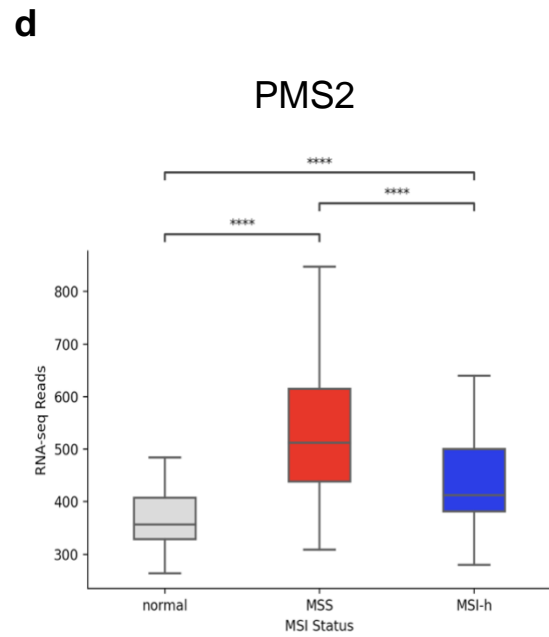
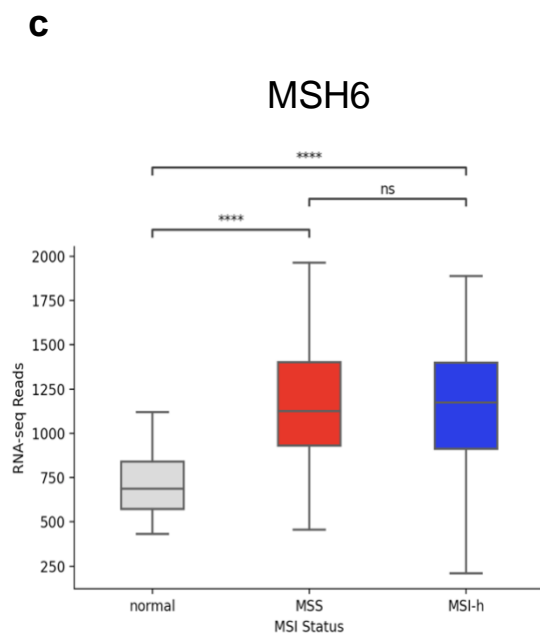
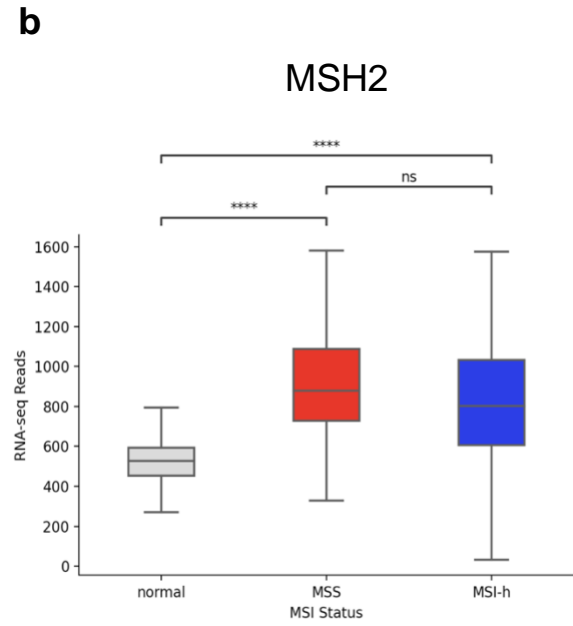
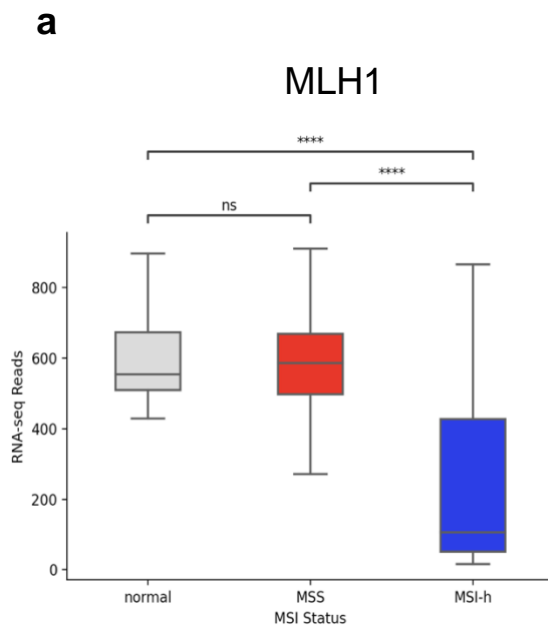
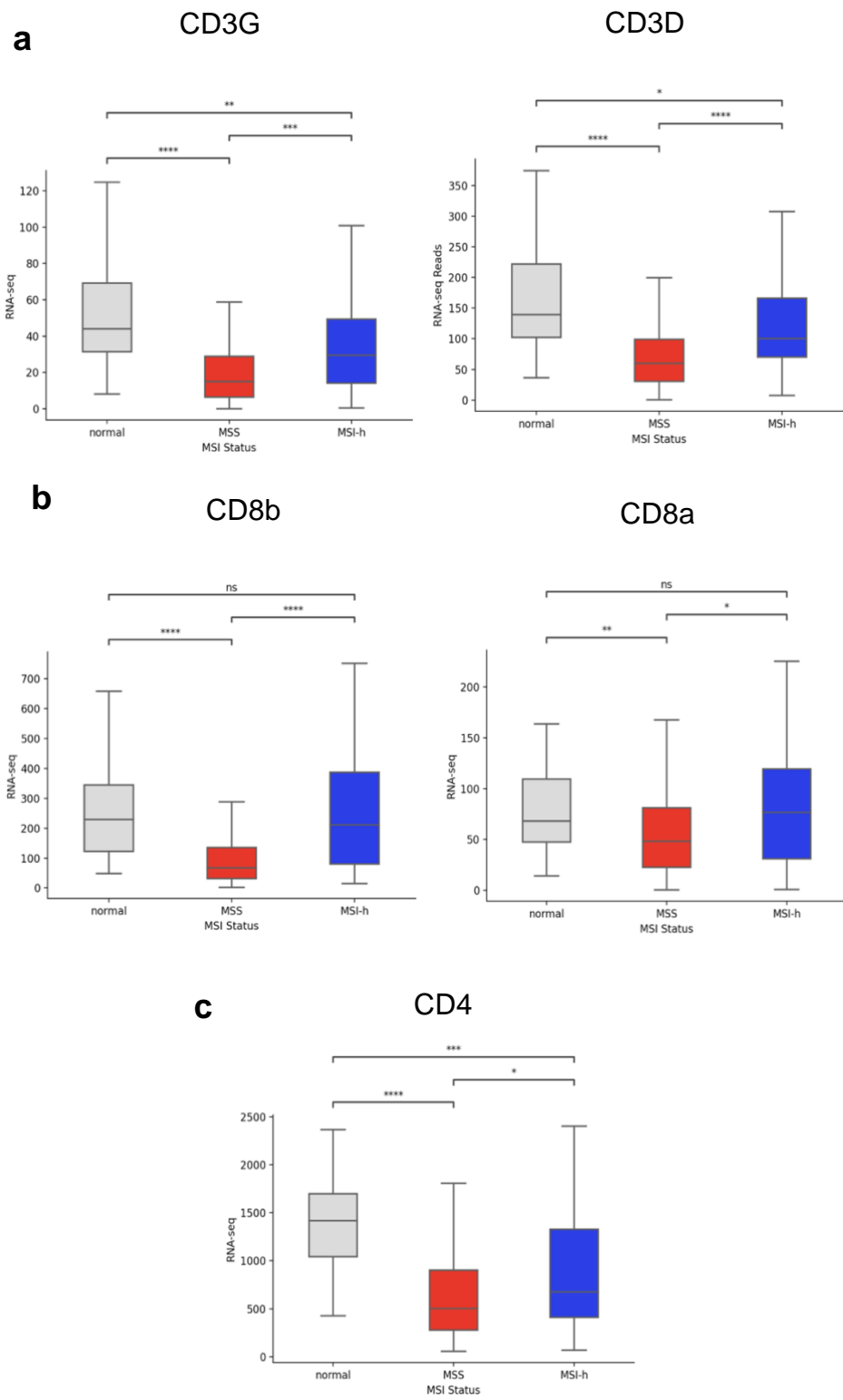


Figure 3.1. MLH1 is downregulated in microsatellite instable human COAD READ tumours.

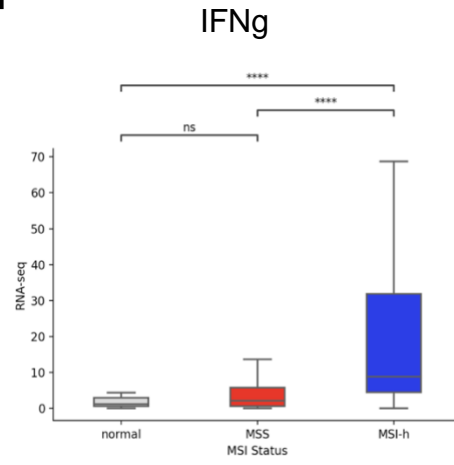
(a) Normalized MLH1, (b) MSH2, (c) MSH6, (d), PMS2 RNA-seq data was obtained from the TCGA database COAD READ dataset and grouped into normal (n=51), MSS (n=257) and MSI-h (n=51) tissues. Statistical analysis was performed by non-parametric Mann-Whitney U test. * $p \leq 0.05$, ** $p \leq 0.01$, *** $p \leq 0.001$, **** $p \leq 0.0001$, ns (not significant).

3.2 MSI-h tumours are associated with higher numbers of T-cells and levels of pro-inflammatory molecules

MSI-h tumours exhibit a high mutational load, which is often associated with an immune-inflamed phenotype. As such, RNAseq levels of mRNAs for genes that characterize T-cells (*CD3G*, *CD3D*), CD8⁺ T-cells (*CD8a*, *CD8b*), CD4⁺ T-cells (*CD4*), pro-inflammatory cytokine interferon gamma (*IFNG*) and cytolytic proteins perforin (*PRFI*) and granzyme B (*GZMB*) were analyzed. I found higher transcript levels of T-cell genes (Fig.3.2a) including those for both CD8⁺ T-cells (Fig.3.2b) and CD4⁺ T-cells (Fig.3.2c) in MSI-h tissues when compared to their microsatellite-stable counterpart. MSI-h tumours also expressed higher levels of mRNA encoding the pro-inflammatory cytokine IFN γ (Fig.3.2d) versus both the MSS and normal samples. Importantly, these highly unstable tumours also exhibit higher levels of mRNAs for cytolysis-associated genes perforin and granzyme B (Fig.3.2e) when compared to both the microsatellite-stable and normal tissues. These data demonstrate that highly unstable MSI-h tumours are both immune infiltrated and inflamed, unlike MSS tumours which lack this immunogenicity. It is also important to note, that when I compared the expression of a number of immune genes in either MSS or MSI-h tumour samples to the expression in normal samples, I observed a decrease in mRNA levels. Tumours have evolved multiple mechanisms in order to limit immune infiltration and evade the immune system.³⁷ For example, one of many immune exclusion mechanisms involves the tumour intrinsic Wnt/beta-catenin pathway.³⁷ This pathway limits T-cell infiltration and promotes immune suppressive cells.³⁷ Tumour cells can also limit production of effector chemokines in order to block effector T-cell recruitment into tumours.³⁷ These immune exclusion mechanisms provide insight into the decrease in immune gene expression observed in tumour samples when compared to normal samples.



d



e

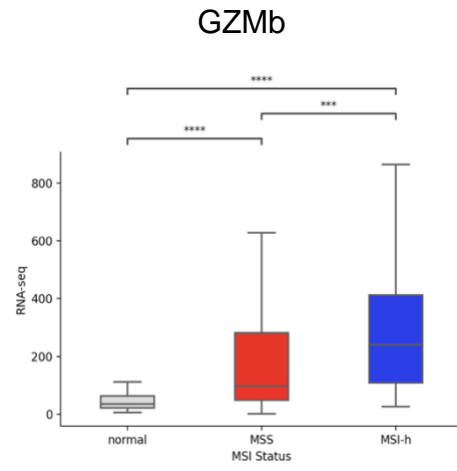
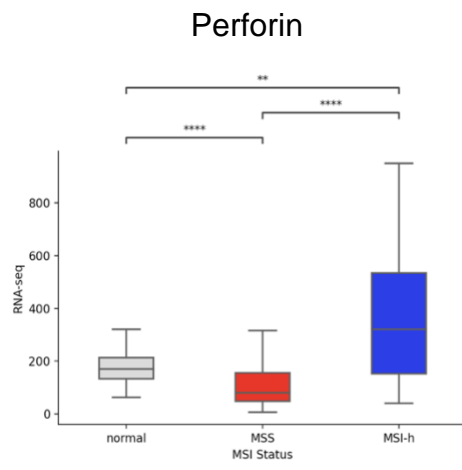


Figure 3.2. MSI-h tumours express higher levels of T-cells marker and proinflammatory genes.

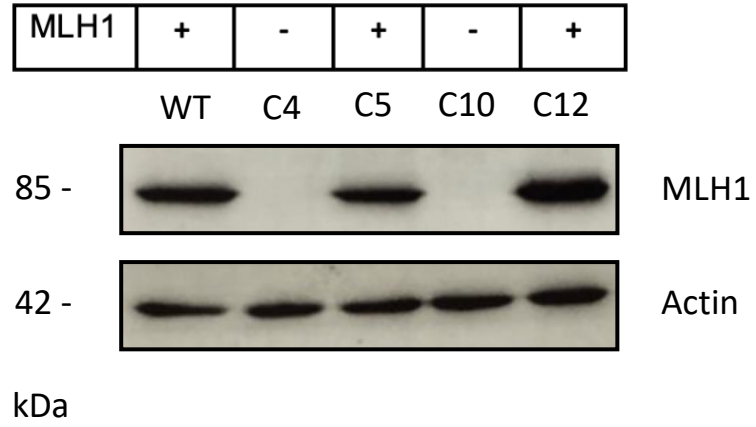
Normalized RNA-seq data for T-cell genes (a) *CD3G*, *CD3D*, (b) *CD8A*, *CD8B* and (c) *CD4* and pro-inflammatory genes (d) *IFNg*, (e) *PRF1* and *GZMB* were obtained from the TCGA database COAD READ dataset and grouped into normal, MSS and MSI-h tissues (n=51, n=257, n=51). Statistical analysis was performed by non-parametric Mann-Whitney U test. * $p \leq 0.05$, ** $p \leq 0.01$, *** $p \leq 0.001$, **** $p \leq 0.0001$, ns (not significant).

3.3 Generating an *MLH1* knock-out mouse neuroblastoma cell line

Neuroblastoma is an immunologically cold tumour that is also refractory to immunotherapy with ICIs³⁵. dMMR tumours, on the other hand, have a high tumour mutational burden and, as seen in Fig.3.2, are immunologically hot. Rene Figueredo, the lab technician in the Koropatnick/Maleki lab, transfected the mouse neuroblastoma cell line neuro-2a with an *MLH1* KO plasmid with the goal of generating an *immunogenic* MMR-deficient neuro-2a cell line for *in vitro* and *in vivo* studies. He then selected multiple clones using FACS sorting specific for GFP fluorescing cells and then compared *MLH1* protein production in the knock-out clones (C4, C5, C10, C12) to *MLH1* produced by the positive control (wild type neuro-2a cells) (Fig.3.3a). Clone 4 did not produce *MLH1* protein, indicated that the *MLH1* gene was successfully knocked-out (Fig.3.3a). This clone was therefore selected as the dMMR clone and will be referred to as the dMMR cell line for the remainder of this thesis. Moreover, clone 12 still produced normal levels of *MLH1* protein, indicating that knock-out was unsuccessful (Fig.3.3a). Clone 12 was therefore established as the control DNA-mismatch repair proficient cell line, along with the parental WT cell line. I will be referring to clone 12 from this point onward as the pMMR cell line.

Moreover, it was important to ensure that both the dMMR and pMMR cell lines had similar baseline proliferation rates *in vitro* before studying their tumour growth *in vivo*. I compared the proliferation rate of the pMMR and dMMR clones and the growth rate as reflected in the fold increase in pMMR cells compared to dMMR cells over 4 days was found not differ significantly (Fig.3.3b).

a



b

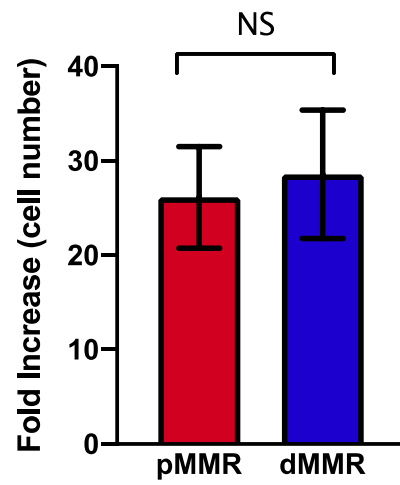


Figure 3.3. Inducing MMR deficiency in neuroblastoma mouse cancer cells and the impact on growth *in vitro*.

(a) Neuro-2a cells were transfected with a CRISPR CAS9 knock-out plasmid specific for the MLH1 gene. Expression of MLH1 in the parental cells and several putative knock-out clones was analyzed by Western Blot. (b) WT neuro-2a cells (pMMR) (n=9) and MLH1 KO neuro-2a cells (dMMR) (n=9) were seeded and counted on day 0 and were counted again on day 4 to analyze the fold increase of each cell line. Statistical analysis was performed by unpaired two-tailed Student's t-test. * $p \leq 0.05$, ** $p \leq 0.01$, *** $p \leq 0.001$, **** $p \leq 0.0001$, NS (not significant). Results are representative of 3 pooled experiments.

3.4 Baseline tumour growth of pMMR and dMMR neuro-2a cells was similar in immunodeficient mice

Previously, I showed that pMMR and dMMR neuro-2a cells have similar baseline proliferation rates *in vitro* (3.3b). In order to test the baseline tumour kinetics of pMMR and dMMR neuro-2a cells *in vivo*, these cells were injected into immunodeficient SHO mice. SHO mice lack both mature B-cells and mature T-cells. Mice bearing pMMR or dMMR tumours were injected subcutaneously at day 0 and left to grow for a 24-day period. I found that baseline tumour kinetics of pMMR and dMMR neuro-2a cells *in vivo* was not significantly different (Fig 3.4).

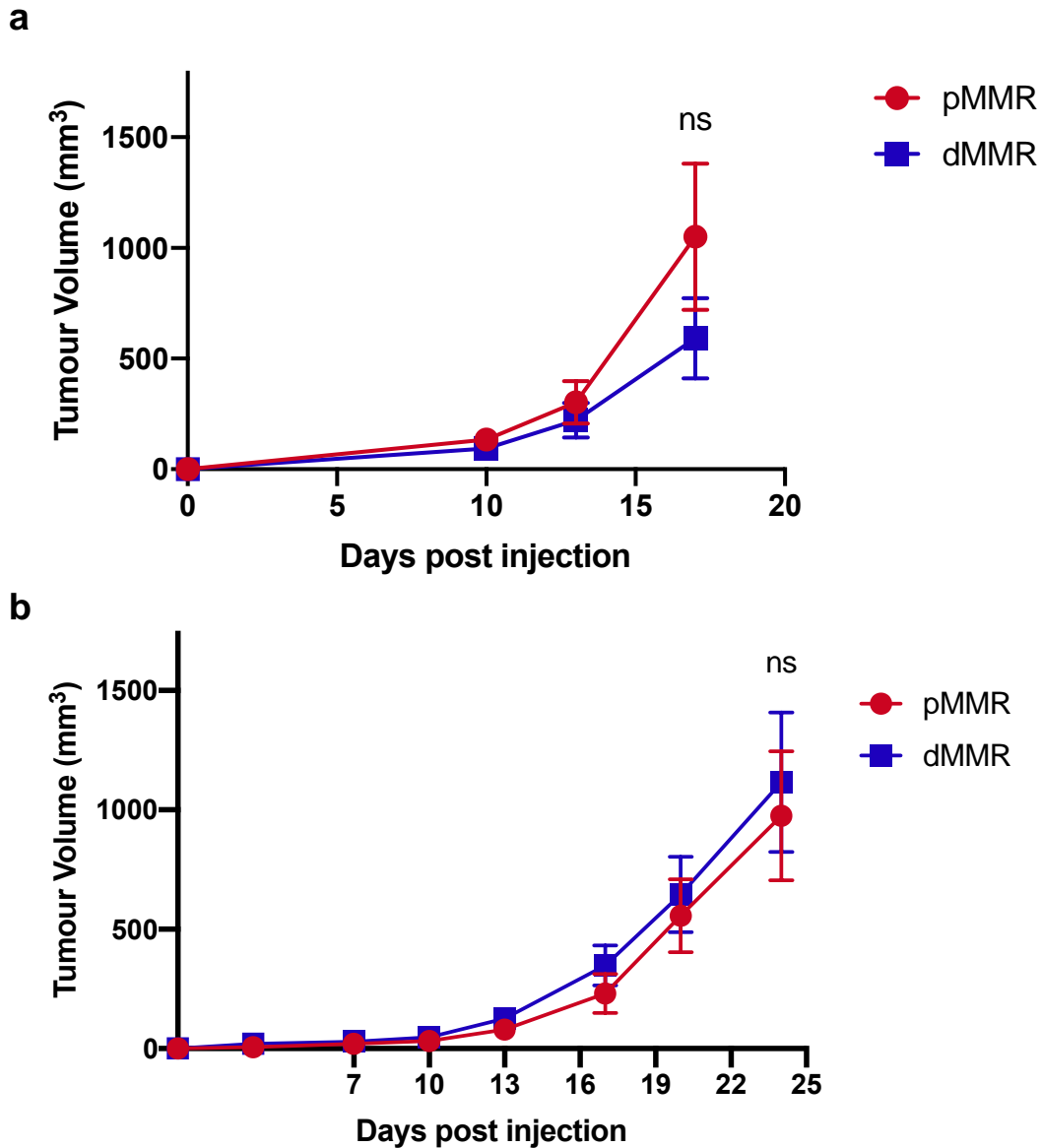


Figure 3.4. Growth of pMMR and dMMR neuro-2a cells in immunodeficient mice was not significantly different.

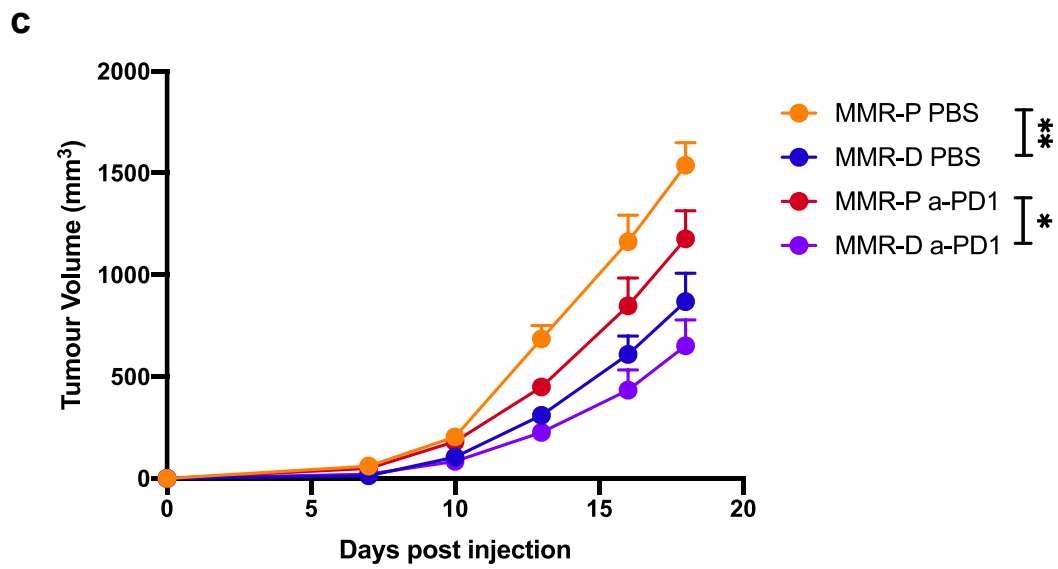
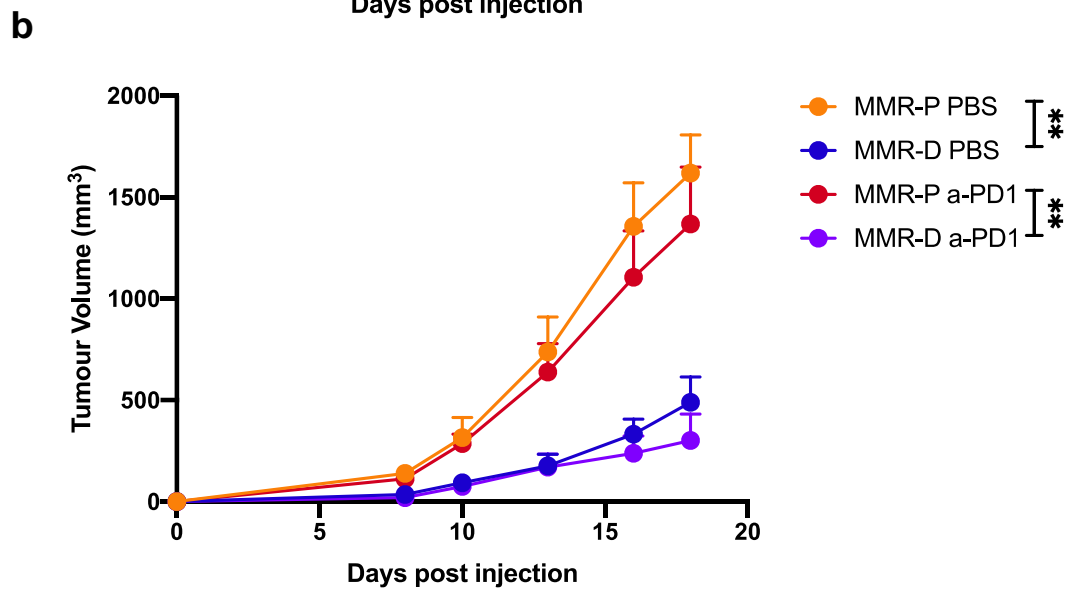
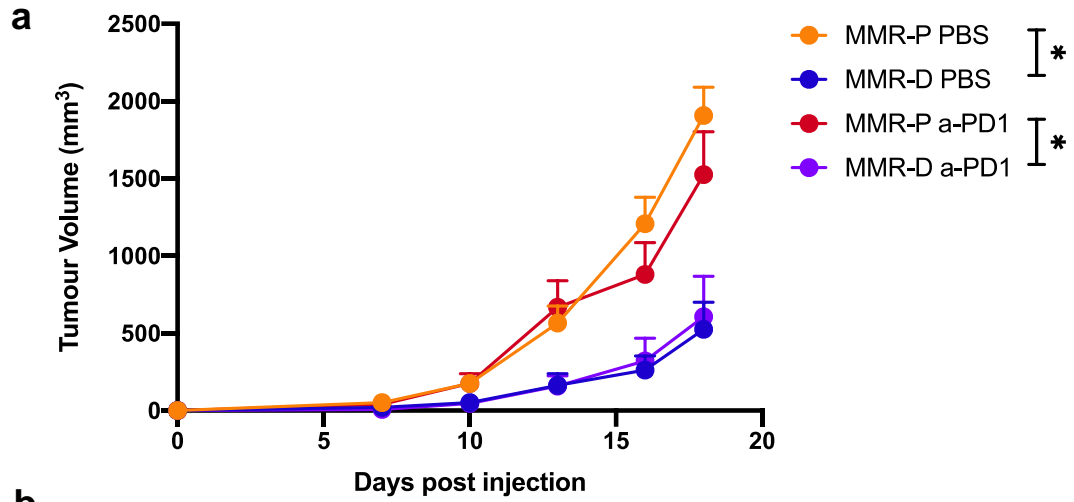
pMMR and dMMR neuro-2a cells were injected subcutaneously into immunodeficient SHO mice and sacrificed when tumours reached $\sim 1400 \text{ mm}^3$ (**a**) $n=5$, $n=5$, (**b**) $n=5$, $n=6$, pMMR and dMMR respectively. Statistical analysis was performed by unpaired two-tailed Student's t-test. * $p \leq 0.05$, ** $p \leq 0.01$, *** $p \leq 0.001$, **** $p \leq 0.0001$, ns (not significant). Results are representative of 2 independent experiments.

3.5 Inducing DNA-MMR deficiency results in an increased anti-tumour response in immunocompetent mice

DNA-mismatch repair deficient tumours have an increased response rate to ICIs. As previously shown (Fig.3.2) this is in large part because these tumours are both immune cell-infiltrated and immune-inflamed. As such, they display high levels of T-cell markers and T-cell activation markers. In order to study the effect of inducing MMR-deficiency in an immunologically cold tumour (neuroblastoma), both pMMR and dMMR cells were injected into immunocompetent A/J mice with a similar MHC background to the neuro-2a cells (H-2^K). Mice were either treated with PBS (control) or an anti-PD1 antibody as described before. Inducing MMR deficiency generated a strong anti-tumour response and significantly hindered tumour growth in immunocompetent mice (Fig.3.5.1a-c). Interestingly, treating with anti-PD1 did not have a statistically significant added benefit in inhibiting tumour growth. This shows that inducing MMR deficiency on its own can trigger an immunogenic rejection of tumours in immune-competent mice. It is important to note that dMMR tumour-bearing mice were only monitored for an 18-day period in this experiment, with corresponding tumour volumes reaching ~300-600mm³. I therefore decided to monitor dMMR tumour growth over a longer period of time (30-day period) in order to study whether treating these highly unstable and potentially immunogenic tumours with ICI would further hinder tumour growth over time (Fig.3.5.1d). Preliminary data shows that inducing dMMR tumours stimulates an initial anti-tumour response. However, after 20 days the majority of dMMR tumour bearing mice not receiving treatment reached the maximally permitted tumour size, whereas most mice receiving the *combination* of MMR induction and anti-PD1 treatment were still well below the ~1400mm³ tumour volume end point (Fig.3.5.1d).

Finally, to study whether starting anti-PD1 treatment earlier could enhance the anti-tumour response of mice bearing dMMR neuro-2a cells, immunocompetent A/J mice were given the ICI treatment starting at day 7 post tumour injection (Fig.3.5.2a, b). Notably, this resulted in the cure of 2 mice bearing dMMR tumours that were treated with α -PD1, and 1 additional mouse exhibiting a significantly reduced level of growth compared to pMMR tumours receiving α -PD1 treatment. (Fig.3.5.2b). However, starting α -PD1 treatment at day

7 did not result in a statistically significant reduction in tumour growth when compared to mice bearing dMMR tumours not receiving α -PD-1 treatment (Fig.3.5.2a, b). It is important to note that these mice were only monitored for an 18-day period in this experiment, with corresponding tumour volumes reaching $\sim 300\text{-}500\text{mm}^3$. In future experiments, I will monitor these mice for a longer period of time to see whether treating dMMR tumour bearing mice with anti-PD1 starting at day 7 has any added benefit in inhibiting tumour growth.



d

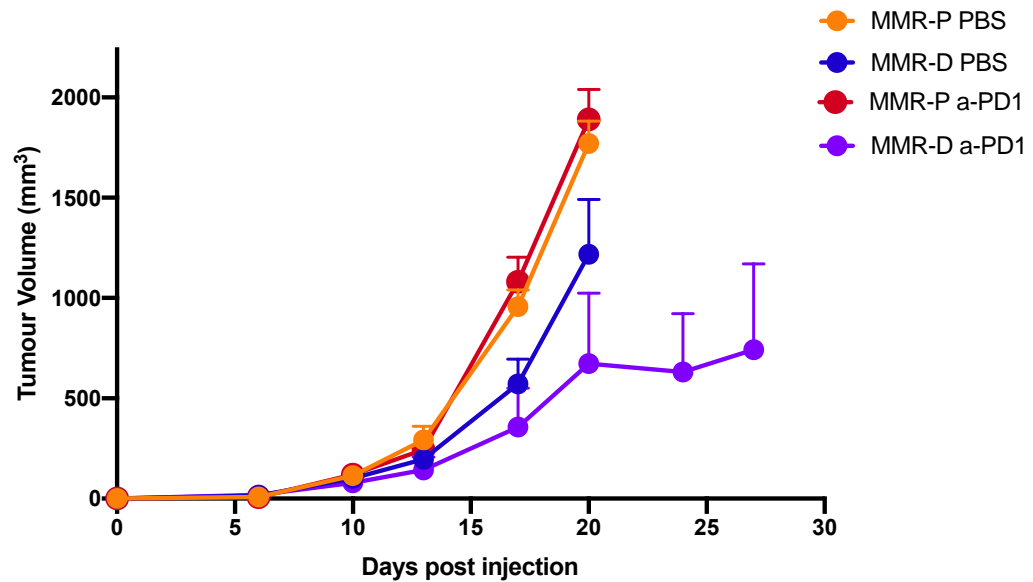
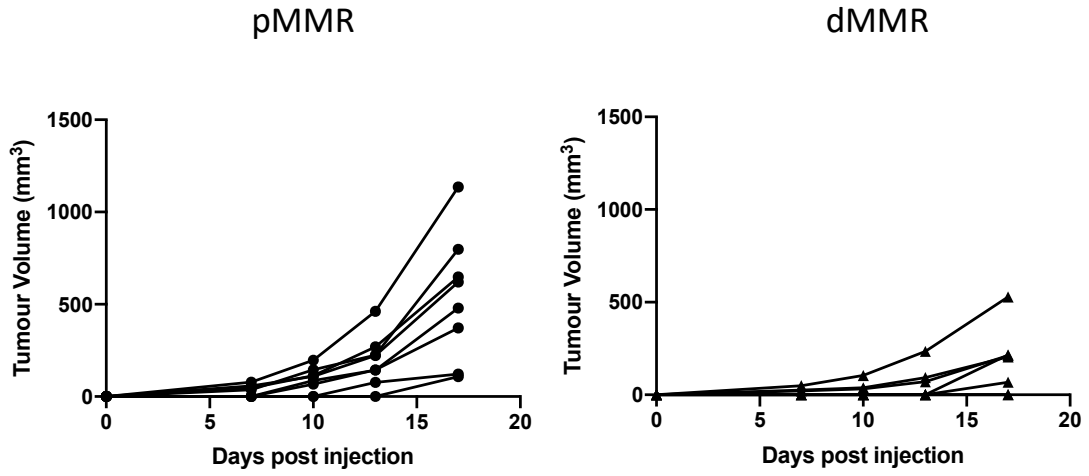


Figure 3.5.1. **Inducing tumour MMR deficiency results in increased anti-tumour response.**

pMMR and dMMR neuro-2a cells were injected subcutaneously into A/J mice and injected i.p at days 10, 13 and 16 with the control PBS or the anti-PD1 treatment (250ug/100ul) and were sacrificed at day 18. Experiments were conducted a total of 3 times. Mice were grouped into pMMR no treatment, dMMR no treatment, pMMR treatment and dMMR treatment groups, (a) n=5, n=4, n=5, n=4, (b) n=5, n=5, n=6, n=6 respectively, (c) n=5, n=5, n=6, n=6, (d) n=5, n=6, n=5, n=6 respectively. Statistical analysis was performed by unpaired two-tailed Student's t-test. * $p \leq 0.05$, ** $p \leq 0.01$, *** $p \leq 0.001$, **** $p \leq 0.0001$, ns (not significant).

a

No treatment



b

Anti-PD1 Treatment

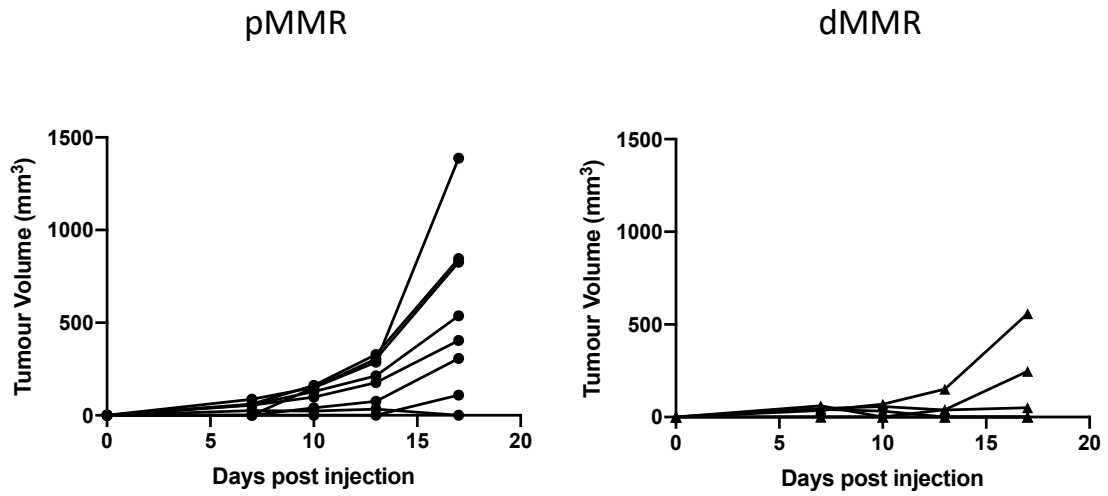


Figure 3.5.2. A combination of inducing MMR-deficiency and treating with anti-PD1 immune checkpoint blockade starting at day 7 can cure a subset of mice.

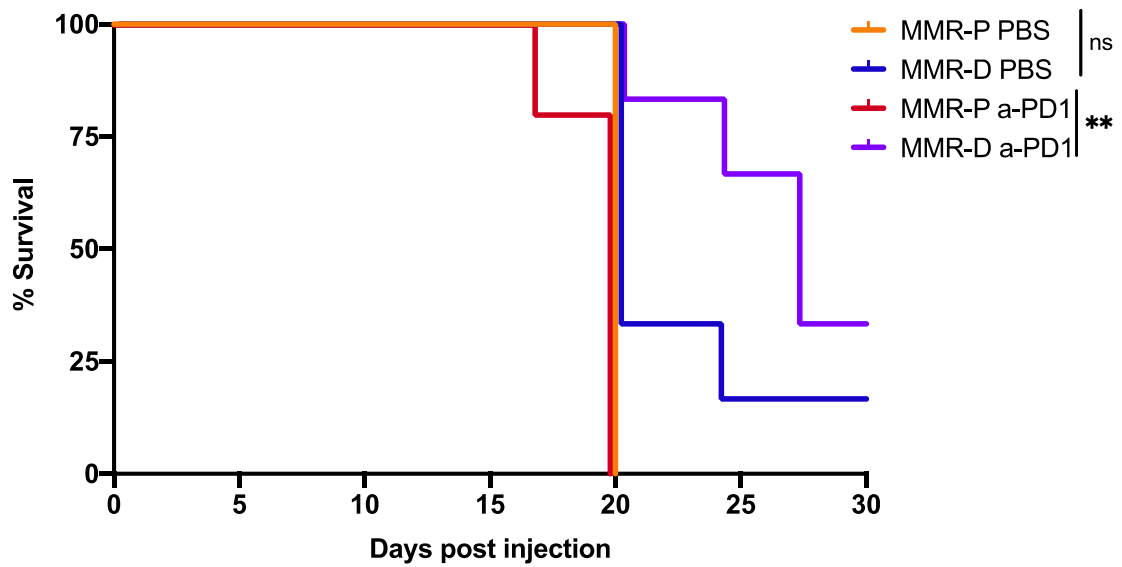
Wild type and dMMR neuro-2a cells were injected subcutaneously into A/J mice and injected i.p at days 7, 10 and 13 **(a)** with the control PBS (n=8, n=7), **(b)** and the treatment anti-PD1 (250ug/100ul) (n=8, n=6), respectively. Results are representative of 2 pooled experiments.

3.6 Combination of inducing MMR-deficiency and treating with anti-PD1 prolongs survival of immune competent mice

DNA mismatch repair-deficient tumours respond favorably to immune checkpoint inhibitors. I therefore wanted to study whether combining MMR-induction of an immunologically cold tumour (neuroblastoma) along with treating with anti-PD1 could prolong survival of immune-competent mice. pMMR and dMMR cells were injected into A/J mice and treated at days 10, 13 and 16 with either the PBS (control) or an anti-PD1 antibody. Moreover, mice were sacrificed when their tumour volume reached $\sim 1400\text{mm}^3$. Notably, there was no significant survival advantage to inducing MMR-deficiency on its own (Fig.3.6a). However, the combination of inducing MMR-deficiency along with treating with anti-PD1 resulted in a significant increase in survival when compared to pMMR bearing mice receiving ICI treatment (Fig.3.6a). This highlights the potential utility of inducing MMR-deficiency to render cold tumours immunogenic and then treating with immune checkpoint blockade.

I also studied the impact of inducing MMR-deficiency on the overall health of mice by analyzing their body weight over time (Fig.3.6b). Mice bearing dMMR-deficient tumours displayed no significant decreases of body weight over time, similarly to their pMMR counterparts (Fig.3.6b).

a



b

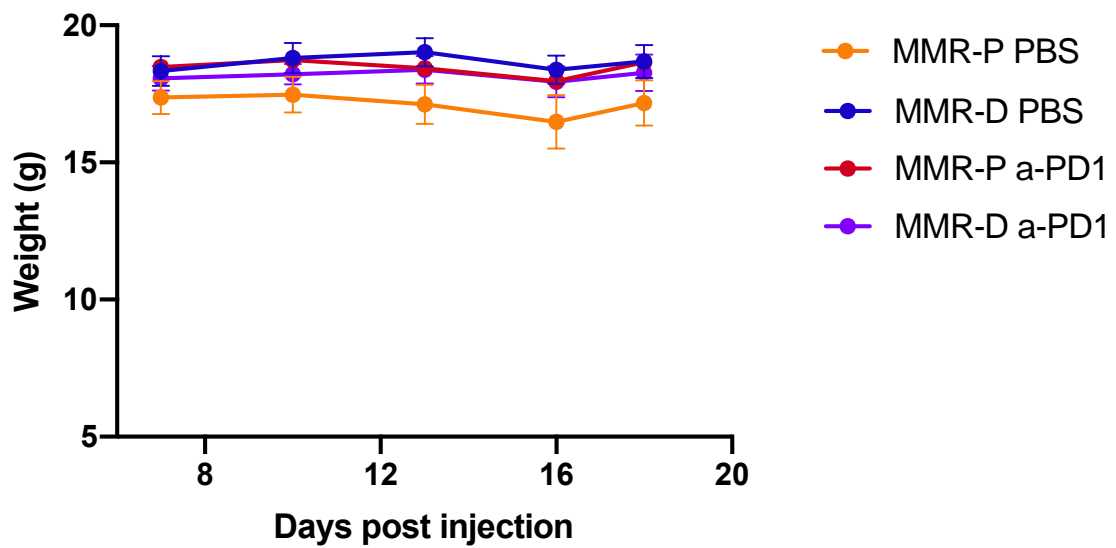


Figure 3.6. Inducing tumour MMR deficiency and treating with anti-PD1 increases survival of mice.

pMMR and dMMR neuro-2a cells were injected subcutaneously into A/J mice and injected i.p at days 10, 13 and 16 with the control PBS and the treatment anti-PD1 (250ug/100ul) and were sacrificed as mice reached $\sim 1400 \text{ mm}^3$. Mice were grouped into pMMR no treatment, dMMR no treatment, pMMR treatment and dMMR treatment groups, (a) n=5, n=6, n=5, n=6. Statistical analysis was performed using the two-sided log-rank (Mantel-Cox) test. * $p \leq 0.05$, ** $p \leq 0.01$, *** $p \leq 0.001$, **** $p \leq 0.0001$, ns (not significant).

3.7 DNA-mismatch repair deficient tumours express higher levels of MHC-I *in vitro*

MHC-I is an antigen-presenting molecule critical for presenting peptides to T-cells and is, therefore, an essential component of immunosurveillance¹⁰. Due to the heightened anti-tumour immunity against dMMR tumours, I speculated that an increase in MHC-I expression on dMMR cells may contribute to immunogenicity. In order to analyze the MHC-I expression on pMMR and dMMR tumours, neuro-2a cells were grown in culture at 3 different time points (8, 9 and 10 weeks). pMMR and dMMR cells were first grown in culture for 8 weeks. Cells were then stained for MHC-I and analyzed by flow cytometry. dMMR cells had a higher mean fluorescence intensity (MFI) of MHC-I when compared to mismatch repair proficient neuro-2a cells (Fig 3.7a). These cells were left to grow an additional week in culture and MHC-I levels analyzed at the 9-week time point (Fig 3.7b). dMMR tumours expressed a higher MFI of MHC-I than their pMMR neuro-2a counterparts at this time point (Fig 3.7b). Finally, cells were left to grow for 10 weeks *in vitro* and dMMR cells still expressed a higher MFI of MHC-I than mismatch repair-proficient neuro-2a cells (Fig 3.7c).

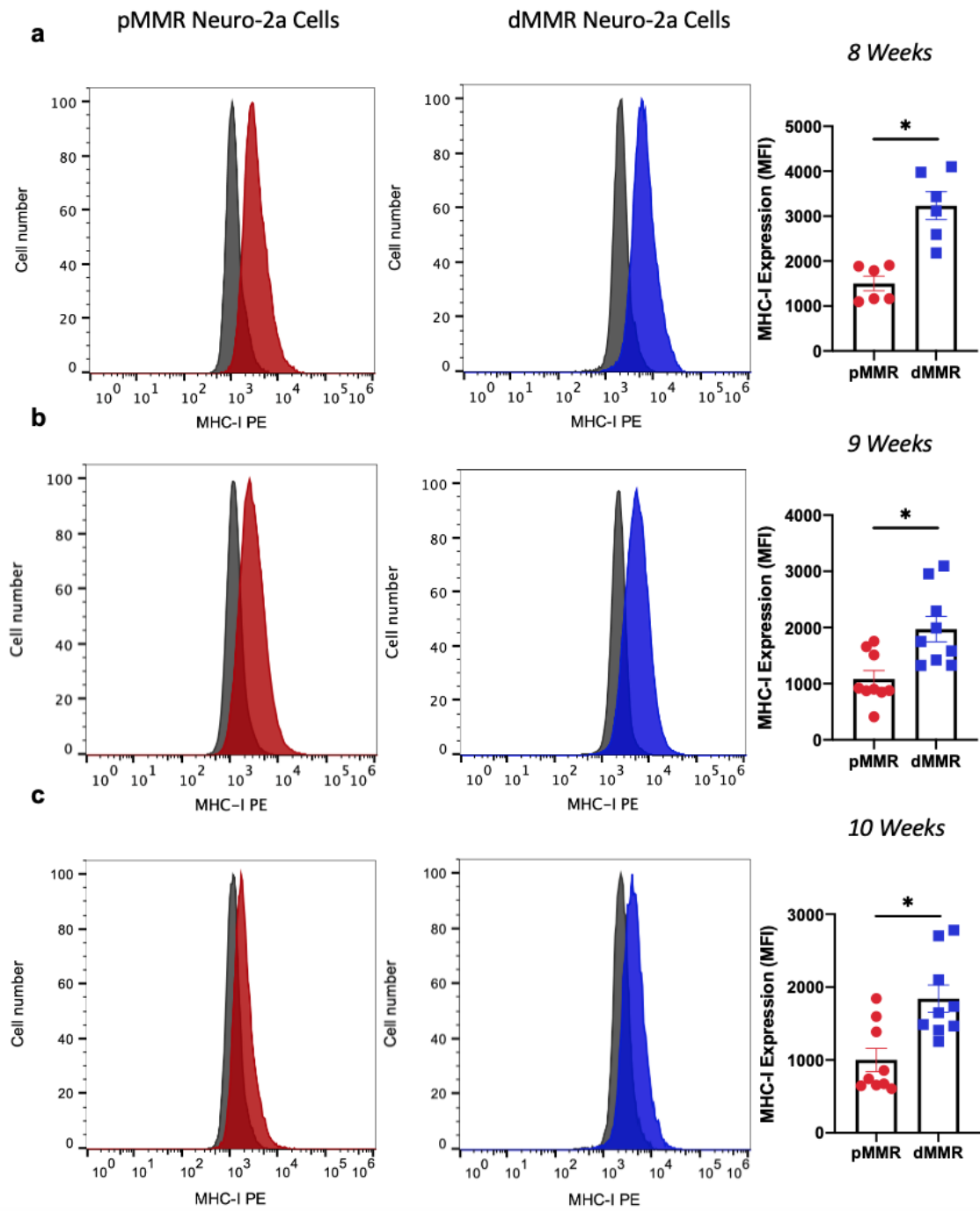


Figure 3.7. Inducing MMR-deficiency enhances MHC-I expression in neuro-2a cells. pMMR and dMMR neuro-2a cells were grown for (a) 8 weeks (b) 9 weeks and (c) 10 weeks *in vitro* and the mean fluorescence intensity of MHC-I was quantified for 3 replicates each (n=3). MFI values are representative of the median fluorescence intensity. Grey histograms display unstained neuro-2a MHC-I expression and the red and blue histograms show stained pMMR and dMMR MHC-I expression, respectively. Statistical analysis was performed by unpaired two-tailed Student's t-test. * $p \leq 0.05$, ** $p \leq 0.01$, *** $p \leq 0.001$, **** $p \leq 0.0001$, ns (not significant). Results are representative of 2 (a) and 3 (b), (c), pooled experiments.

3.8 Colorectal cancer patients with highly microsatellite instable tumours express higher levels of MHC-I related genes

I showed that inducing dMMR *in vitro* results in a higher mean fluorescence intensity (MFI) of MHC-I (Fig.3.7). We, therefore, set out to study whether such differences in MHC-I levels existed in highly microsatellite-*instable* (MSI-h) human tumours when compared to microsatellite-*stable* (MSS) samples using the COAD READ cohort of the TCGA database. I found no differences in the gene expression (mRNA) levels of *HLA-A* and *HLA-B* between the MSS and MSI-h tumour samples (Fig.3.8a, b). However, I found that *HLA-C* transcript levels were significantly higher in MSI-h samples when compared to MSS samples (Fig.3.8c). Importantly, I also found a significant increase in *B2M* (which encodes the β_2 microglobulin protein, a component of the MHC-I complex) gene transcript levels in MSI-h tumour tissues when compared to MSS tumour tissues (Fig.3.8d). These findings demonstrate that certain MHC-I-associated gene transcript levels are upregulated in MSI-h samples when compared to MSS samples. This further elucidates the increased immunogenicity of highly microsatellite-*instable* tumours when compared to the less immunogenic microsatellite-*stable* tumours. In order to better understand MHC-I expression in the context of an anti-tumour response, I originally set out to analyze MHC-I expression of cells cultured from murine neuroblastoma tumours grown *in vivo*. However, I ran into technical challenges as I could not acquire a GD2 (marker specific for neuroblastoma cells) specific antibody to analyze MHC-I expression exclusively on tumour cells.

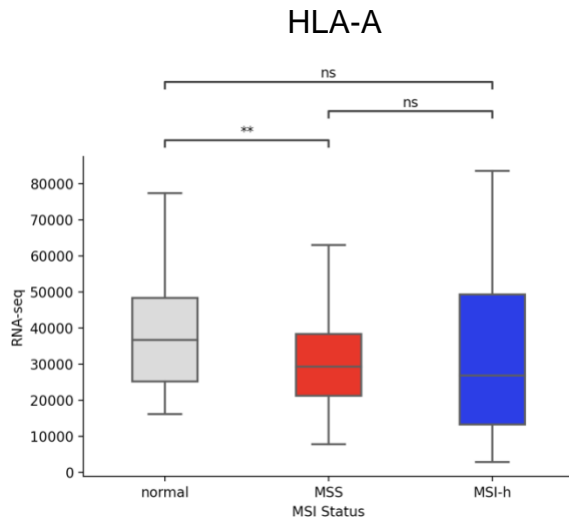
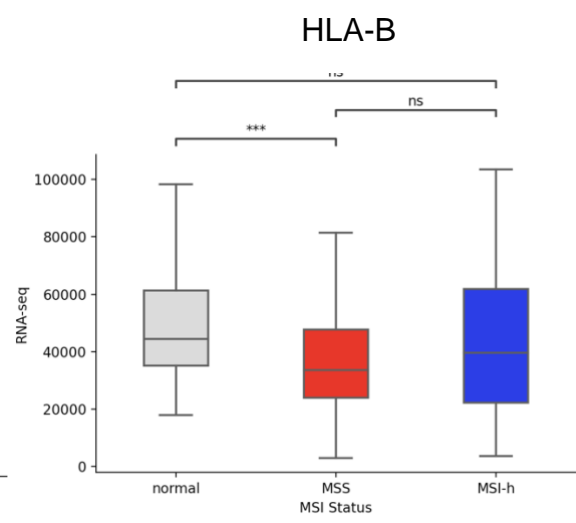
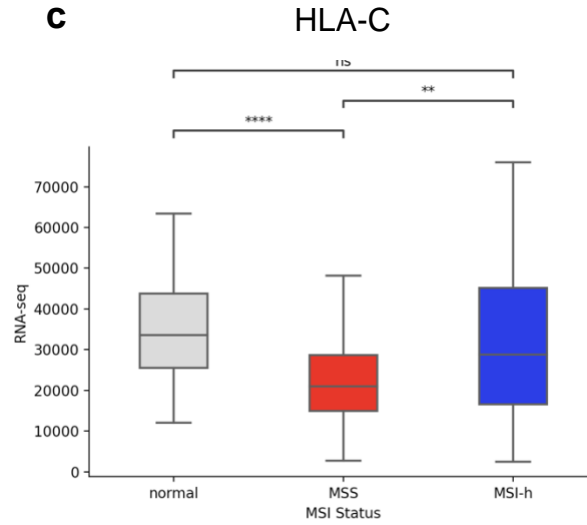
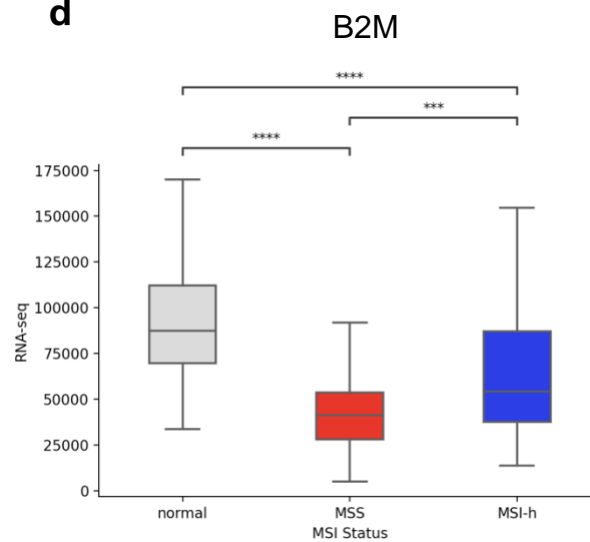
a**b****c****d**

Figure 3.8. MSI-h tumours express higher levels of MHC-I genes.

Normalized RNA-seq data for MHC-I genes *HLA-A*, *HLA-B*, *HLA-C* and *B2M* was obtained from the TCGA database COAD READ dataset and grouped into normal, MSS and MSI-h tissues (n=51, n=257, n=51). * $p \leq 0.05$, ** $p \leq 0.01$, *** $p \leq 0.001$, **** $p \leq 0.0001$, ns (not significant).

3.9 Effect of inducing DNA-MMR repair in neuro-2a cells on PD-L1 expression

I previously showed that inducing MMR-deficiency in neuro-2a cells results in an increase in MHC-I expression (Fig.3.7). I next studied whether inducing such deficiency affects the expression of PD-L1 on neuro-2a cells. PD-L1 is a marker that mediates immunosuppression and tumours that express PD-L1 are more responsive to immune checkpoint inhibitor treatment. Previous studies have shown the highly microsatellite instable tumours (MSI-h), which respond well to ICI, express higher levels of PD-L1 when compared to their microsatellite stable (MSS) counterparts³⁸. I again used the TCGA COAD READ RNA-seq data to confirm this. I found that patients with MSI-h tumours expressed higher levels of PD-L1 when compared to both MSS samples and normal samples (Fig.3.9.1).

I then studied the effect of inducing MMR-deficiency on the expression of PD-L1 on neuro-2a cells *in vitro*. pMMR and dMMR tumours, neuro-2a cells were grown in culture at 3 different time points (8, 9 and 10 weeks). I found that at 8 weeks, there was no significant difference in PD-L1 expression between pMMR and dMMR neuro-2a cells (Fig.3.9.2a). After 9 weeks and 10 weeks in culture, MMR-deficient neuro-2a cells had significantly higher levels of PD-L1 protein compared to MMR-proficient neuro-2a cells (Fig.3.9.2b, c). These findings support the observation of higher PD-L1 protein levels in MSI-h tumours in patients²⁴. More specifically, our results demonstrate an increase in PD-L1 protein level after MMR deficiency is induced *in vitro*. This model, therefore, does not include immune system pressures and therefore there may be another mechanistic reason for upregulation of these molecules.

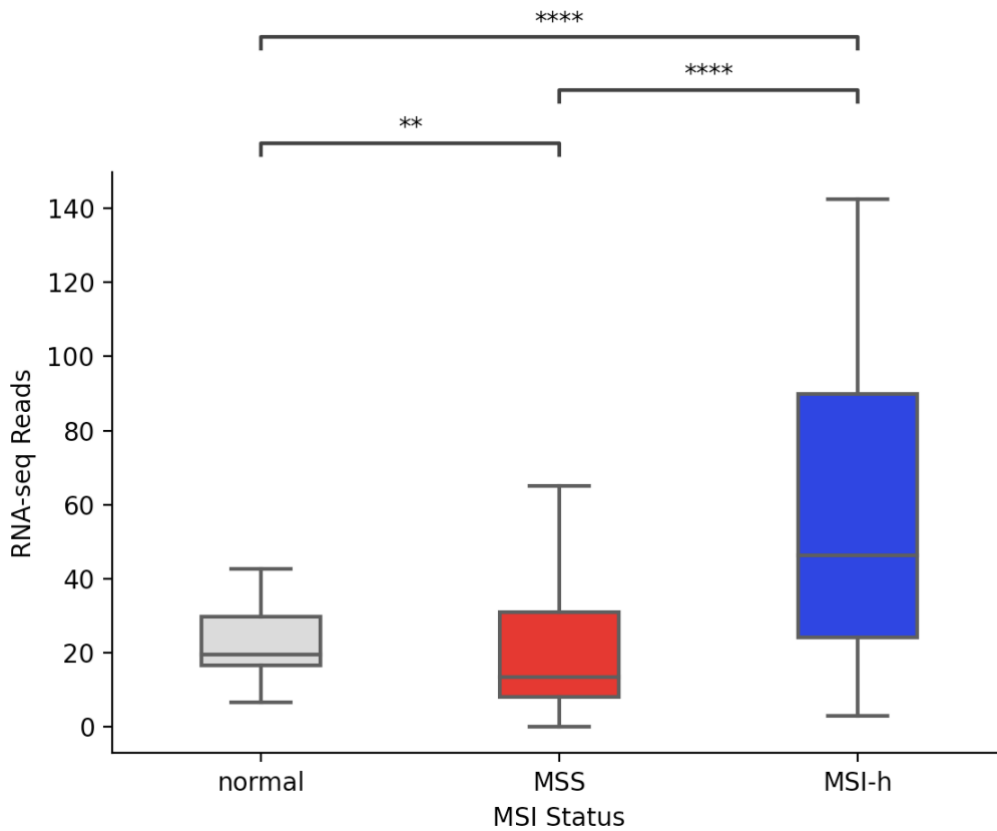


Figure 3.9.1 MSI-h colorectal tumours express higher levels of PD-L1 mRNA.

Normalized RNA-seq data for CD274 (PD-L1) was obtained from the TCGA database COAD READ dataset and grouped into normal, MSS and MSI-h tissues (n=51, n=257, n=51). * $p \leq 0.05$, ** $p \leq 0.01$, *** $p \leq 0.001$, **** $p \leq 0.0001$, ns (not significant).

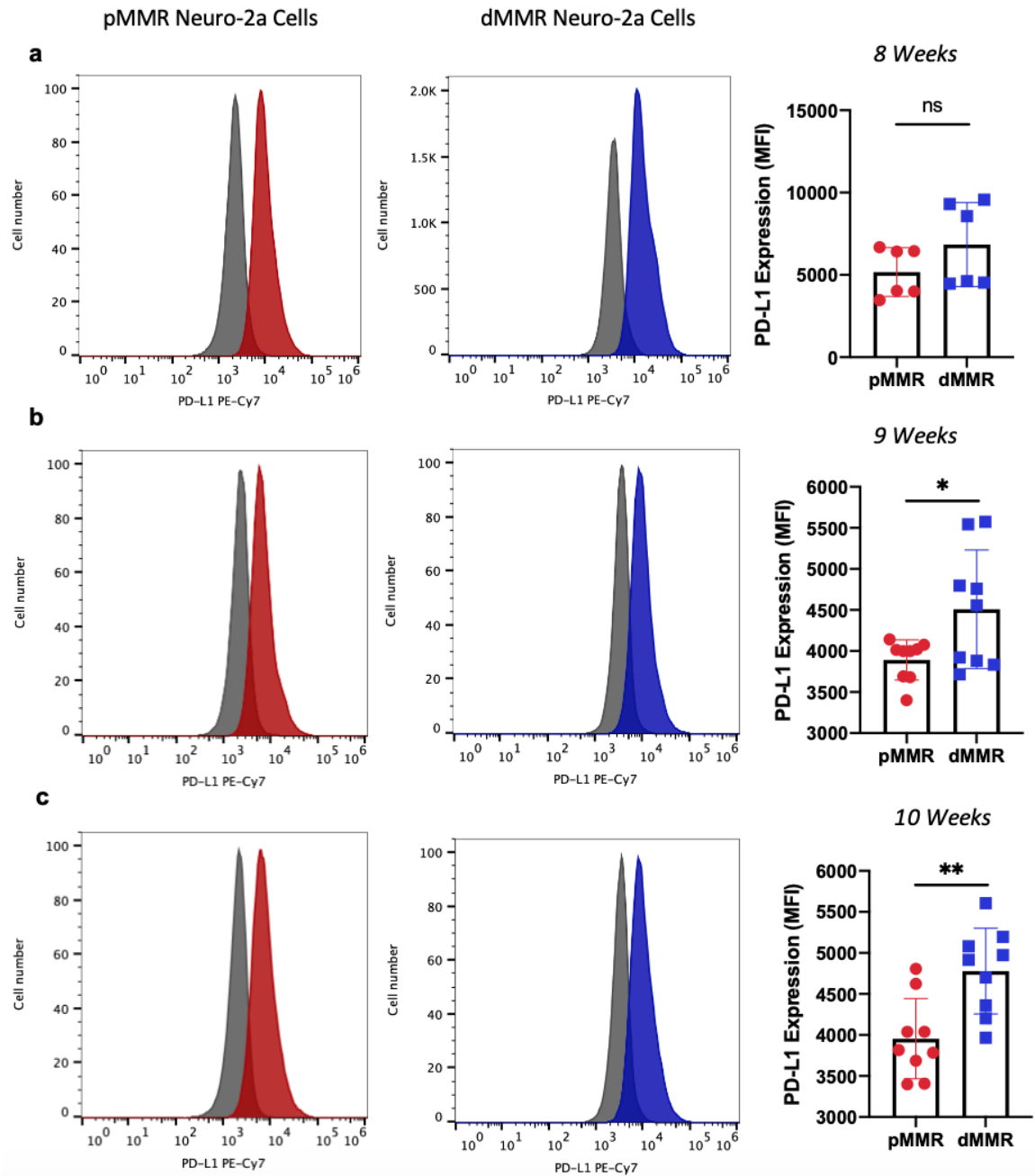


Figure 3.9.2 Effect of inducing MMR-deficiency on PD-L1 expression.

pMMR and dMMR neuro-2a cells were grown for (a) 8 weeks (b) 9 weeks and (c) 10 weeks *in vitro* and the mean fluorescence intensity of PD-L1 was quantified for 3 replicates each (n=3). MFI values are representative of the median fluorescence intensity. Grey histograms display unstained neuro-2a MHC-I expression and the red and blue histograms show stained pMMR and dMMR MHC-I expression, respectively. Statistical analysis was performed by unpaired two-tailed Student's t-test. * $p \leq 0.05$, ** $p \leq 0.01$, *** $p \leq 0.001$, **** $p \leq 0.0001$, ns (not significant). Results are representative of 2 (a) and 3 (b), (c), pooled experiments.

3.10 Effect of inducing MMR-deficiency and treating with anti-PD1 on T-cell infiltration of the tumour-draining lymph nodes

I previously showed that inducing MMR-deficiency elicits an anti-tumour response that hinders tumour growth (Fig.3.5.1). Moreover, MMR-deficient tumours are often highly infiltrated with T-cells. I therefore wanted to explore whether inducing MMR-deficiency and treating with anti-PD1 affected T-cell infiltration into tumour-draining lymph nodes. I injected mice with either pMMR or dMMR neuro-2a tumour cells and treated tumour-bearing mice with anti-PD1 at days 10, 13 and 16. Mice were then sacrificed on day 18 and the tumour-draining lymph nodes from each group were pooled together. Cells isolated from the lymph node were stained for T-cell markers and analyzed using multicolour flow cytometry. My preliminary results show that dMMR tumours treated with anti-PD1 had higher infiltration of T-cells (Fig.3.10). However, it is important to note that these results are representative of a single experiment and that this experiment needs to be repeated with additional control groups not treated with anti-PD1 antibody.

Tumour draining lymph nodes - α PD-1 Treatment

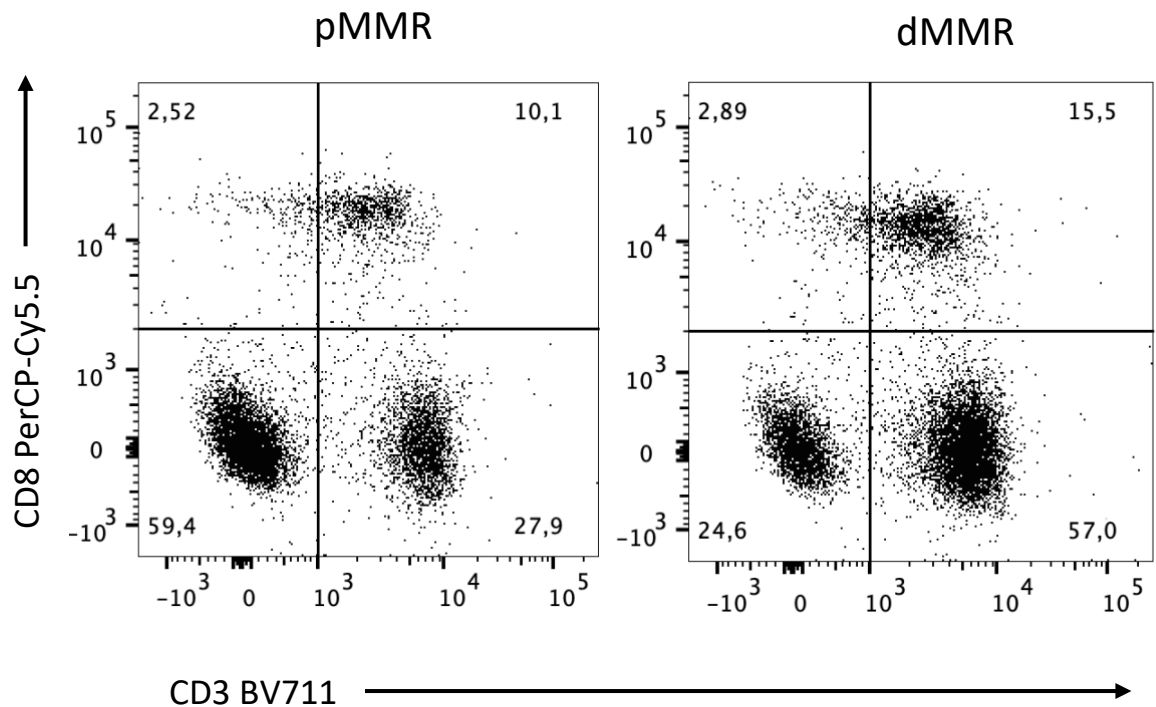


Figure 3.10. **Inducing MMR-deficiency enhances T-cell recruitment to tumour draining lymph nodes in response to anti-PD1 treatment.**

pMMR and dMMR neuro-2a cells were injected subcutaneously into A/J mice and treated with anti-PD1 at days 10, 13 and 16. These cells were gated as a percentage of all live single cells. Pooled lymph nodes were harvested, and T-cell populations were analyzed by flow cytometry.

3.11 T-cell infiltration into tumours in response to dMMR induction and anti-PD1 treatment

I have shown that inducing MMR deficiency results in an increased anti-tumour response (Fig.3.5). Moreover, dMMR tumours show increased T-cell infiltration (Fig.3.2). I therefore injected mice with either dMMR or pMMR neuro-2a cells and treated with either PBS or anti-PD1 antibody at days 10, 13 and 16. Mice were sacrificed at day 18 and tumours were pooled together and stained for T-cell markers, analyzed using multicolour flow cytometry. This experiment was conducted a total of 3 times (5-6 mice in each group), with representative results from each separate experiment presented in the results below. Note that each experiment will be represented as follows: experiment #1, experiment #2, experiment #3.

In the first and third experiments, I found that dMMR tumours had higher percentages of CD3⁺ cells than pMMR tumours in both the control (PBS treatment) and anti-PD1 treatment groups (Fig.3.11a, c). In the second experiment I found that dMMR tumours had higher T-cell infiltration than pMMR tumours in the non-treatment PBS group. However, in the anti-PD1 treated mice, dMMR tumours did not have significantly higher levels of T-cells when compared to pMMR tumours (Fig.3.11b). These results illustrate a trend of higher T-cell levels in dMMR induced tumours when compared to pMMR tumours. This may suggest that inducing MMR deficiency is stimulating an increased T-cell response into neuroblastoma tumours.

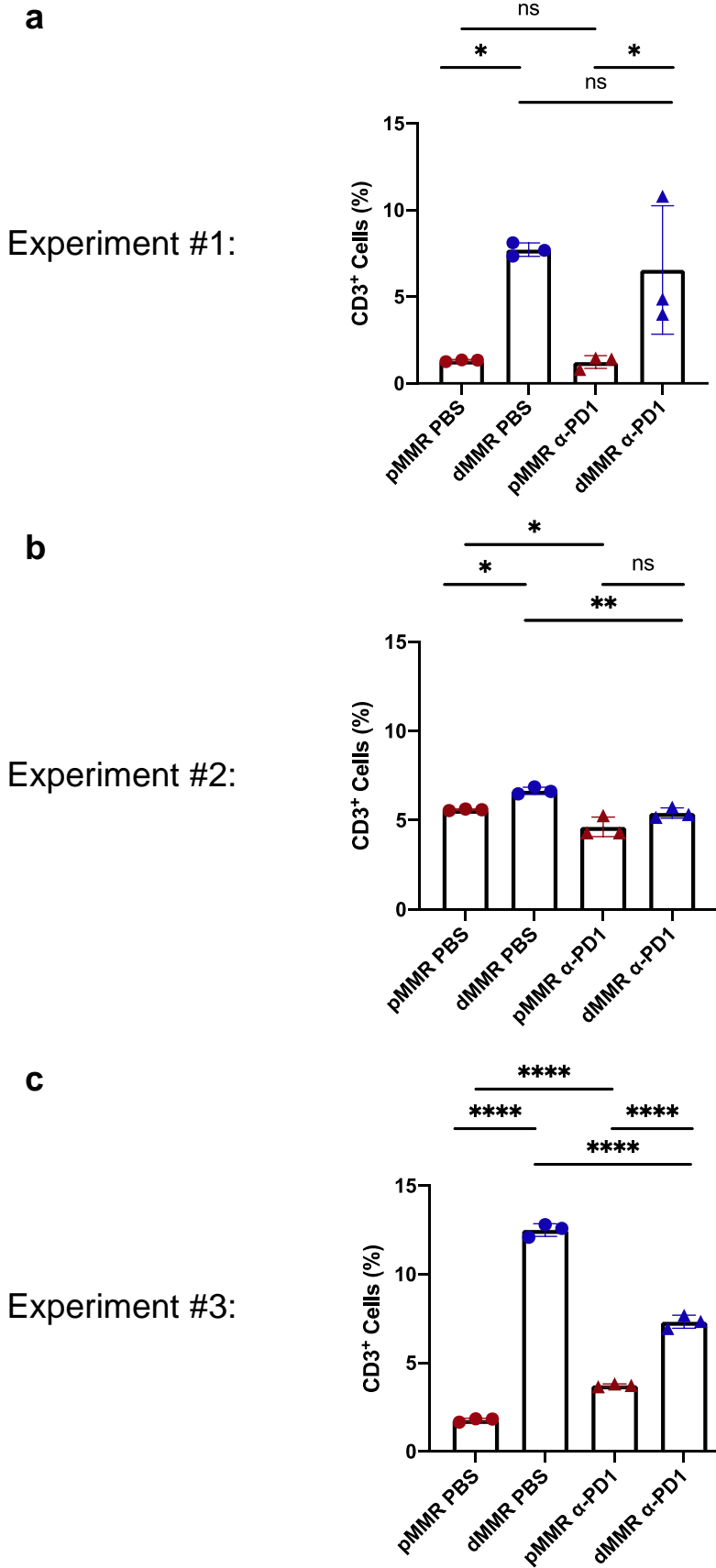


Figure 3.11. Effect of inducing MMR-deficiency on T-cell infiltration of mouse neuroblastoma tumours.

pMMR and dMMR neuro-2a cells were injected subcutaneously into A/J mice and injected i.p at days 10, 13 and 16 with the control PBS and the treatment anti-PD1 (250ug/100ul) and were sacrificed at day 18. Tumours from each treatment group were pooled together. Cells from the tumour single cell suspension were stained with a live/dead dye and live, singlet, lymphocytes were gated. Cells are presented as a percentage of live cells. Results are representative of 3 independent experiments. Mice were grouped into pMMR no treatment, dMMR no treatment, pMMR treatment and dMMR treatment groups, **(a)** n=5, n=4, n=5, n=4 **(b)** n=5, n=5, n=6, n=6, **(c)** n=5, n=5, n=6, n=6 respectively. These cells were gated as a percentage of all live single cells. Data represents technical replicates. Statistical analysis was performed using one-way ANOVA. * $p \leq 0.05$, ** $p \leq 0.01$, *** $p \leq 0.001$, **** $p \leq 0.0001$, ns (not significant).

3.12 CD8⁺ T-cell infiltration into tumours in response to dMMR induction and anti-PD1 treatment

Cytotoxic T-cells play an essential role in the anti-tumour immune response. I therefore studied the effect of inducing dMMR on the stimulation of CD8⁺ T-cells in mouse neuroblastoma tumours with the same experimental setup as previously described (3.11). This experiment was conducted a total of 3 times (with 5-6 mice in each group), with representative results from each separate experiment presented in the results below. Note that each experiment will be represented as follows: experiment #1, experiment #2, experiment #3.

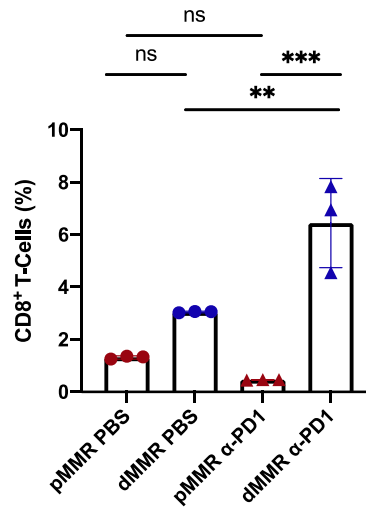
In my first experiment, I observed that tumours with induced MMR deficiency had increased CD8⁺ T-cell infiltration compared to pMMR tumours (Fig.3.12a). Moreover, dMMR tumours in the anti-PD-1 treatment groups also had higher levels of CD8⁺ T-cells when compared to pMMR tumours from the anti-PD1 treatment group (Fig.3.12a).

The second and third experiments yielded similar results to the first. Specifically, dMMR tumours again displayed an increased CD8⁺ T-cell infiltration compared to pMMR tumours (Fig.3.12b, c). The same trends were observed in the anti-PD1 treatment groups (Fig.3.12b, c).

These results suggest that inducing dMMR in neuroblastoma tumours may stimulate an increase in CD8⁺ T-cell infiltration into these immunologically cold tumours.

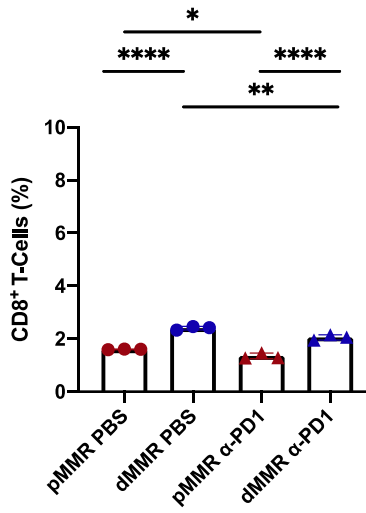
a

Experiment #1:



b

Experiment #2:



c

Experiment #3:

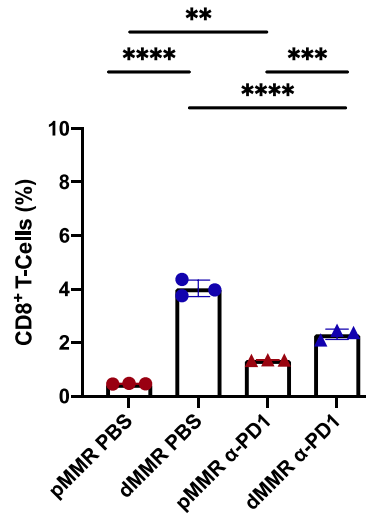


Figure 3.12. Effect of inducing MMR-deficiency on CD8⁺ T-cell infiltration into mouse neuroblastoma tumours.

pMMR and dMMR neuro-2a cells were injected subcutaneously into A/J mice and injected i.p at days 10, 13 and 16 with the control PBS and the treatment anti-PD1 (250ug/100ul) and were sacrificed at day 18. Tumours from each treatment group were pooled together. Cells from the tumour single cell suspension were stained with a live/dead dye and live, singlet, lymphocytes were gated. Cells are presented as a percentage CD3⁺ cells. Results are representative of 3 independent experiments. Mice were grouped into pMMR no treatment, dMMR no treatment, pMMR treatment and dMMR treatment groups, **(a)** n=5, n=4, n=5, n=4 **(b)** n=5, n=5, n=6, n=6, **(c)** n=5, n=5, n=6, n=6 respectively. These cells were gated as a percentage of all live single cells. Data represents technical replicates. Statistical analysis was performed using one-way Anova. * $p \leq 0.05$, ** $p \leq 0.01$, *** $p \leq 0.001$, **** $p \leq 0.0001$, ns (not significant).

3.13 The effect of inducing MMR deficiency and treating with anti-PD1 on T-cell activation and exhaustion

I previously showed that dMMR tumours are highly infiltrated with T-cells and show signs of immune activation (Fig 3.2). I therefore wanted to study whether inducing dMMR in a genomically-stable cold tumour (neuroblastoma) resulted in any differences in the phenotype of T-cells isolated from tumours. I therefore injected pMMR and dMMR neuro-2a cells into A/J mice and treated at days 10, 13 and 16 with either the PBS (control) or an anti-PD1 antibody. I then euthanized mice at day 18, isolated T-cells from tumours as described in the *Materials and Methods* section and analyzed them using flow cytometry. This experiment was conducted 3 times, with experiments 1 and 3 generating results in agreement with each another. However, experiment 2 showed conflicting data and, therefore this experiment will be repeated in order to resolve the discrepancy. In experiment 1, I found that there were no significant differences in the levels of immune activation markers between mice bearing either pMMR or dMMR tumours and without anti-PD-1 treatment (PBS-treated controls) (Fig.3.13a). Moreover, when mice bearing pMMR tumours were treated with anti-PD1 there was a significant increase in the expression of activation and exhaustion markers (Fig.3.13a). However, dMMR tumours in mice treated with anti-PD-1 resulted in a significant decrease in the level of activation and exhaustion markers when compared to pMMR tumours treated with anti-PD-1 (Fig.3.13a). These findings are of interest as a decrease in exhaustion markers in dMMR tumours may be a sign of effective antigen clearance³⁹.

In the second experiment, I observed similar results for the levels of exhaustion markers in the control, PBS treatment group (Fig.3.13b). For certain exhaustion markers I saw a slight increase in level in the dMMR group (Fig.3.13b). However, in contrast to my first and third experiments, there were *higher* levels of exhaustion markers in mice with dMMR tumours receiving anti-PD-1 treatment.

Results of the third experiment (Fig.3.13c) were in agreement with the results of experiment one (Fig.3.13a).

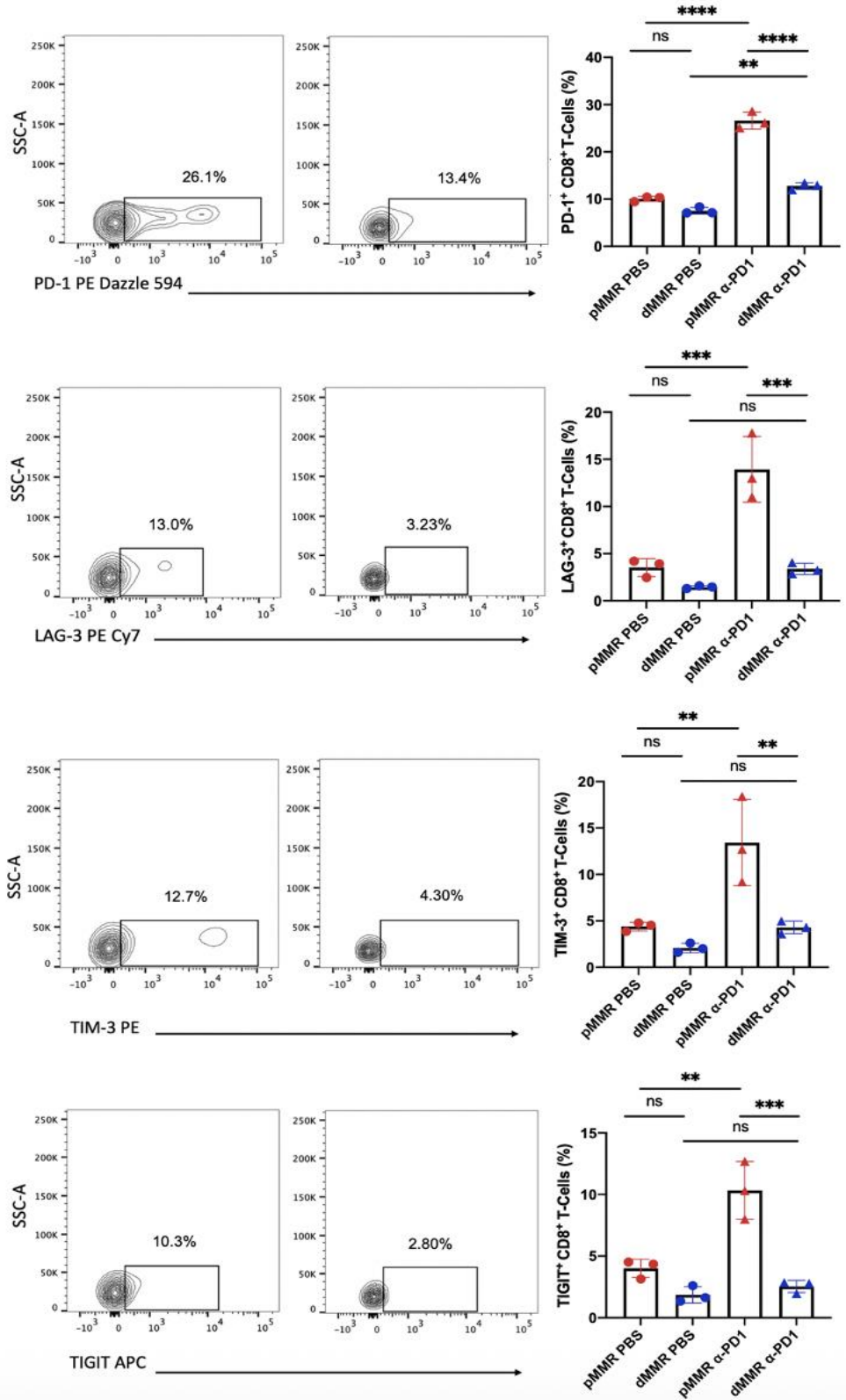
a

Experiment #1

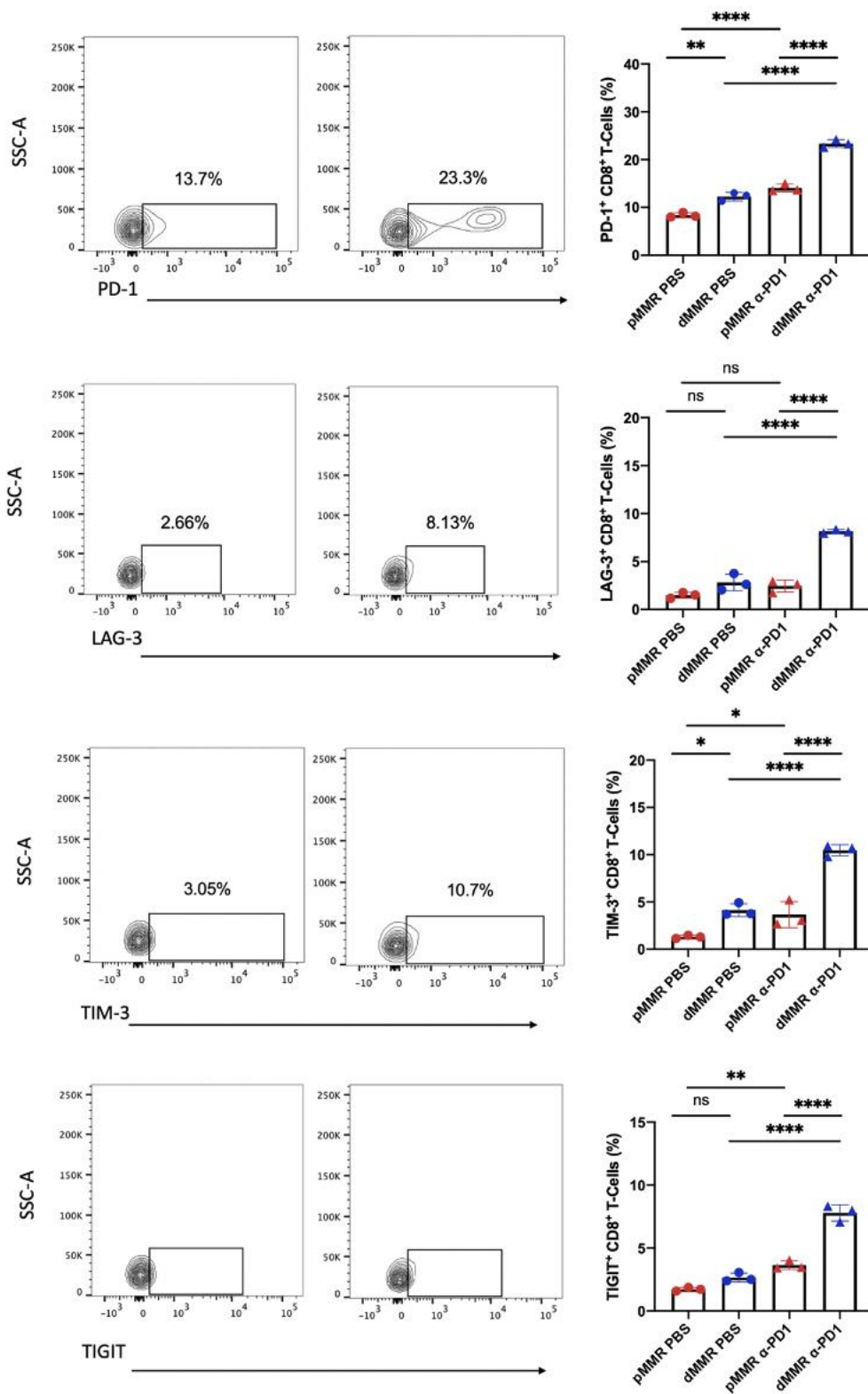
α PD-1 Treatment.

pMMR

dMMR



b Experiment #2
α PD-1 Treatment pMMR dMMR



c

Experiment #3

*α*PD-1 Treatment

pMMR

dMMR

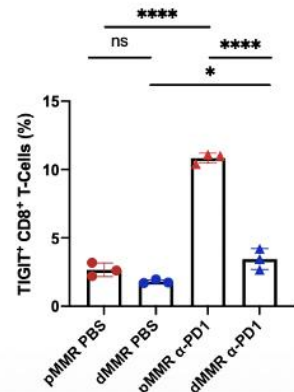
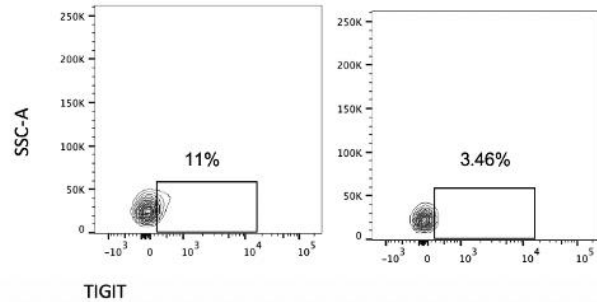
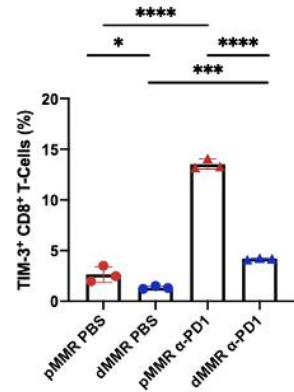
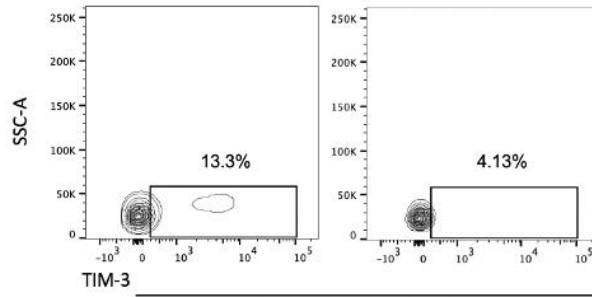
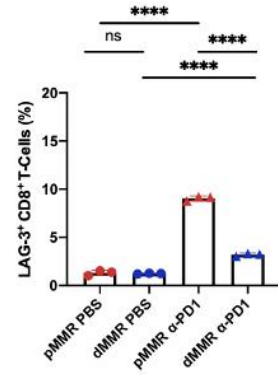
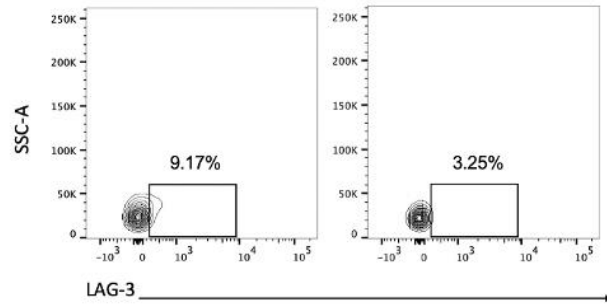
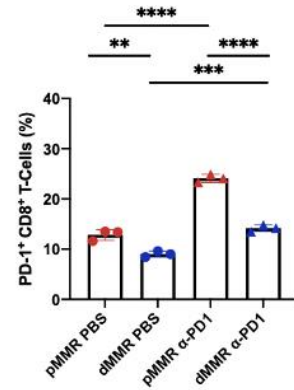
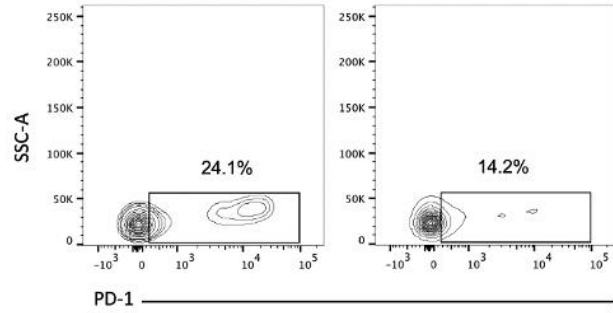


Figure 3.13. Tumour infiltrating lymphocyte activation and exhaustion in mice bearing induced DNA mismatch repair deficient tumours.

pMMR and dMMR neuro-2a cells were injected subcutaneously into A/J mice and injected i.p at days 10, 13 and 16 with the control PBS and the treatment anti-PD1 (250ug/100ul) and were sacrificed at day 18. Tumours from each treatment group were pooled together. Cells from the tumour single cell suspension were stained with a live/dead dye and live, singlet, lymphocytes were gated. Cells are presented as a percentage CD3⁺ cells. Results are representative of 3 independent experiments. Mice were grouped into pMMR no treatment, dMMR no treatment, pMMR treatment and dMMR treatment groups, **(a)** n=5, n=4, n=5, n=4 **(b)** n=5, n=5, n=6, n=6, **(c)** n=5, n=5, n=6, n=6 respectively. These cells were gated as a percentage of all live CD8⁺ T-cells. Data represents technical replicates. Statistical analysis was performed using one-way Anova. * p ≤ 0.05, ** p ≤ 0.01, *** p ≤ 0.001, **** p ≤ 0.0001, ns (not significant).

3.14 The effect of inducing MMR-deficiency and treating with anti-PD1 blockade on T-cell cytotoxic activity

In the previous section (3.13), I showed the effect of inducing MMR-deficiency and treating with anti-PD1 on T-cell activation and exhaustion. I next wanted to analyze the functional activity of T-cells in response to MMR-induction and anti-PD1 treatment. As CD8⁺ T-cells target cancer cells, they release cytolytic granules as an effector mechanism⁴⁰. During this process the granule membrane fuses with the cytoplasmic membrane and the result is the expression of lysosomal associated proteins, such as CD107a, on the cell surface⁴⁰. I therefore studied the expression of CD107a on CD8⁺ T-cells from tumours of mice following the same experimental setup as previous described (3.13).

In one set of experiments, I found there to be no significant differences in the expression of CD107a on CD8⁺ T-cells in pMMR and dMMR tumour bearing mice receiving the control PBS (Fig.3.14a). However, there was a significant increase in this degranulation marker in mice bearing pMMR tumours and receiving anti-PD1 treatment (Fig.3.14a). Moreover, the combination of dMMR induction and anti-PD1 did not increase CD107a levels on CD8⁺ T-cells (Fig.3.14a).

In my second experiment, I found that mice bearing dMMR tumours receiving no treatment expressed higher levels of the CD107a degranulation marker on CD8⁺ T-cells compared to their pMMR counterparts (Fig.3.14b). The same result was observed in the anti-PD1 treatment group, as the dMMR bearing mice had higher levels of CD107a⁺CD8⁺ T-cells than the pMMR tumour-bearing mice (Fig.3.14b).

Results for experiment 3 are similar to experiment 1, following the same trend in CD107a expression (Fig.3.14c). Due to the conflicting results, this experiment needs to be repeated.

α PD-1 Treatment

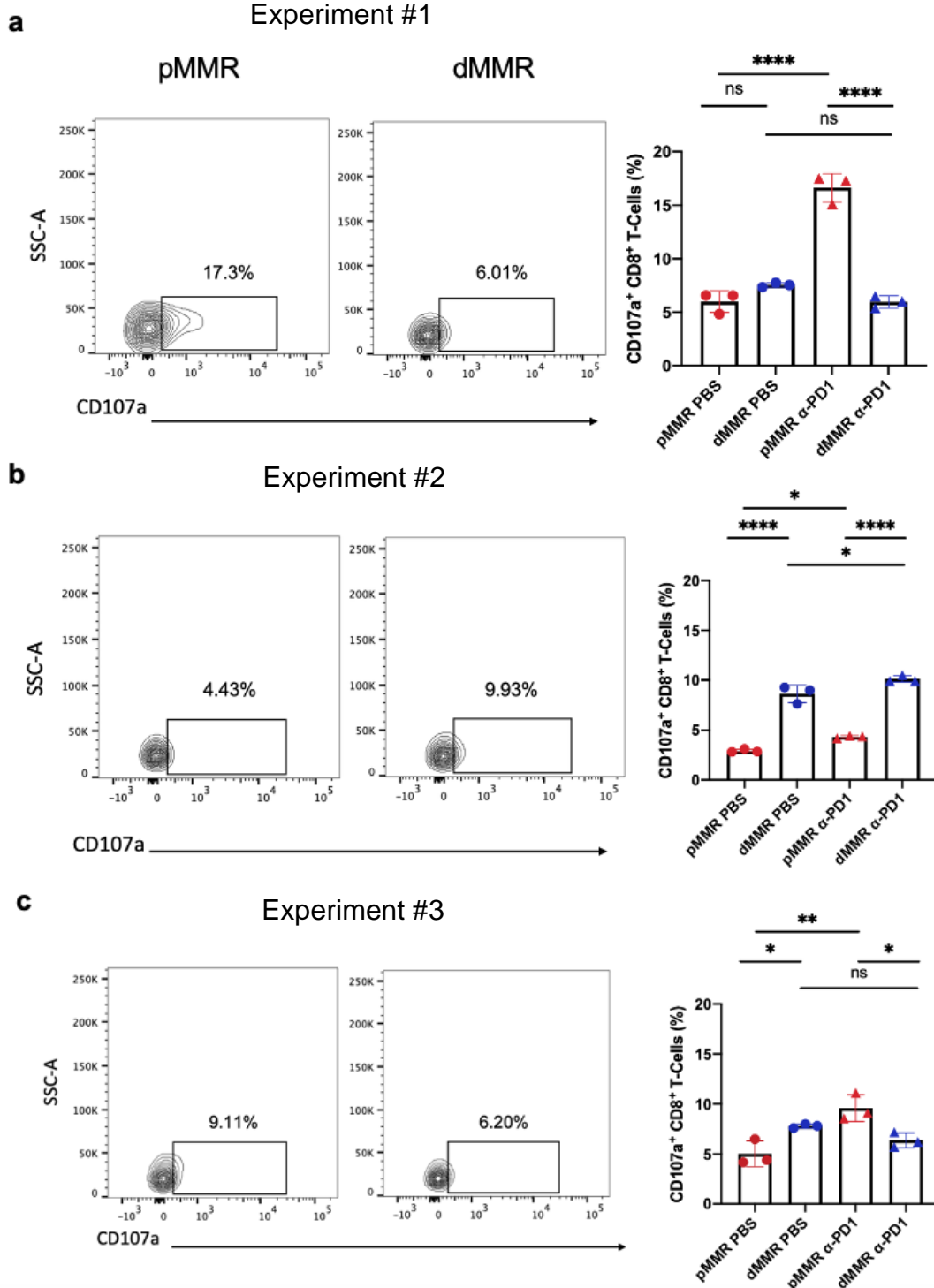


Figure 3.14. CD8⁺ T-cell degranulation activity from tumours following MMR-induction and anti-PD1 treatment.

pMMR and dMMR neuro-2a cells were injected subcutaneously into A/J mice and injected i.p at days 10, 13 and 16 with the control PBS and the treatment anti-PD1 (250ug/100ul) and were sacrificed at day 18. Tumours from each treatment group were pooled together. Cells from the tumour single cell suspension were stained with a live/dead dye and live, singlet, lymphocytes were gated. Cells are presented as a percentage CD3⁺ cells. Results are representative of 3 independent experiments. Mice were grouped into pMMR no treatment, dMMR no treatment, pMMR treatment and dMMR treatment groups, (a) n=5, n=4, n=5, n=4 (b) n=5, n=5, n=6, n=6, (c) n=5, n=5, n=6, n=6 respectively. These cells were gated as a percentage of all live CD8⁺ T-cells. Data represents technical replicates. Statistical analysis was performed using one-way Anova. * p ≤ 0.05, ** p ≤ 0.01, *** p ≤ 0.001, **** p ≤ 0.0001, ns (not significant).

3.15 Effect of inducing MMR-deficiency and treating with anti-PD1 on CD39⁺ PD1⁺ CD8⁺ T-cells infiltrated into tumours

I previously analyzed a number of T-cell exhaustion markers from TILs isolated from pMMR or dMMR tumours in control mice (PBS treatment) or being treated with anti-PD1 (Fig.3.11). Moreover, CD39 is an important molecule expressed on the surface of T-cells which converts ATP to AMP⁴¹. Under inflammatory conditions, CD39 leads to the production of immunosuppressive adenosines⁴¹. The expression of CD39 on T-cells has been linked to T-cell exhaustion and dysfunction⁴¹. I therefore used the same experimental setup as previously mentioned, and isolated T-cells from the tumours and stained for both CD39 and the activation/exhaustion marker PD-1 (3.13).

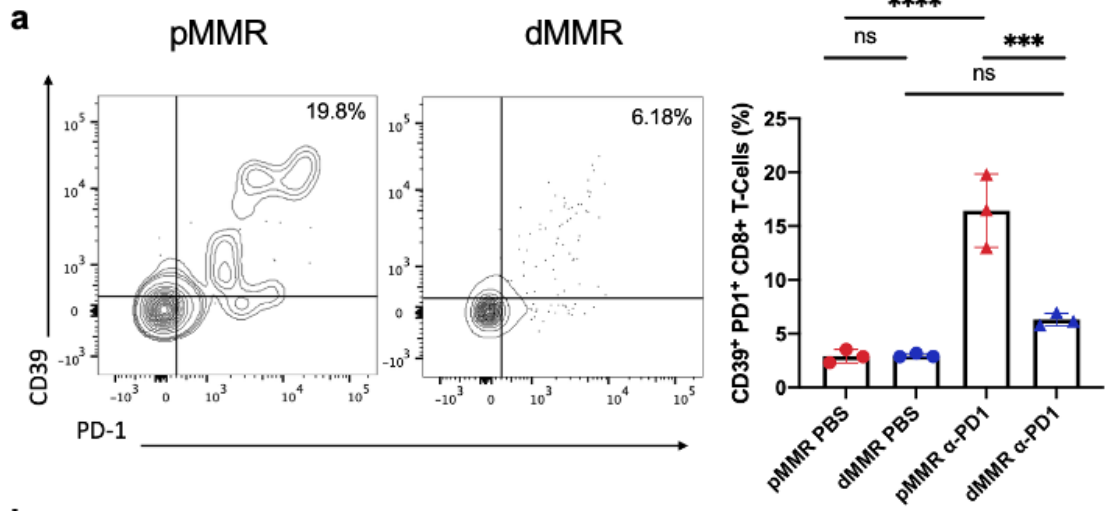
In my first experiment, I found no significant differences in the CD8⁺ T-cell population co-expressing CD39 and PD1 (Fig.3.15a). Moreover, pMMR tumour bearing mice receiving anti-PD1 treatment expressed significantly higher levels of CD39⁺PD1⁺CD8⁺ T-cells (Fig.3.15a). However, the combination of dMMR and anti-PD1 treatment resulted in a significant decrease in this exhausted T-cell population (Fig.3.15a).

In my second experiment, I found that dMMR tumour-bearing mice had slightly higher numbers of CD39⁺PD1⁺CD8⁺ T-cells compared to pMMR tumour-bearing mice (control groups, treated with PBS, in both cases) (Fig.3.15b). Moreover, this was observed in the anti-PD1 treatment groups, with the dMMR tumour-bearing mice displaying higher levels of CD39, PD1 double positive CD8⁺ T-cells (Fig.3.15b).

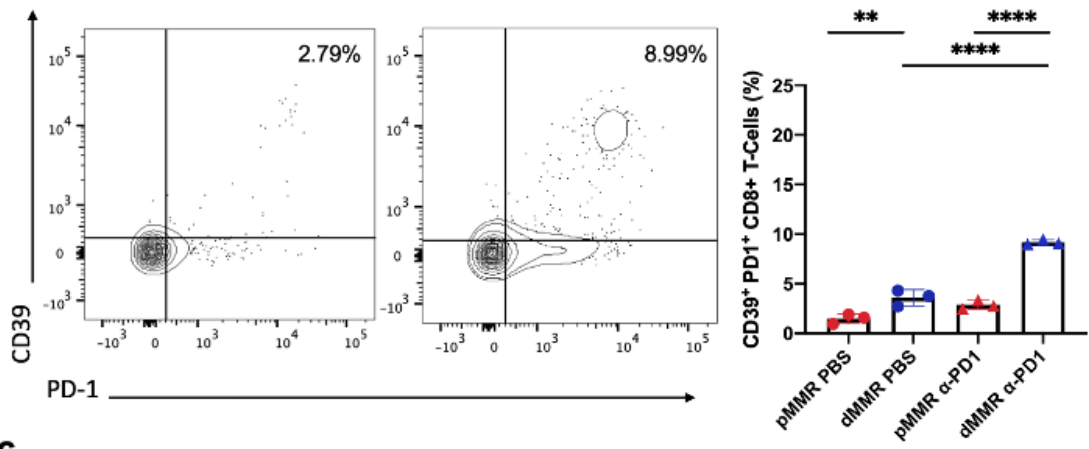
The third experiment (Fig.3.15c) yielded results similar to those of experiment one (Fig.3.15a). Due to the conflicting nature of these results, this experiment needs to be repeated.

*α*PD-1 Treatment

Experiment #1



b Experiment #2



c Experiment #3

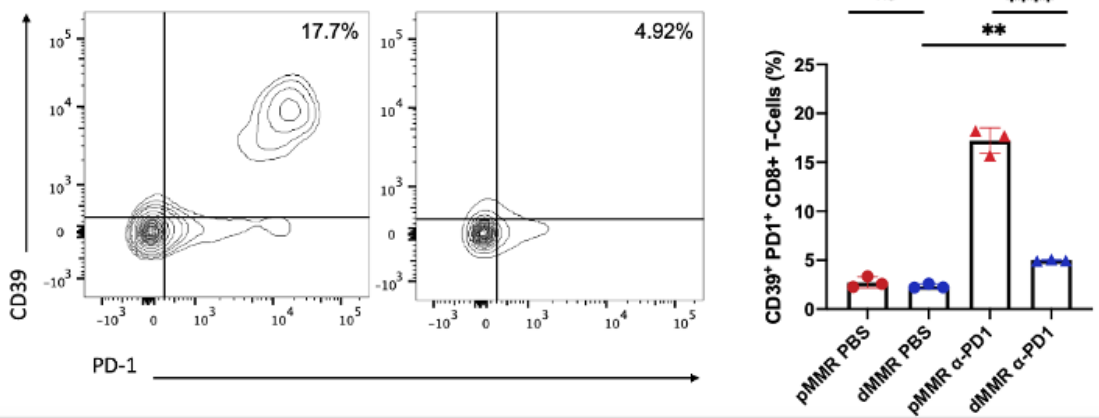


Figure 3.15. Tumour infiltrating lymphocyte exhaustion in mice bearing induced DNA mismatch repair deficient tumours.

pMMR and dMMR neuro-2a cells were injected subcutaneously into A/J mice and injected i.p at days 10, 13 and 16 with the control PBS and the treatment anti-PD1 (250ug/100ul) and were sacrificed at day 18. Tumours from each treatment group were pooled together. Cells from the tumour single cell suspension were stained with a live/dead dye and live, singlet, lymphocytes were gated. Cells are presented as a percentage CD3⁺ cells. Results are representative of 3 independent experiments. Mice were grouped into pMMR no treatment, dMMR no treatment, pMMR treatment and dMMR treatment groups, (a) n=5, n=4, n=5, n=4 (b) n=5, n=5, n=6, n=6, (c) n=5, n=5, n=6, n=6 respectively. These cells were gated as a percentage of all live CD8⁺ T-cells. Data represents technical replicates. Statistical analysis was performed using one-way Anova. * $p \leq 0.05$, ** $p \leq 0.01$, *** $p \leq 0.001$, **** $p \leq 0.0001$, ns (not significant).

3.16 Effect of inducing MMR-deficiency and treating with anti-PD1 on stimulating immunosuppressive T-regulatory cells in tumours

T-regulatory T-cells are an important immunosuppressive population that dampens the immune response. These cells play an important role in immune escape. I therefore wanted to study whether the superior anti-tumour immune response against dMMR tumours (Fig.3.6) could be explained by less infiltration of Tregs into these tumours. Following the same experimental strategy as previously described (3.13), mice were euthanized on day 18 and stained for the Treg cell markers CD4⁺ and CD25⁺. I conducted 3 experiments in total with varying results. I found that in experiment 1 (Fig.3.16a) there were no significant differences in the Treg population in between pMMR and dMMR tumour-bearing mice receiving the control PBS. There was also no difference in the Treg populations between pMMR and dMMR tumour bearing mice treated with anti-PD-1. Moreover, in experiment 2 (Fig.3.16b), there were no significant differences in Treg percentages in response to induced dMMR, either in control mice (PBS-treated) or after anti-PD-1 treatment: however, anti-PD-1 treatment resulted in a slight but significant increase in Tregs in mice with both pMMR and dMMR tumours. The third experiment yielded the same significant increase in Tregs in response to anti-PD-1 treatment in mice with dMMR tumours, but no difference in Tregs between PBS-treated mice with pMMR and dMMR tumours and no difference in Tregs between anti-PD-1-treated mice with pMMR and dMMR tumours.

Overall, this experiment requires repetition with a strategy that achieves higher n values than those indicated in Figure 3.15. The low n used to obtain the data shown does not generate sufficient statistical power to yield interpretable results. In addition, FOXP3 needs to be incorporated into this staining, in order to properly identify T-reg cells. Nevertheless, these preliminary results suggest that Tregs cells may not play a significant role in the anti-tumour response elicited against dMMR tumours.

α PD-1 Treatment

Experiment #1

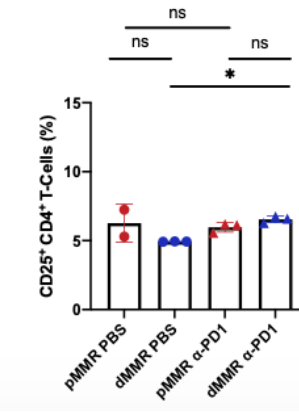
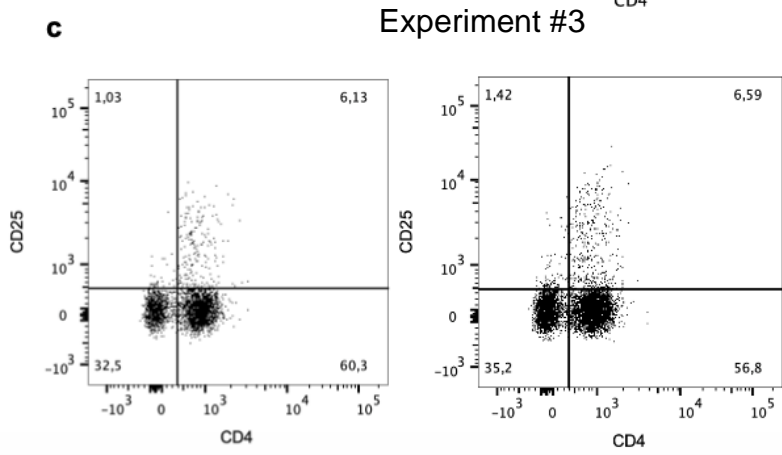
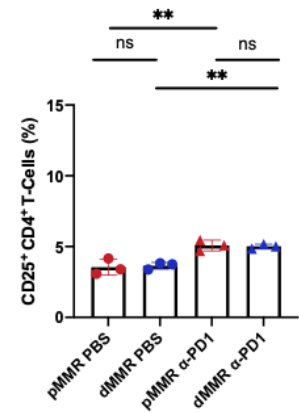
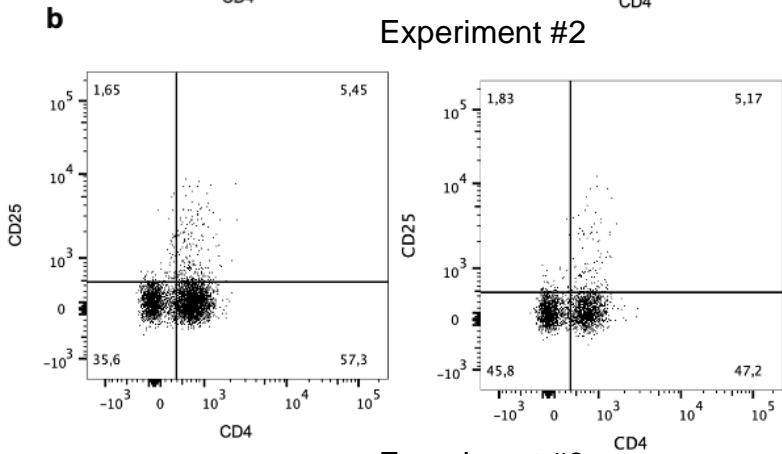
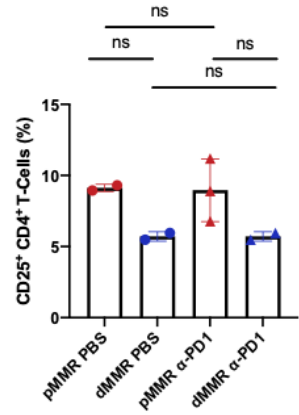
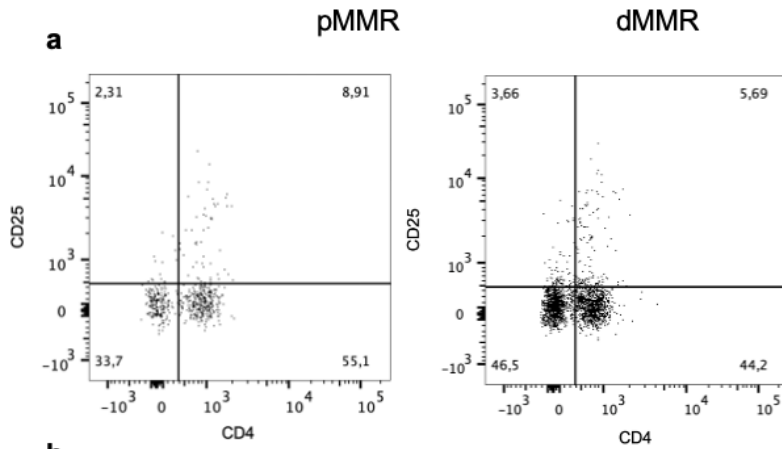


Figure 3.16. T-regulatory cell infiltration into pMMR and dMMR tumours.

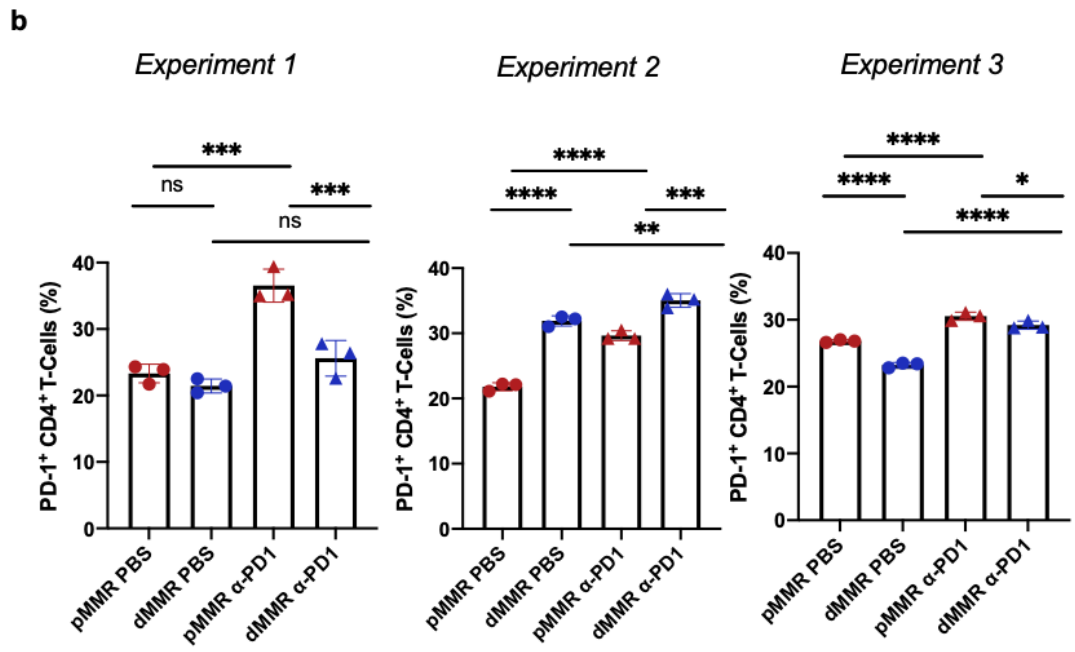
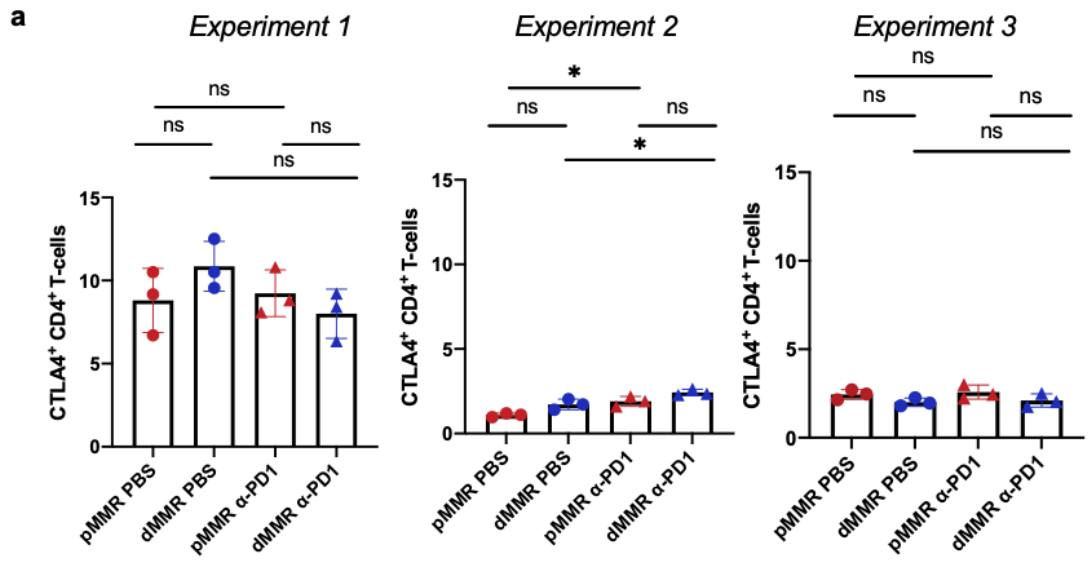
pMMR and dMMR neuro-2a cells were injected subcutaneously into A/J mice and injected i.p at days 10, 13 and 16 with the control PBS and the treatment anti-PD1 (250ug/100ul) and were sacrificed at day 18. Tumours from each treatment group were pooled together. Cells from the tumour single cell suspension were stained with a live/dead dye and live, singlet, lymphocytes were gated. Cells are presented as a percentage CD3⁺ cells. Results are representative of 3 independent experiments. Mice were grouped into pMMR + PBS treatment (control), dMMR + PBS treatment (control), pMMR + anti-PD-1 treatment, and dMMR + anti-PD-1 treatment groups, (a) n=5, n=4, n=5, n=4 (b) n=5, n=5, n=6, n=6, (c) n=5, n=5, n=6, n=6 respectively. These cells were gated as a percentage of all live CD3⁺ cells. Data represents technical replicates. Statistical analysis was performed using one-way Anova. * p ≤ 0.05, ** p ≤ 0.01, *** p ≤ 0.001, **** p ≤ 0.0001, ns (not significant).

3.17 Effect of inducing MMR deficiency and treating with anti-PD1 on CD4⁺ T-cell activation and exhaustion

I previously studied CD8⁺ T-cell exhaustion (Fig.3.13). I next set out to investigate whether inducing MMR deficiency affects CD4⁺ T-cell activation and exhaustion and whether anti-PD1 further impacts CD4⁺ T-cell exhaustion. CD4⁺ T-cells are an important subset of cells that can directly target cancer cells or act as “helper cells” and aid in the activation of cytotoxic CD8⁺ T-cells⁴². Exhaustion of such cells can lead to a weakened anti-tumour response⁴². I therefore studied the effect of inducing dMMR on CD4⁺ T-cell exhaustion, following the same experimental design used to generate the data shown in Figure 3.13. I first analyzed the levels of the immune checkpoint molecule CTLA4, which plays a role in hindering T-cell activation⁴². As T-cells become activated and exhausted they express higher levels of CTLA4⁴². This experiment was repeated 3 times, and over the 3 experiments I did not see any significant differences in CTLA4 expression on CD4⁺ T-cells in response to MMR induction (Fig.3.17a).

I next set out to study the levels of the PD-1 immune checkpoint molecule on CD4⁺ T-cells in pMMR and dMMR tumours (Fig.3.17b). In my first and third experiments I found a lower percentage of CD4⁺ T-cells that express PD-1 in dMMR tumours in both the groups treated with PBS and anti-PD1 (Fig.3.17b). However, this was not observed in experiment 2 (Fig.3.17b).

Moreover, exhausted T-cells often co-express multiple immune checkpoint molecules. I therefore studied populations of CD4⁺ T-cells that co-express the PD-1 and TIM-3 immune checkpoint molecules. In experiments 1 and 3, I found that dMMR tumours in both the non-treatment and the anti-PD1 treatment groups had a lower percentage of CD4⁺ T-cells that co-expressed these exhaustion markers (Fig.3.17c). However, in experiment 2 I found conflicting results, and this experiment therefore needs to be repeated (Fig.3.17c).



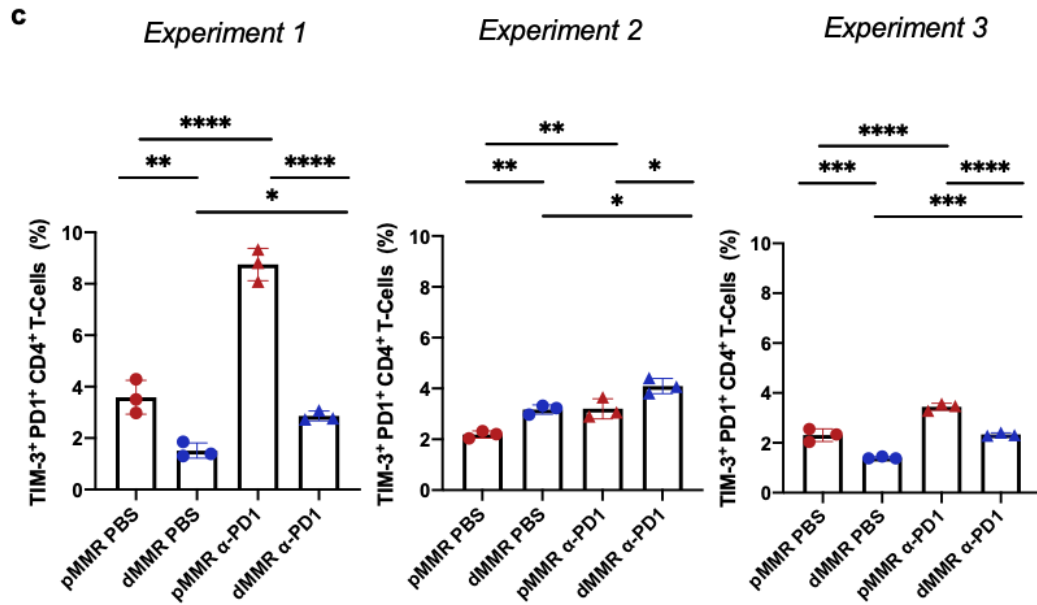


Figure 3.17. CD4⁺ T-cell exhaustion in pMMR and dMMR tumours.

pMMR and dMMR neuro-2a cells were injected subcutaneously into A/J mice and injected i.p at days 10, 13 and 16 with the control PBS and the treatment anti-PD1 (250ug/100ul) and were sacrificed at day 18. Tumours from each treatment group were pooled together. Cells from the tumour single cell suspension were stained with a live/dead dye and live, singlet, lymphocytes were gated. Cells are presented as a percentage CD3⁺ cells. Results are representative of 3 independent experiments. Mice were grouped into pMMR no treatment, dMMR no treatment, pMMR treatment and dMMR treatment groups, (a) n=5, n=4, n=5, n=4 (b) n=5, n=5, n=6, n=6, (c) n=5, n=5, n=6, n=6 respectively. These cells were gated as a percentage of all live CD4⁺ T-cells. Data represents technical replicates. Statistical analysis was performed using one-way Anova. * p ≤ 0.05, ** p ≤ 0.01, *** p ≤ 0.001, **** p ≤ 0.0001, ns (not significant).

3.18 A combination of inducing MMR-deficiency and anti-PD1 treatment results in a significant decrease in dysfunctional T-cells

I have shown the effect of inducing MMR deficiency and treating with anti-PD1 on CD8⁺ T-cell exhaustion. Another important subset of CD8⁺ T-cells are dysfunctional CD38⁺PD-1⁺CD8⁺ T-cells⁴³. More recently, studies have shown that these cells are generated when tumours are not properly primed with antigens prior to anti-PD1 treatment⁴³. I therefore wanted to investigate whether dysfunctional T-cells are upregulated in a similar manner in this study. This model incorporates MMR-proficient (pMMR) tumours, which have a low tumour mutational burden and therefore would not be considered *antigenically primed*. Moreover, this model also includes MMR deficient (dMMR) tumours which, in theory, have a higher tumour mutational burden and would be considered *antigenically primed*. I followed the same experiment strategy as used to generate the data shown in Figure 3.13. Similar to the study conducted by Verma *et al.* I did not find any significant differences in the percentage of dysfunctional CD38⁺PD-1⁺CD8⁺ T-cells from both poorly antigenically primed and antigenically primed tumours (pMMR and dMMR) (Fig.3.17). However, I found a significant increase in this dysfunctional population in the potentially *non-antigenically* primed genomically stable pMMR tumours receiving anti-PD1 treatment (Fig.3.18). Interestingly, dMMR tumours, which are genomically unstable and theoretically antigenically primed, showed a significant decrease in their dysfunctional CD38⁺PD-1⁺CD8⁺ T-cell population (Fig.3.18). These observations are similar to what has been observed by Verma *et al.* and underscore the potential importance of combining MMR induction along with PD-1 blockade in order to properly prime tumours before anti-PD1 treatment to reduce T-cell dysfunction and resistance to anti-PD1 therapy. It is important to note that these results are preliminary, and this experiment needs to be repeated to further validate these findings.

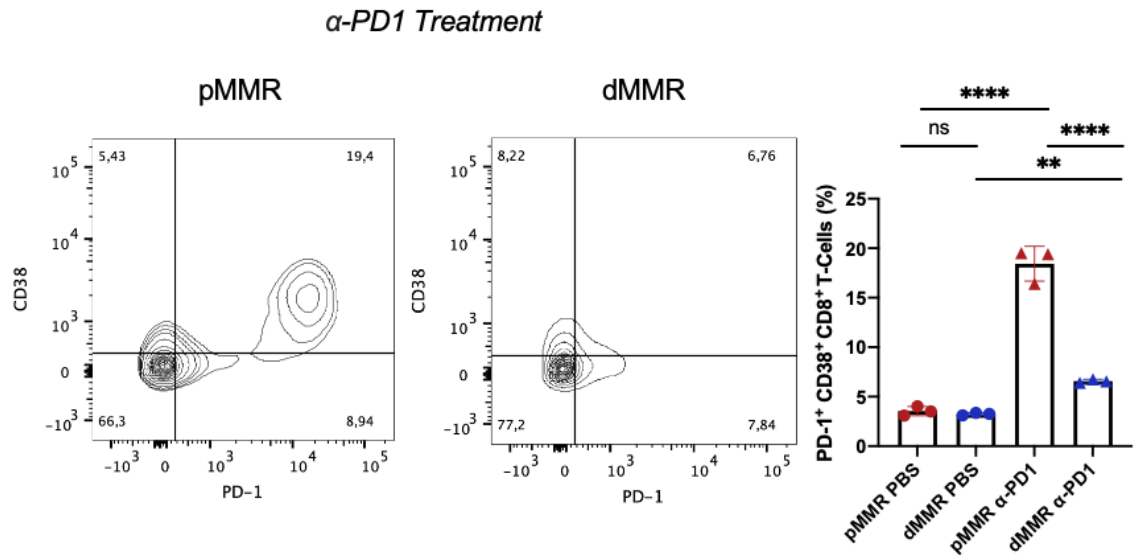


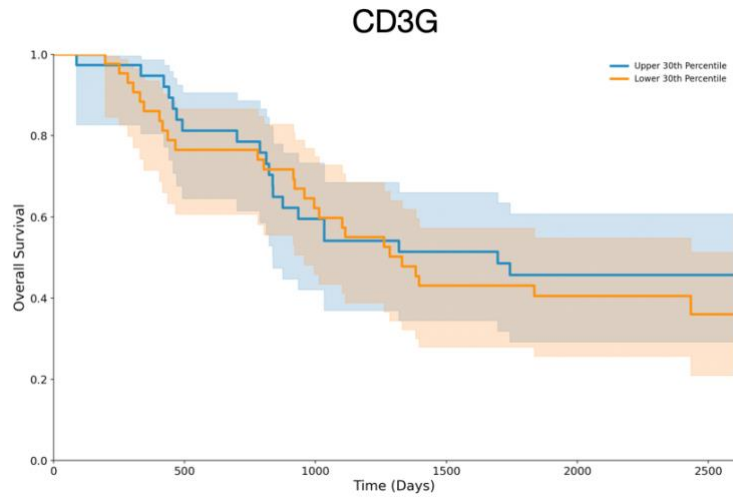
Figure 3.18. A combination of MMR-induction and anti-PD1 treatment results in a decrease in dysfunctional T-cells.

pMMR and dMMR neuro-2a cells were injected subcutaneously into A/J mice and injected i.p at days 10, 13 and 16 with the control PBS and the treatment anti-PD1 (250ug/100ul) and were sacrificed at day 18. Tumours from each treatment group were pooled together. Cells from the tumour single cell suspension were stained with a live/dead dye and live, singlet, lymphocytes were gated. Cells are presented as a percentage CD3⁺ cells. Results are representative of 3 independent experiments. Mice were grouped into pMMR no treatment, dMMR no treatment, pMMR treatment and dMMR treatment groups, n=5, n=5, n=6, n=6 respectively. These cells were gated as a percentage of all live CD8⁺ T-cells. Data represents technical replicates. Statistical analysis was performed using one-way Anova. * p ≤ 0.05, ** p ≤ 0.01, *** p ≤ 0.001, **** p ≤ 0.0001, ns (not significant).

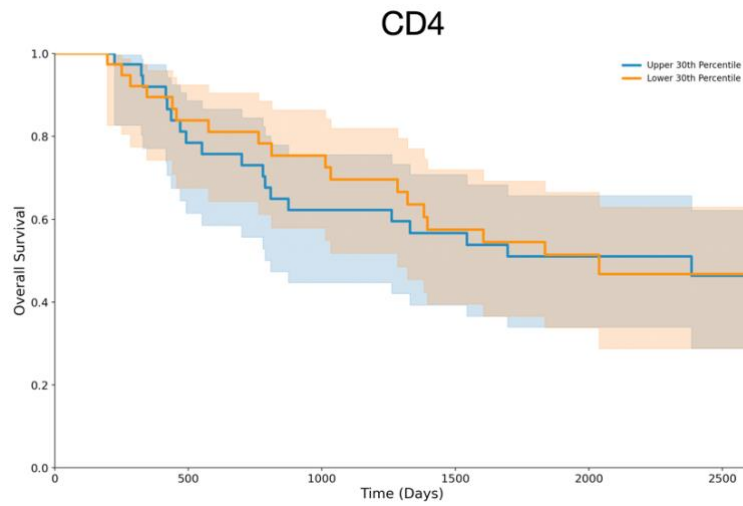
3.19 Immune markers associated with improved overall survival in high-risk neuroblastoma patients

I previously showed that inducing dMMR in immunologically cold murine neuroblastoma tumours, stimulates an anti-tumour immune response characterized by a slower tumour growth rate (Fig.3.5.1). Moreover, I have also shown that this enhanced immune response in dMMR neuroblastoma tumours is accompanied by higher T-cell infiltration (Fig.3.11) and higher CD8⁺ T-cell infiltration (Fig.3.12). I next aimed to study whether the expression of immune markers in neuroblastoma patient tumours had any effect on overall survival. I computationally mined the TARGET database, which focuses on sequencing hard to treat high-risk neuroblastoma patients who have a worse clinical outcome. I found that CD3 and CD4 immune markers were not associated with improved prognosis. Interestingly, CD8 gene expression was associated with a statistically significant improved overall survival of high-risk neuroblastoma patients. CD8⁺ T-cells are effector cells that play an important role in the anticancer immune response. Moreover, CD8⁺ T-cells are a major target of anti-PD1 immune checkpoint inhibitor treatment. Here, I show the impact of CD8 gene expression in the immunologically cold neuroblastoma tumours, on the overall survival of patients. Moreover, I have also shown that by inducing dMMR in murine neuroblastoma tumours, this induces higher CD8⁺ T-cell infiltration. This is notable because, here I show that CD8 gene expression is associated with improved prognosis in high-risk neuroblastoma patients.

a



b



c

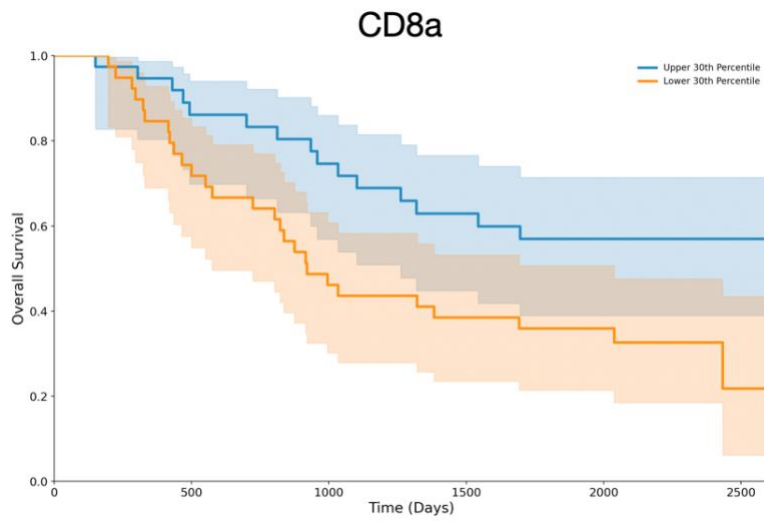


Figure 3.19. CD8a expression is associated with improved overall survival in high-risk neuroblastoma patients.

Overall survival of high-risk neuroblastoma patients stratified according to gene expression of immune markers (a) CD3G, (b) CD4, (c) CD8a. Statistical analysis was performed using the 2-sided log-rank test. Blue = overall survival of patients with gene expression in the upper 30th quartile, Orange = overall survival of patients with gene expression in the lower 30th quartile. Shaded areas represent pointwise 95% confidence intervals.

Chapter 4

Discussion

Over the past decade there has been a shift in oncology to move from only using radiation, chemotherapy and surgery, to utilizing drugs that can mobilize the immune system to recognize and target tumours²⁷. These therapies include immune checkpoint inhibitors (ICIs) that can bind to “immune checkpoint” molecules which serve to dampen the immune response, re-invigorating anti-tumour T-cells²⁷. Patients that respond to ICIs often show durable remissions with improved overall survival⁴⁴. However, the majority of patients still do not respond to ICIs¹⁰. Many factors influence response to ICIs; however, it has become evident that the immunological tumour microenvironment can both limit and promote ICI response²⁷. “Hot” tumour microenvironments tend to be heavily infiltrated with immune cells and show signs of T-cell activation. As such, when patients with hot tumours are treated with ICIs, the pre-existing T-cells in the tumour become re-invigorated and these patients respond better to ICI treatment²⁷. More recently, the TMB has become an important biomarker of a “hot” tumour microenvironment¹⁰. Patients with a higher TMB accumulate more mutations that produce foreign peptides, which allow the tumour to be detected as non-self¹⁰. This consequently results in more T-cell infiltration into the tumour and better response to ICIs¹⁰. An important group of patients with high TMB are a subset of patients with microsatellite instability arising from MMR deficiency¹⁰. In this thesis, I therefore wanted to explore whether inducing a deficiency in DNA-MMR repair, in an immunologically cold tumour, could turn this tumour “hot” and induce an anti-tumour immune response. Moreover, I also wanted to investigate whether inducing DNA-MMR deficiency could further sensitize these tumours ICIs.

Over the past few years, MMR-deficiency and ICI treatment has been studied by a number of groups. Germano *et al.* showed that inducing DNA-MMR deficiency in murine colorectal and pancreatic cell lines, hindered tumour growth in immune competent mice³³. Their MMR-deficient cells were left to grow *in vitro* for ~133 days to accumulate mutations and were injected into immunocompetent mice³³. They observed a significant decrease in tumour growth when compared to mice injected with the control cells³³. In this model, I

similarly induced MMR-deficiency by generating an MLH1 KO cell line (Fig.3.3a). However, I chose to study neuroblastoma, a solid tumour associated with a highly immunosuppressive tumour microenvironment that is refractory to ICI. Similarly, I observed that inducing MMR-deficiency in neuro-2a cells generated a stronger immune response in immune competent mice when compared to the control MMR-proficient cells (Fig.3.5). However, this level of immunogenicity was attained after leaving cells to grow for only ~56 days *in vitro*. Moreover, mice injected with MMR-deficient cells that also received anti-PD1 treatment showed a slight decrease in tumour growth when compared to dMMR tumour bearing mice from the non-treatment group, however, this difference was not significant. It is important to note that I could not show that inducing MMR deficiency further sensitized mice to ICI after 18 days *in vivo*. However, I monitored dMMR induced tumours for a longer period of time in order to study a potential added benefit to treating with anti-PD1. I also conducted a survival experiment in order to investigate the overall survival benefit of inducing MMR deficiency and treating with anti-PD1. Mice were monitored for over 30 days and I showed that the combination of inducing MMR-deficiency in neuro-2a cell line and treating with anti-PD1 significantly prolongs mouse survival when compared to mice bearing MMR proficient tumours treated with anti-PD1(Fig.3.6a).

I also studied the immunogenic phenotype of both pMMR and dMMR tumours for any underlying differences in immunogenicity prior to tumour injection into immune competent mice and found that dMMR tumours express higher levels of MHC-I *in vitro* (Fig.3.7). I further mined the TCGA database and similarly found that in the COAD READ cohort, MSI-h patients who often have a deficiency in their DNA-MMR machinery, displayed higher levels of certain MHC-I related genes when compared to MSS tumour samples (Fig.3.8). Interestingly, I also found that dMMR tumours express higher levels of PD-L1 *in vitro* (Fig.3.9.2), similar to immunogenic MSI-h patients' tumours (3.9.1). However, this finding was *in vitro* and there may be other mechanistic differences to explain this increase in PD-L1 expression.

To my knowledge, this is the first study of the immune phenotype associated with an increased anti-tumour response in *induced* dMMR tumour bearing mice. My preliminary data shows that dMMR mice receiving anti-PD1 treatment showed a higher infiltration of CD8⁺ T-cells into tumour draining lymph nodes when compared to pMMR tumour bearing mice. Moreover, I also studied the T-cell phenotype in tumours and found that dMMR bearing mice had higher levels of both T-cells and CD8⁺ T-cells when compared to pMMR tumour bearing mice. These findings are in agreement with a dMMR induced model by Mandal *et al*, where they targeted the DNA-MMR repair gene *MSH2* (as opposed to *MLH1*) and showed higher T-cell infiltration in dMMR induced tumours⁴⁶. This finding is important as I also show that CD8 gene expression in neuroblastoma patients is associated with improved survival. Therefore, this increase in CD8⁺ T-cell infiltration in response to dMMR is particularly significant in our neuroblastoma model, as we show that neuroblastoma patients with higher CD8 gene expression have a better prognosis.

In addition to altered numbers of T-cells, I also examined T-cell exhaustion, which is characterized by increased immune checkpoint expression and reduced T-cell function, which limits the T-cell response against tumours. Specifically, I studied the expression of a number of immune checkpoint molecules on CD8⁺ T-cells from pMMR tumours and dMMR tumours in order to establish any differences in T-cell exhaustion in these immunologically distinct tumours. Interestingly, I did not find a significant difference in T-cell exhaustion in pMMR and dMMR tumours not receiving treatment (Fig.3.13a, c). However, in 2 of my experiments I found that mice receiving a combination of MMR induction and anti-PD1 treatment had lower levels of T-cell exhaustion when compared to pMMR tumours (Fig.3.13a, c). Studies have shown that effective antigen recognition and clearance results in lower T-cell exhaustion levels³⁹. This combination of inducing MMR-deficiency, resulting in a potential increase in neoantigens, and then treating with anti-PD1 could reduce T-cell exhaustion. It is important to note that a third experiment showed conflicting results, and this therefore needs to be repeated (Fig.3.13b). Finally, I studied the CD4⁺ T-cell phenotype in response to MMR induction and anti-PD1 treatment. In order to study exhaustion, I analyzed expression of immune checkpoint molecules such as CTLA-4, PD-1 and TIM-3. Consistent with my previous findings, there were only slight difference

in the expression of immune checkpoint molecules in CD4⁺ T-cells from pMMR or dMMR tumours not receiving treatment. Interestingly, I found that pMMR bearing mice treated with anti-PD1 display an increase in CD4⁺ T-cell exhaustion, however combining MMR-induction of neuroblastoma tumours in combination with anti-PD1 results in a decrease in T-cell exhaustion.

Finally, I aimed to study the dysfunctional T-cell phenotype in MMR-induced tumours treated with anti-PD1. Dysfunctional T-cells are an important population of T-cells that often hinder anti-tumour immunity and can lead to resistance to anti-PD1 therapy⁴³. A study conducted by *Verma et al* showed that treating with anti-PD1 prior to antigenically priming tumours results in a significant increase in the CD38⁺PD-1⁺CD8⁺ dysfunction T-cell population⁴³. However, they showed that vaccinating mice in order to prime these tumours with antigen prior to anti-PD1 treatment resulted in a significant decrease in these dysfunctional T-cells⁴³. In this model, preliminary results similarly demonstrate that inducing MMR-deficiency in order to antigenically prime immunologically cold neuroblastoma tumours and then treating with anti-PD1 results in a significant decrease in dysfunctional T-cells when compared to pMMR tumours receiving anti-PD1 treatment.

In this study, I have established key differences in the T-cell immune phenotype in tumours between pMMR and dMMR tumour bearing mice receiving no treatment and receiving anti-PD1 treatment. It is important to note that the experiments characterizing changes in T-cell phenotype need to be repeated, as one of my experiments showed conflicting results. Additionally, in my future studies I will aim to not only establish differences in the T-cell phenotype from pMMR and dMMR tumour bearing mice, but also whether these T-cells differ in their cytotoxic capabilities. Another limitation of my study is that all my *in vivo* experiments utilized a subcutaneous model for neuroblastoma tumour growth in mice. Although, this model allows for tumours to be readily measured, this does have its limitations as neuroblastoma tumours in patients grow in the adrenal medulla. The subcutaneous tumour microenvironment therefore does not accurately represent the complex architecture associated with tumour growth in the adrenal medulla. However, orthotopic injections into the adrenal medulla are technically challenging and were

therefore difficult to implement for my experiments. Moreover, another technical challenge in this study is that the generation of random neoantigens, which can be quite immunogenic, can induce a strong anti-tumour response in the absence of any treatment. This is a technical challenge in this project, as I grow the cells in culture for injection into mice, they can develop random mutations that can render them more or less immunogenic because of the induced mismatch repair deficiency. This phenomenon has been also reported in other cancer models with higher TMB³⁴. In my future studies, I aim to repeat my *in vivo* tumour growth experiments, however, I will culture the neuroblastoma cells over a longer period of time *in vitro* in order to investigate whether this leads to an increase in neoantigen production and a heightened anti-tumour response once injected into immune competent mice.

Immune checkpoint inhibitors have improved the survival of many cancer patients over the years. However, a major challenge in treating patients with “cold tumours” is the poorly immunogenic tumour microenvironment. To my knowledge, this study is the first to show that inducing MMR-deficiency in the poorly immunogenic, ICI refractory murine neuroblastoma tumours, as a mechanism to render these tumours immunologically “hot”, results in a heightened anti-tumour response in immune competent mice. My data also demonstrates that inducing MMR-deficiency in poorly immunogenic neuroblastoma tumours and treating with anti-PD1 prolonged survival of mice. Neuroblastoma tumours are highly immunosuppressive, and this study demonstrates the potential of inducing MMR-deficiency in these tumours to overcome their highly tumour suppressive TME and further sensitize these tumours to ICI treatment. This study also provides a mechanistic understanding of the impact of inducing MMR-deficiency and treating with anti-PD1 on T-cell exhaustion and dysfunction.

References

- 1 Hanahan, D., & Weinberg, R. Hallmarks of Cancer: The Next Generation. *Cell (Cambridge)*. **144**, 646–674 (2011).
- 2 Fares, J., Fares, M.Y., Khachfe, H.H. *et al.* Molecular principles of metastasis: a hallmark of cancer revisited. *Sig Transduct Target Ther*. **5**, 28 (2020).
- 3 O’Donnell, J.S., Teng, M.W.L. & Smyth, M.J. Cancer immunoediting and resistance to T cell-based immunotherapy. *Nat Rev Clin Oncol*. **16**, 151–167 (2019).
- 4 Mittal D, Gubin MM, Schreiber RD, Smyth MJ. New insights into cancer immunoediting and its three component phases--elimination, equilibrium and escape. *Curr Opin Immunol*. **27**,16-25 (2014).
- 5 Bhatia A, Kumar Y. Cancer-immune equilibrium: questions unanswered. *Cancer Microenvironment: Official Journal of the International Cancer Microenvironment Society*. **4**, 209-217 (2011).
- 6 Kim, Ryungsa et al. “Cancer immunoediting from immune surveillance to immune escape.” *Immunology* vol. **121**, 1-14 (2007).
- 7 Keenan, T.E., Burke, K.P. & Van Allen, E.M. Genomic correlates of response to immune checkpoint blockade. *Nat Med*. **25**, 389–402 (2019).
- 8 Raval, Raju R et al. “Tumour immunology and cancer immunotherapy: summary of the 2013 SITC primer.” *Journal for immunotherapy of cancer*. **2**,14 (2014).
- 9 Roth, David B. “V(D)J Recombination: Mechanism, Errors, and Fidelity.” *Microbiology spectrum* vol. **2**,6 (2014).
- 10 Choucair, K., Morand, S., Stanbery, L. *et al.* TMB: a promising immune-response biomarker, and potential spearhead in advancing targeted therapy trials. *Cancer Gene Ther*. (2020).
- 11 Han S, Toker A, Liu ZQ, Ohashi PS. Turning the Tide Against Regulatory T Cells. *Front Oncol*. **9**, 279 (2019).
- 12 Zhang, Nu, and Michael J Bevan. “CD8(+) T cells: foot soldiers of the immune system.” *Immunity*. **35**, 161-8 (2011).
- 13 Audiger C, Rahman MJ, Yun TJ, Tarbell KV, Lesage S. The Importance of Dendritic Cells in Maintaining Immune Tolerance. *J Immunol*. **198**, 2223-2231 (2017).

- 14 HPio R, Ajona D, Ortiz-Espinosa S, Mantovani A, Lambris JD. Complementing the Cancer-Immunity Cycle. *Front Immunol.* **10**, 774 (2019).
- 15 Embgenbroich, Maria, and Sven Burgdorf. "Current Concepts of Antigen Cross-Presentation." *Frontiers in Immunology.* **9**, 1643–1643 (2018).
- 16 Waldman AD, Fritz JM, Lenardo MJ. A guide to cancer immunotherapy: from T cell basic science to clinical practice. *Nat Rev Immunol.* **20**, 1-18 (2020).
- 17 Marhelava, Katsiaryna et al. "Targeting Negative and Positive Immune Checkpoints with Monoclonal Antibodies in Therapy of Cancer." *Cancers* **11**, 1756 (2019).
- 18 Buchbinder, Elizabeth I, and Anupam Desai. "CTLA-4 and PD-1 Pathways: Similarities, Differences, and Implications of Their Inhibition." *American journal of clinical oncology.* **39**, 98-106 (2016).
- 19 Leach, D. R., Krummel, M. F. & Allison, J. P. Enhancement of antitumour immunity by CTLA-4 blockade. *Science.* **271**, 1734–1736 (1996).
- 20 Yarchoan, M., Johnson, B., Lutz, E. *et al.* Targeting neoantigens to augment antitumour immunity. *Nat Rev Cancer.* **17**, 209–222 (2017).
- 21 Chan, D., Gibson, H., Aufiero, B. *et al.* Differential CTLA-4 expression in human CD4⁺ versus CD8⁺ T cells is associated with increased NFAT1 and inhibition of CD4⁺ proliferation. *Genes Immun* **15**, 25–32 (2014).
- 22 Bowyer S, Prithviraj P, Lorigan P, Larkin J, McArthur G, Atkinson V, Millward M, Khou M, Diem S, Ramanujam S, Kong B, Liniker E, Guminski A, Parente P, Andrews MC, Parakh S, Cebon J, Long GV, Carlino MS, Klein O. Efficacy and toxicity of treatment with the anti-CTLA-4 antibody ipilimumab in patients with metastatic melanoma after prior anti-PD-1 therapy. *Br J Cancer.* **10**,1084-9 (2016).
- 23 Francisco, L. M., Sage, P. T. & Sharpe, A. H. The PD-1 pathway in tolerance and autoimmunity. *Immunol. Rev.* **236**, 219–242 (2010).
- 24 Iwai, Y. et al. Involvement of PD-L1 on tumour cells in the escape from host immune system and tumour immunotherapy by PD-L1 blockade. *Proc. Natl Acad. Sci. USA* **99**, 12293–12297 (2002).
- 25 Joller, N. & Kuchroo, V. K. Tim-3, Lag-3, and TIGIT. *Curr. Top. Microbiol. Immunol.* **410**, 127–156 (2017)

- 26 Raskov, Hans, Adile Orhan, Jan Pravsgaard Christensen, and Ismail Gögenur. “Cytotoxic CD8+ T Cells in Cancer and Cancer Immunotherapy.” *British Journal of Cancer*. (2020).
- 27 Binnewies, M. et al. Understanding the tumour immune microenvironment (TIME) for effective therapy. *Nat. Med.* **24**, 541–550. (2018)
- 28 Duan Q, Zhang H, Zheng J, and Zhang L. Turning Cold into Hot: Firing up the Tumor Microenvironment. *Trends Cancer*. **6**, 605-18 (2020)
- 29 Ganesh, K., Stadler, Z.K., Cercek, A. *et al.* Immunotherapy in colorectal cancer: rationale, challenges and potential. *Nat Rev Gastroenterol Hepatol* **16**, 361–375 (2019).
- 30 Richman, Susan. “Deficient mismatch repair: Read all about it (Review).” *International journal of oncology*. **47**,1189-202 (2015).
- 31 Boland, C Richard, and Ajay Goel. “Microsatellite instability in colorectal cancer.” *Gastroenterology*. **138**, 2073-2087 (2010).
- 32 Vilar, E., Gruber, S. Microsatellite instability in colorectal cancer—the stable evidence. *Nat Rev Clin Oncol* **7**, 153–162 (2010).
- 33 Germano, G., Lamba, S., Rospo, G. *et al.* Inactivation of DNA repair triggers neoantigen generation and impairs tumour growth. *Nature* **552**, 116–120 (2017).
- 34 Mandal, R., Samstein, R., Lee, K. *et al.* Genetic diversity of tumors with mismatch repair deficiency influences anti–PD-1 immunotherapy response. *Science* **364**, 485–491 (2019).
- 35 Brodeur, G., Bagatell, R. Mechanisms of neuroblastoma regression. *Nat Rev Clin Oncol* **11**, 704–713 (2014).
- 36 Cheung, Nai-Kong V, and Michael A Dyer. “Neuroblastoma: developmental biology, cancer genomics and immunotherapy.” *Nature reviews. Cancer*. **13**, 397-411(2013).
- 37 Spranger S. Mechanisms of tumor escape in the context of the T-cell-inflamed and the non-T-cell-inflamed tumor microenvironment. *International immunology*, **8**, 383–391(2016).
- 38 Llosa, Nicolas J., et al. The vigorous immune microenvironment of microsatellite instable colon cancer is balanced by multiple counter-inhibitory checkpoints. *Cancer discovery*. **5**, 43-51 (2015).
- 39 Wherry, E. T cell exhaustion. *Nat Immunol* **12**, 492–499 (2011).

40 Lorenzo-Herrero S, Sordo-Bahamonde C, Gonzalez S, López-Soto A. CD107a Degranulation Assay to Evaluate Immune Cell Antitumor Activity. *Methods Mol Biol* **1884**,119-130 (2019).

41 Moesta, A.K., Li, X. & Smyth, M.J. Targeting CD39 in cancer. *Nat Rev Immunol* (2020).

42 Borst, J., Ahrends, T., Bąbała, N. *et al.* CD4⁺ T cell help in cancer immunology and immunotherapy. *Nat Rev Immunol* **18**, 635–647 (2018).

43 Verma, V., Shrimali, R.K., Ahmad, S. *et al.* PD-1 blockade in subprimed CD8 cells induces dysfunctional PD-1⁺CD38^{hi} cells and anti-PD-1 resistance. *Nat Immunol* **20**, 1231–1243 (2019).

44 Akinleye, A., Rasool, Z. Immune checkpoint inhibitors of PD-L1 as cancer therapeutics. *J Hematol Oncol* **12**, 92 (2019).

46 Mandal, R., Samstein, R., Lee, K. *et al.* Genetic diversity of tumors with mismatch repair deficiency influences anti-PD-1 immunotherapy response. *Science* **364**, 485–491 (2019).

Curriculum Vitae

MIKAL EL-HAJJAR

Education

BS Western University, Bachelor of Science Honors May 2018
Honors Double Major
Microbiology and Immunology and French Studies

Honors and Awards

Western Scholar 2014-2015
First year students entering Western University with a final admission average of 90% or higher are eligible for Western Scholars. This program provides opportunities for outstanding students to learn and grow as both students and global citizens in an engaging, enriching, and inspiring environment.

Dean's Honor List 2014-2018
The Dean of each Faculty establishes an Honor List containing the names of all full-time students registered in that Faculty who completed a **minimum of 4.0 courses** during the previous fall/winter Session (September-April) and earned an average for the session of **80%** or more with **no failed courses**.

Western Continuing Admission Scholarship 2014-2018
Scholarship available to only students with entering averages of 95% or higher. The value of the award will be \$2,500 per year for four years.

BioCanRx Travel Award Recipient 2019
Travel award for the Summit of Cancer Immunotherapy which includes diverse lineup of internationally recognized speakers, scientific presentations, poster sessions, panel discussions, trainee workshops and networking opportunities.

Research Experience

Volunteering Position, Western University 2015-2017
Advisor: Dr. Jimmy Dikeakos
Shadowing experience of master's and PhD students.

Masters Candidate, Western University, Victoria Hospital 2018-Present
Advisors: Drs. James Koropatnick and Saman Maleki
Clinical trial experience, Mimic Trial (Melanoma)

Abstracts and Presentations and Publications

Abstracts

El-Hajjar M, Maleki S, Koropatnick J et al (2018) Understanding the immune phenotype of anti-tumour T-cells in tumours deficient in DNA mismatch repair. Infection & Immunity Research Forum (IIRF), Western University, London, Ontario

El-Hajjar M, Maleki S, Koropatnick J et al (2019) Identifying immune mechanisms responsible for increased sensitivity to anti-PD1 immunotherapy in tumours with induced mismatch repair deficiency. Summit for Cancer Immunotherapy, BioCanRX, Victoria, British Columbia

El-Hajjar M, Maleki S, Koropatnick J et al (2019) Understanding the Immune Phenotype of Anti-Tumour T-cells in Tumours Deficient in DNA Mismatch Repair. London Health Research Day, London, Ontario

El-Hajjar M, Maleki S, Koropatnick J et al (2019) Identifying immune mechanisms responsible for increased sensitivity to anti-PD1 immunotherapy in tumours with induced mismatch repair deficiency. Oncology Research & Education Day, London, Ontario

Maleki S, Lenehan JG, Burton J, Silverman M, Nair Parvathy S, **El-Hajjar M**, Krishnamoorthy M. “*Combination of fecal microbiota transplantation from healthy donors with anti-PD1 immunotherapy in treatment-naïve advanced or metastatic melanoma patients*” **Late-Breaking Poster**, SITC Annual Meeting, International Conference, National Harbour, MD, November 2019

Maleki S, Lenehan J, Burton J, Silverman M, Parvathy SN, **El-Hajjar M** and Krishnamoorthy M. P864 Combination of fecal microbiota transplantation from healthy donors with anti-PD1 immunotherapy in treatment-naïve advanced or metastatic melanoma patients. Journal for Immunotherapy of Cancer. March 2020

Presentations

The effect of inducing mismatch repair deficiency on low tumour mutation burden tumours and anti-tumour immunity. Infection & Immunity Research Forum (IIRF) November 8th, 2019

Inducing DNA-Mismatch Repair Deficiency in Tumours: A Strategy to Enhance Anti-Tumour Immunity. Immuno-Oncology Symposium, LHSC, London, Ontario, February 6, 2020

Peer Reviewed Publications

Faizah Alotaibi, Mateusz Rytelowski, Rene Figueredo, Ronak Zareardalan, Meng Zhang, Peter J Ferguso, Saman Maleki Vareki, Yousef Najajreh, **Mikal El-Hajjar**, Xiufen Zheng, Wei-ping Min, James Koropatnick. 2020. CD5 blockade enhances ex vivo CD8+ T cell activation and tumour cell cytotoxicity. Eur. J. Immunol. 50: 695-704. Impact Factor 5.179.

Professional Training

ACVS Certification in Basic Animal Care and Use

Western University, 2018

ACVS Certification in Mouse IP and SQ Injections

Western University, 2018

ACVS Certification in Rodent and Mouse Gas Anesthesia

Western University, 2018

Biosafety and WHIMIS Certified

Western University, 2018

Teaching Experience

Teach Assistant (TA) for the Microbiology and Immunology 2500a fall 2020 term at Western University